STORY OF SURVIVAL: *ASPERGILLUS FUMIGATUS*,

AN ACCIDENTAL FUNGAL PATHOGEN

by

Shin-Yong Earl Kang, Jr.

(Under the Direction of Michelle Momany)

ABSTRACT

Aspergillus fumigatus is a ubiquitous saprophytic fungus well adapted to survive a wide range of environmental conditions including that of the human host. Infection is caused by inhalation of conidia, which are usually cleared in healthy individuals but can cause chronic or invasive aspergillosis in immunocompromised individuals. Over the last 30 years, mortality rates of those with invasive aspergillosis have increased to 90-100% even with treatment due to the rapid emergence of antifungal resistant isolates. Resistance is thought to be derived in the environment from off-target exposure to agricultural fungicides, the same class of antifungals used in clinics. Therefore, it is imperative for us to understand its ecology and biology to identify novel drug targets to prevent the growth of *A. fumigatus* in humans. In this dissertation we first examine the population structure of environmental *A. fumigatus* collected in Georgia and Florida and analyzed genomes of susceptible and resistant clinical isolates to understand how resistance may be evolving. Then we tested the effect of sporulation environment on conidial germination using a high throughput germination assay to identify conditions which resulted in fast and slow rate of germination in genetically identical spores. Finally, we performed transcriptomic analysis on conidia to better understand what regulates its development and ability to germinate. In conclusion we found that the conidial stage of *A. fumigatus* life cycle is inherently stressful and by repurposing conidial transcriptional programs it is able to adapt to the stressful environmental conditions.

INDEX WORDS: fungicide resistance, heterogeneity, conidia, transcriptomics, environment

STORY OF SURVIVAL: *ASPERGILLUS FUMIGATUS,* AN ACCIDENTAL FUNGAL PATHOGEN

by

SHIN-YONG EARL KANG, JR.

B.S., University of California, San Diego, 2011

A Dissertation Submitted to the Graduate Faculty of The University of Georgia in Partial Fulfillment of the Requirements for the Degree

DOCTOR OF PHILOSOPHY

ATHENS, GEORGIA

2019

STORY OF SURVIVAL: *ASPERGILLUS FUMIGATUS,*

AN ACCIDENTAL FUNGAL PATHOGEN

by

SHIN-YONG EARL KANG, JR.

Major Professor:	Michelle Momany
Committee:	Chang Hyun Khang James Leebens-mack Xiaorong Lin Zachary Lewis

Electronic Version Approved:

Ron Walcott
Interim Dean of the Graduate School
The University of Georgia
December 2019

DEDICATION

I would like to dedicate this to my friends and mentors who believed in me and gave me the strength to complete this journey.

TABLE OF CONTENTS

CHAPTER 1

INTRODUCTION

Aspergillus fumigatus is a ubiquitous saprophytic fungus that plays an essential role in recycling environmental carbon and nitrogen[1], and is able to utilize a wide variety of carbon and nitrogen sources. Its natural ecological niche is soil and decaying organic debris, and have been isolated from garden soils[2, 3], compost piles[4], forest soils[5], and sewage sludge[6, 7]. Isolates are also tolerant of a range of pH between 2.0 to 10.5[8] and temperatures between 4°C and 65°C.[9] It has also been identified an endophytic fungus and known to produce phytochemicals such as gibberellin and taxols[10-12]. These phytochemicals are an example of the vast number of secondary metabolites *A. fumigatus* is able to produce. Its genome encodes for a high number of efflux pumps, transporters, catalases, superoxide dismutases, glutathione transferases for the detoxification of reactive oxygen species (ROS)[13-15].

While *Aspergillus fumigatus* is not the most prevalent fungus in the world, it is one of the most ubiquitously found fungus due to the efficient distribution of its airborne conidia[16]. Conidia are the asexual propagules of *A. fumigatus* and are abundantly produced in long chains under nutrient deficient conditions and/or exposure to oxidative stress[17]. Disturbances to the environment by rain or wind can disperse conidia over many long distances[16, 18, 19]. Conidia can withstand UV, extreme temperatures and desiccation due to its highly organized rodlet layer and melanized cell wall[1, 20]. Interestingly, the ornate cell wall structure is predicted to facilitate dispersion by animals[21] and specific cell wall proteins are recognized by swarming bacteria which can also facilitate dispersion[22].

However, airborne conidia are the infectious propagules of *A. fumigatus* and are responsible for over 8,000,000 global cases of fungal disease[23] (Table 1.1). Adults are estimated to inhale between 10-1000 conidia daily. The 2-3 um conidia are able to get deep into the lung alveoli where conidial germination is initiated by the presence of water and glucose and begins to swell, releasing cell wall proteins and endotoxins into our system. In healthy individuals the foreign particles trigger an immune

response and conidia / early germlings are cleared. Repeated exposure to a large dose of conidia can cause an allergic response known as "Farmer's lung", and in rare cases exposure can overwhelm the immune system of a healthy individual and cause death[24]. In immunocompromised or neutropenic individuals conidia and germlings are not cleared and can cause life threatening aspergillosis without treatment[25].

Recommended treatment for aspergillosis is with the use of antifungal class of azoles[26]. Azoles primarily target lanosterol demethylase genes (cyp51A / Erg11) in the ergosterol synthesis pathway. The first generation broad-spectrum azole available for clinical use against aspergillosis was itraconazole first introduced in the 1980s[27]. However, this itraconazole had low bioavailability and resistance was observed in AIDs patients. An improved itraconazole was approved in 1992 and treatment failure was reported within years[28]. Voriconazole, a second generation azole, was discovered in the late 1990s and due to its fungicidal nature and efficacy it was approved for clinical use in 2002.

Shortly after, pan-azole resistance to due to a tandem repeat of 34bp in the promoter region and a L98H codon change was being reported in Europe. Analysis of culture collections found that the first TR_{34}/L98H resistant isolate occurred in 1998 and since then the single resistance mechanism had spread throughout Europe and globally[29, 30]. Since aspergillosis is caused by conidia produced in the environment, epidemiologists went looking in the environment for isolates harboring TR_{34}/L98H resistance mechanisms and found it in agricultural settings where demethylation inhibitor (DMI) fungicides were being used[29]. Then in 2011, a novel TR_{46}/Y121F/T289A mutation associated with voriconazole resistance was reported in the Netherlands[31, 32]. Since then there has been an increase in global reports of TR_{46}/Y121F/T289A isolates and additional novel TR isolates from both clinical and environmental settings[33-35]. The rapid emergence of antifungal resistance in *Aspergillus fumigatus* combined with the lag in antifungal discovery makes it imperative that we understand the ecology and biology of *A. fumigatus* in hopes of identifying novel drug targets.

In Chapter 2, we surveyed Georgia and Florida for azole resistant isolates in agricultural settings and found TR_{46}/Y121F/T289A isolates from two sites in different regions of Georgia. The TR_{46} isolates

were resistant to antifungal voriconazole and agricultural fungicide tebuconazole as previously reported[36]. Analysis of the genome showed that TR resistant isolates carried genetic markers for resistance to other commonly used agricultural fungicides that are not used in clinical settings. For the first time we showed that *A. fumigatus* is gaining accidental resistance to fungicides in the environment globally.

Whole genome sequencing and phylogeny showed that there are four distinct clades within *A. fumigatus* as previously reported[37]. We also analyzed publically available whole genome sequences of resistant isolates. Cyp51A TR resistant isolates all clustered in one clade along with isolates from the Netherlands and UK while resistant isolates with no known mechanism of resistance were distributed throughout the tree. We identified near isogenic pairs of resistant and susceptible isolates for future studies. Interestingly, SplitsTree analysis suggests that there is very little or no recombining between the four clades which suggests the clade containing TR resistant isolates may be a subspecies of *A. fumigatus*.

In Chapter 3, we tested the effect of nine sporulation conditions on germination rate of *Aspergillus fumigatus*. We found that the sporulation environment causes phenotypic changes in genetically identical conidia. The germination rate and variation in germination was carefully analyzed. We identified conditions which resulted in fast germinating, synchronous population of conidial germlings and identified conditions which resulted in slow germinating, variable population of conidial germlings. We suggest that the inherent variability during germination is a form of bet hedging.

In Chapter 4, transcriptomic analysis was performed on the conditions identified in Chapter 3. We found that fast germinating conidia were enriched in genes encoding transmembrane proteins and catabolic processes. Slow germinating conidia were enriched in genes involved in cell wall synthesis. We also report that germination phenotypes correlates with specific secondary metabolite clusters. Then we compare the conidial transcriptome to hyphal transcriptome to identify conidial regulators.

Table 1.1 Burden of Fungal Diseases caused by *Aspergillus fumigatus* [a] [23]

Fungal Disease	Annual incidence	Global burden	Comments
Allergic bronchopulmonary aspergillosis in asthma		~4,800,000	Adults only, rare in children
Allergic bronchopulmonary aspergillosis in cystic fibrosis		~6675	Adults only, starts from age 4
Chronic pulmonary aspergillosis		~3,000,000	
Invasive aspergillosis	>300,000		From about 10 million at risk annually

[a] Adapted from Bongomin et al, 2017

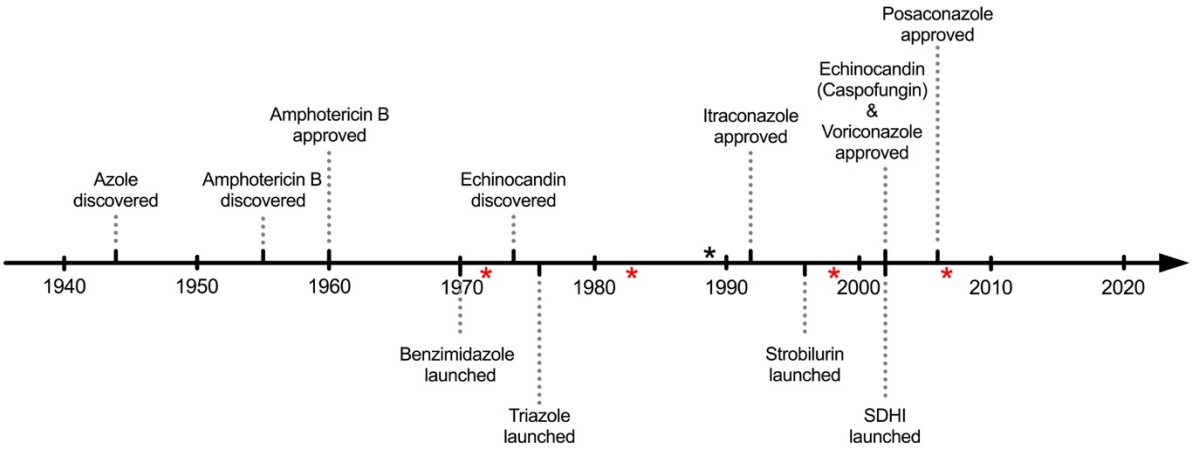

Figure 1.1. Timeline of antifungal and fungicides. Clinical antifungal discovery and FDA approval is shown on top of the timeline[38]. Agricultural broad-spectrum foliar fungicide launched is shown on the bottom of the timeline[39]. Red asterisk following fungicide launched indicates when resistance to the fungicide was first documented following the launch of fungicide[40]. Black asterisk indicates earliest documented case of triazole resistance in *Aspergillus fumigatus* from clinical sample isolated in 1989[41].

References

1. Latge, J.P. Aspergillus fumigatus and aspergillosis. *Clin Microbiol Rev* **12**, 310-50 (1999).
2. Haas, D.*, et al.* Culturable fungi in potting soils and compost. *Medical Mycology* **54**, 825-834 (2016).
3. Jensen, H.L. The fungus flora of the soil. *Soil Sci* **31**, 123-158 (1931).
4. Anastasi, A., Varese, G.C. & Marchisio, V.F. Isolation and identification of fungal communities in compost and vermicompost. *Mycologia* **97**, 33-44 (2005).
5. Miller, J.H., Giddens, J.E. & Foster, A.A. A Survey of the Fungi of Forest and Cultivated Soils of Georgia. *Mycologia* **49**, 779-808 (1957).
6. Millner, P.D., Marsh, P.B., Snowden, R.B. & Parr, J.F. Occurrence of Aspergillus-Fumigatus during Composting of Sewage Sludge. *Appl Environ Microb* **34**, 765-772 (1977).
7. Kothary, M.H., Chase, T. & Macmillan, J.D. Levels of Aspergillus-Fumigatus in Air and in Compost at a Sewage-Sludge Composting Site. *Environ Pollut A* **34**, 1-14 (1984).
8. Wheeler, K.A., Hurdman, B.F. & Pitt, J.I. Influence of pH on the growth of some toxigenic species of Aspergillus, Penicillium and Fusarium. *Int J Food Microbiol* **12**, 141-9 (1991).
9. Kwon-Chung, K.J. & Sugui, J.A. Aspergillus fumigatus--what makes the species a ubiquitous human fungal pathogen? *PLoS Pathog* **9**, e1003743 (2013).
10. Khan, A.L.*, et al.* Gibberellins producing endophytic Aspergillus fumigatus sp LH02 influenced endogenous phytohormonal levels, isoflavonoids production and plant growth in salinity stress. *Process Biochem* **46**, 440-447 (2011).
11. Liu, J.Y.*, et al.* Aspergillus fumigatus CY018, an endophytic fungus in Cynodon dactylon as a versatile producer of new and bioactive metabolites. *Journal of Biotechnology* **114**, 279-287 (2004).
12. Sun, D., Ran, X. & Wang, J. [Isolation and identification of a taxol-producing endophytic fungus from Podocarpus]. *Wei Sheng Wu Xue Bao* **48**, 589-95 (2008).
13. Nierman, W.C.*, et al.* What the Aspergillus genomes have told us. *Medical Mycology* **43**, S3-S5 (2005).
14. Kwon-Chung, K.J. & Sugui, J.A. Aspergillus fumigatus-What Makes the Species a Ubiquitous Human Fungal Pathogen? *Plos Pathogens* **9**, (2013).
15. Burns, C.*, et al.* Identification, cloning, and functional expression of three glutathione transferase genes from Aspergillus fumigatus. *Fungal Genetics and Biology* **42**, 319-327 (2005).

16. Taha, M.P., Pollard, S.J., Sarkar, U. & Longhurst, P. Estimating fugitive bioaerosol releases from static compost windrows: feasibility of a portable wind tunnel approach. *Waste Manag* **25**, 445-50 (2005).

17. Ebbole, D.J. The Conidium. *Cellular and Molecular Biology of Filamentous Fungi* 577-590 (2010).

18. Siqueira, V.M., *et al.* Filamentous fungi in drinking water, particularly in relation to biofilm formation. *Int J Environ Res Public Health* **8**, 456-69 (2011).

19. Warris, A., *et al.* Molecular epidemiology of Aspergillus fumigatus isolates recovered from water, air, and patients shows two clusters of genetically distinct strains. *J Clin Microbiol* **41**, 4101-6 (2003).

20. Brakhage, A.A. & Liebmann, B. Aspergillus fumigatus conidial pigment and cAMP signal transduction: significance for virulence. *Medical Mycology* **43**, S75-S82 (2005).

21. Calhim, S., *et al.* Fungal spore diversity reflects substrate-specific deposition challenges. *Scientific Reports* **8**, 5356 (2018).

22. Ingham, C.J., Kalisman, O., Finkelshtein, A. & Ben-Jacob, E. Mutually facilitated dispersal between the nonmotile fungus Aspergillus fumigatus and the swarming bacterium Paenibacillus vortex. *P Natl Acad Sci USA* **108**, 19731-19736 (2011).

23. Bongomin, F., Gago, S., Oladele, R.O. & Denning, D.W. Global and Multi-National Prevalence of Fungal Diseases-Estimate Precision. *J Fungi (Basel)* **3**, (2017).

24. Russell, K., *et al.* Gardening can seriously damage your health. *Lancet* **371**, 2056 (2008).

25. Dagenais, T.R.T. & Keller, N.P. Pathogenesis of Aspergillus fumigatus in Invasive Aspergillosis. *Clinical Microbiology Reviews* **22**, 447-465 (2009).

26. Patterson, T.F., *et al.* Executive Summary: Practice Guidelines for the Diagnosis and Management of Aspergillosis: 2016 Update by the Infectious Diseases Society of America. *Clin Infect Dis* **63**, 433-42 (2016).

27. Hector, R. The many lives of itraconazole. *Expert Opin Ther Pat* **13**, 141-148 (2003).

28. Koltin, Y. & Hitchcock, C.A. The search for new triazole antifungal agents. *Current Opinion in Chemical Biology* **1**, 176-182 (1997).

29. Snelders, E., *et al.* Emergence of azole resistance in Aspergillus fumigatus and spread of a single resistance mechanism. *PLoS Med* **5**, e219 (2008).

30. Verweij, P.E., Lestrade, P.P., Melchers, W.J. & Meis, J.F. Azole resistance surveillance in Aspergillus fumigatus: beneficial or biased? *J Antimicrob Chemother* **71**, 2079-82 (2016).

31. Camps, S.M.T., van der Linden, J.W.M., Melchers, W.J.G. & Verweij, P.E. A new resistance mechanism emerging in clinical Aspergillus fumigatus isolates in The Netherlands. *Mycoses* **54**, 56-57 (2011).

32. van der Linden, J.W., *et al.* Aspergillosis due to voriconazole highly resistant Aspergillus fumigatus and recovery of genetically related resistant isolates from domiciles. *Clin Infect Dis* **57**, 513-20 (2013).

33. Verweij, P.E., Chowdhary, A., Melchers, W.J. & Meis, J.F. Azole Resistance in Aspergillus fumigatus: Can We Retain the Clinical Use of Mold-Active Antifungal Azoles? *Clin Infect Dis* **62**, 362-8 (2016).

34. Alvarez-Moreno, C., *et al.* Fungicide-driven alterations in azole-resistant Aspergillus fumigatus are related to vegetable crops in Colombia, South America. *Mycologia* **111**, 217-224 (2019).

35. Hare, R.K., *et al.* In Vivo Selection of a Unique Tandem Repeat Mediated Azole Resistance Mechanism (TR120) in Aspergillus fumigatus cyp51A, Denmark. *Emerging Infectious Diseases* **25**, 577-580 (2019).

36. Cui, N., *et al.* Tebuconazole induces triazole-resistance in Aspergillus fumigatus in liquid medium and soil. *Science of the Total Environment* **648**, 1237-1243 (2019).

37. Garcia-Rubio, R., *et al.* Genome-Wide Comparative Analysis of Aspergillus fumigatus Strains: The Reference Genome as a Matter of Concern. *Genes (Basel)* **9**, (2018).

38. Gubbins, P.O. & Anaissie, E.J., *CHAPTER 7 - Antifungal therapy*, in *Clinical Mycology (Second Edition)*, E.J. Anaissie, M.R. McGinnis, and M.A. Pfaller, Editors. 2009, Churchill Livingstone: Edinburgh. p. 161-195.

39. Klittich, C.J. Milestones in Fungicide Discovery: Chemistry that Changed Agriculture. *Plant Health Progress* **9**, 31 (2008).

40. Lucas, J.A., Hawkins, N.J. & Fraaije, B.A., *Chapter Two - The Evolution of Fungicide Resistance*, in *Advances in Applied Microbiology*, S. Sariaslani and G.M. Gadd, Editors. 2015, Academic Press. p. 29-92.

41. Denning, D.W., *et al.* Itraconazole resistance in Aspergillus fumigatus. *Antimicrob Agents Chemother* **41**, 1364-8 (1997).

CHAPTER 2

AZOLE RESISTANCE IN ENVIRONMENTAL ISOLATES OF *ASPERGILLUS FUMIGATUS* IN GEORGIA AND FLORIDA[1]

[1] Kang, S.E., Momany, M., Brewer, M.T. To be submitted to Nature Microbiology.

Abstract

Aspergillus fumigatus causes over 300,000 annual cases of life-threatening infections in susceptible human hosts and antifungal class of azoles or demethylation inhibitors (DMI) are the most effective treatment. Azoles target lanosterol demethylase gene (cyp51A) in the ergosterol pathway and are highly effective against fungal pathogens of both humans and plants leading to their widespread use in clinical and agricultural settings. Emerging resistance to clinical azoles have become a major global problem over the last two decades, where identical mutations in cyp51A have been found in isolates from both clinical and agricultural settings. Shared cyp51A genotypes suggest that clinical azole resistance might have had an agricultural origin, however, until now, independent origins of this mutation could not be ruled out. Here we show that cyp51A mutant azole-resistant isolates of *A. fumigatus* from clinical and agricultural settings are genetically related and also carry mutations conferring resistance to succinate-dehydrogenase inhibitors (SDHI), quinone outside inhibitors (QoI) and benzimidazoles, fungicides used exclusively in agricultural settings. This is the first report of a clear marker for the agricultural origin of resistance to a clinical antifungal drugs. We anticipate that our work will increase appreciation for the role of antimicrobials directed against plant pathogens in reducing the effectiveness of clinical antimicrobials.

Introduction

Fungi cause over 1.5 million deaths annually and are responsible for 25% of crop loss annually. The filamentous fungus *Aspergillus fumigatus* is a saprophyte that is well adapted to surviving in a variety of environments including soil, compost and decaying plant material. It is a ubiquitous fungus due to its asexual production of abundant airborne asexual spores. It has evolved to utilize a wide range of carbon and nitrogen sources which has also allowed it to survive in immunocompromised hosts causing serious disease. *A. fumigatus* is responsible for over 300,000 annual cases of life-threatening invasive aspergillosis and approximately 8,000,000 global cases of fungal disease including allergic bronchopulmonary aspergillosis in asthma and chronic pulmonary aspergillosis.[1, 2]

The antifungal class of azoles which targets the lanosterol demethylase gene (cyp51A) in the ergosterol pathway are the most effective treatment.[3] The rapid rise of resistance to clinical azoles due to mutations in cyp51A have become a major global problem over the last two decades. Mutations in cyp51A coupled with tandem repeat duplication in the promoter region of the gene known as TR_{34}/L98H and TR_{46}/Y121F/T289A confers pan-azole resistance and resistance to voriconazole respectively. Identification of the same mutations in agricultural and clinical strains has led to the idea that azole resistance in clinical isolates of *A. fumigatus* might have an agricultural origin;[4] however, independent evolution of the same azole resistance mutations cannot be ruled out.

Reports in 2015 of cyp51A azole resistant isolates from patients in the United States has prompted the CDC to determine whether environmental isolates harboring the TR mutations exist in the United States.[5, 6] A 2015 survey of azole resistant *A. fumigatus* in agricultural settings in the United States resulted in isolates harboring TR_{34}/L98H mutation; however, isolates harboring TR_{46}/Y121F/T289A were not isolated.[7] As a continuation of the CDC survey for azole resistant isolates in the environment we collected soil and plant debris samples between 2017-2018 from 61 sites across Georgia and Florida where heavy DMI fungicide use has been reported by the US Department of Interior National Water-Quality Assessment Project.

Materials and Methods

Environmental sampling Soil, plant debris, or compost was collected from 61 agricultural sites in Georgia or Florida, USA, between July 2017 and March 2018. Sites included 53 sites that had been recently treated with triazole fungicides, two sites within a pecan processing facility, two sites that were in organic production with no triazole use in at least 10 years, and four compost piles with an unknown history of fungicide use on the plant material prior to composting (Table 2.1). Each site was defined as a different field location, different crop at the same field location, or different triazole fungicide treatment. Soil core and compost samples were taken at a depth of approximately 10 cm. Plant debris was sampled

from the center of cull piles. For each site 4 samples were collected at separate locations to minimize the collection of clones.

Isolation and storage Samples were processed as described previously by Snelder et al. 2009 and Hurst et al. 2017 with some modifications. Briefly, 2 g of soil was suspended in 15 ml of sterile 0.1M sodium pyrophosphate. Samples were vortexed for 30 sec and settled for 1 min. From the supernatant, 100 ul was pipetted on Sabouraud dextrose agar (SDA) supplemented with 50 µg/ml chloramphenicol (Sigma Aldrich) and 5 µg/ml gentamicin (Research Products International). The plates were incubated for 2-4 days at 45°C to select for thermotolerant fungi. Single colonies of *Aspergillus fumigatus* isolates were replicate plated onto SDA supplemented with 3 µg/ml tebuconazole (Bayer Corp) and SDA to screened for resistance. All isolates were streaked for single colony isolation, and a single was stored at -80°C in 15% glycerol.

Susceptibility testing of *A. fumigatus* Environmental *A. fumigatus*, clinical strains and controls were tested for antifungal susceptibility under conditions described in the Clinical Laboratory Standard Institute M38-A2 reference method (CLSI 2008). Antifungals tested included tebuconazole (TCI America, Oregon, USA), itraconazole (Thermo Sci Acros Organics, New Jersey, USA), voriconazole (Thermo Sci Acros Organics, New Jersey, USA), and pozaconazole (Apexbio Technology, Texas, USA) diluted in DMSO. Briefly, isolates were grown on complete media slants for 5-7 days at 37°C and harvested with 2 ml of 0.02% Tween-20 solution. Inoculum was adjusted to 0.09 – 0.13 OD at 530 nm using a spectrophotometer. Final density of 2 – 5 x 10^4 conidia/ml in 100 µl was added to 100 mL of RPMI 1640 (Thermo Sci Gibco, California, USA) in microtiter plates with final concentration of drugs ranging from 0.015 to 16 mg/L. Plates were incubated at 37°C for 48 hrs and MIC end points were read visually. MIC end point was defined as the lowest concentration at which there was 100% inhibition of growth compared to drug-free control wells. Azole resistance was defined as MIC > 1 mg/L of azole.

DNA extraction High molecular weight genomic DNA of *A. fumigatus* isolates was extracted using a modified CTAB protocol as described previously.[8] Briefly, ~100 mg of mycelia collected from

cultures that had been incubated overnight in liquid complete medium[9] were transferred to 2 ml tubes containing ~200 µl of 0.5 mm disruption glass beads (RPI, catalog #9831) and three 3 mm steel beads and lyophilized. Lyophilized cells were pulverized using GeneGrinder at 1750 rpm for 30 sec. Resulting powdered mycelia were incubated in 1 ml of CTAB lysis buffer (100 mM Tris pH 8.0, 10 mM EDTA, 1% CTAB, 1% BME) for 30min at 65C. The samples were then treated with chloroform (500 µl) twice and DNA in the upper layer was precipitated in ice cold isopropanol. The precipitated DNA samples were washed with 70% ethanol twice, air dried, and dissolved in 100 µl sterile water. DNA was quantified using NanoDrop One (Thermo Sci, New Jersey, USA).

Library preparation and whole genome sequencing Genomic DNA was sheared to a mean size of 600 bp using a Covaris LE220 focused ultrasonicator (Covaris Inc., Woburn, MA). DNA fragments were Ampure (Beckman Coulter Inc., Indianapolis, IN) cleaned and used to prepare dual-indexed sequencing libraries using NEBNext Ultra library prep reagents (New England Biolabs Inc., Ipswich, MA) and barcoding indices synthesized in the CDC Biotechnology Core Facility. Libraries were analyzed for size and concentration, pooled and denatured for loading onto flowcell for cluster generation. Sequencing was performed on an Illumina Hiseq using 300x300 cycle paired-end sequencing kit. On completion, sequence reads were filtered for read quality, base called and demultiplexed using Casava v1.8.4.

SNP calling Trimmed reads were aligned to AF293 reference genome using Burrows-Wheeler Aligner (BWA) alignment tool and duplicate reads were marked using Picard v2.16.0. Single nucleotide polymorphisms (SNPs) were called with SAMtools mpileup v1.6 with option -I to exclude insertions and deletions then with BCFtools v1.9 with option –c. Bases with phred quality score lower than 40 were filtered using SAMtools seqtk v1.2.

Phylogeny reconstruction SNP data were converted into interleaved Phylip format and maximum likelihood trees were constructed using IQ-TREE v1.6.5[10]. Ultrafast bootstrap approximation with 1000 bootstrap replicates was used to determine the best tree[11]. SplitsTree analysis was performed using SplitsTree4[12] without weights to better visualize potential connections between isolates.

Cyp51A sequencing. For all environmental isolates from this study, Cyp51a was amplified using Q5 Hot Start High-Fidelity 2x Master Mix Protocol (NEB) from 100ng of genomic DNA with 0.5 µM forward primer 5' - CGG GCT GGA GAT ACT ATG GCT and 0.5 uM reverse primer 5' - GTA TAA TAC ACC TAT TCC GAT CAC ACC in 20 µl reactions. Amplification was performed at 98°C for 2 min followed by 30 cycles of 98°C for 15 sec, 62°C for 15 sec, and 72°C for 2:30 min and then one cycle of 72°C for 5 minutes. Amplicons were sanger sequenced (Eurofins genomics, USA) using primers 5' - GCA TTC TGA AAC ACG TGC GTA G, 5' - GTC TCC TCG AAA TGG TGC CG, and 5' - CGT TCC AAA CTC ACG GCT GA. Promoter sequences were aligned to A1163 genomic sequence v43 from Ensembl. Coding sequences were translated to protein sequences and aligned to A1163 cyp51a GenBank sequence EDP50065. Sequence analysis was performed using Geneious v11.1.5 (Biomatters, Auckland, NZ).

Genome analysis Cleaned whole genome sequence reads for each isolate were *de novo* assembled using SPAdes v3.12.0 with option --careful and trained to AF293 reference genome using option --trusted-contigs.[13] GenBank sequences for benA (EDP56324), cyp51a (EDP50065), cytB (AFE02831), and sdhB (EDP51777) were blasted against *de novo* assembled scaffolds using BLAST+ v2.7.1. Blast hits were extracted from assembly using BEDtools v2.26.0. Sequence analysis was performed using Geneious v11.1.5 (Biomatters, Auckland, NZ).

Agricultural fungicide phenotype assay Benzimidazole assay plates contained 10 µg/ml Benomyl (Sigma Aldrich, diluted from10 mg/ml stock in DMSO) in in SDA. Quinone outside inhibitors (QoI) assay plates contained 10 µg/ml of azoxystrobin (AZ) (Sigma Aldrich analytical-grade, diluted from 10 mg/mL stock in acetone) and 100 µg/ml Salicylhydroxamic acid (SHAM) (Sigma Aldrich analytical-grade, diluted from 100 mg/ml stock in methanol) in SDA. Succinate-dehydrogenase inhibitor (SDHI) assay plates contained 3 µg/ml of boscalid (BASF Corp, diluted from 3 mg/ml stock in acetone) in SDA. Negative controls included isolates without mutations and SDA plate without drugs. Isolates were streaked from inoculum adjusted to 0.09 – 0.13 OD at 530 nm and incubated at 37°C for 48 hrs.

Results

Sites sampled included 55 that had been treated with DMI fungicides, two sites from 1 processing facility that dealt with plant material from various sources, 2 organic sites with no DMI fungicide use in at least 10 years, and four compost piles of unknown history (Table 2.1). Out of the 61 sites sampled, *A. fumigatus* was isolated from 53 sites. A total of 704 isolates were collected, 123 (17.6%) grew on SDA amended with 3 µg/mL tebuconazole.

Susceptibility testing was performed on all 123 isolates. An additional 49 isolates that did not grow on SDA amended tebuconazole plates were selected from sites that resulted in isolates that grew on SDA amended tebuconazole plates for a total of 172 isolates. Minimal Inhibitory Concentrations (MICs) ranged from 0.5 to >16 µg/µL for tebuconazole, 0.5 to 2 µg/µL for itraconazole, 0.125 to >16 µg/ml for voriconazole, and 0.06 to 1 µg/µL. 12/172 isolates exhibited MIC of ≥16µg/µL for tebuconazole and voriconazole, 11/172 isolates exhibited MIC of >1µg/µL for itraconazole and 15/172 isolates exhibited MIC of >1µg/µL for pozaconazole (Table 2.2). Isolate eAF609 exhibited MIC of 2-4µg/µL for tebuconazole however was susceptible to all other azoles.

Sequencing of Cyp51A, including 1000bp upstream of the start site and 286bp downstream of stop site, of all 172 isolates revealed that all 12 isolates with MIC of ≥16µg/µL for tebuconazole and voriconazole all contained TR_{46}/Y121F/T289A mutation previously documented as being voriconazole resistant[14]. 11 isolates had an I242V mutation and 5 isolates had Y46F/V172M/T248N/E255D/K427E mutations found in reference isolate Af293. MIC values of the 16 isolates without tandem repeats in the promoter region of Cyp51a had slightly elevated value compared to sensitive reference isolate A1163; however, were still below what is considered clinically resistant (Table 2.3).

To determine the genetic relatedness of the isolates, at least one isolate pre-screened as resistant and/or sensitive from each site were selected at random for whole genome sequencing and phylogenetic analysis using IQ-TREE (Figure 2.1). To our surprise, clones were rarely sequenced from the same site. There was also no discernable correlation between crop, location, and resistance. However, four cyp51A

TR_{46} mutants that were whole genome sequenced (eAF222, eAF233, eAF234, eAF513) clustered on a single branch along with two susceptible isolates (eAF537, eAF095). This suggests that the TR_{46}/Y121F/T289A mutations may have developed independently multiple times or that the mutation can be lost. SplitsTree analysis of environmental isolates suggest that there may be four distinct clades or populations of *Aspergillus fumigatus* (Figure 2.2).

Next to see if agricultural and clinical resistant isolates display genetic relatedness, we included publicly available whole genome sequences of clinical resistant isolates (Figure 2.3). Azole resistant isolates were distributed along the tree suggesting that azole resistance has developed independently multiple times. Pan-azole resistant isolates with TR mutations in cyp51A clustered into a clade along with isolates from the Netherlands and several isolates from the UK. This suggests that isolates with the TR_{46}/Y121F/T289A mutation have been introduced from Europe where the mutation was first discovered[15].

Genomes of all environmental *A. fumigatus* in this study and resistant isolates examined were analyzed for mutations in target sites of other single-site inhibitors: B-tubulin (benA) for benzimidazoles, Mitochondrial cytochrome B (cytB) for quinone outside inhibitors (QoIs) and succinate dehydrogenase (sdhA-D) for succinate dehydrogenase inhibitors (SDHIs)[16]. We BLASTed amino acid sequences of cyp51b, benA, cytB, sdhA, sdhB, sdhC, and sdhD against the *de novo* assembled scaffold genomes of all isolates[17]. To our surprise only isolates with cyp51a TR azole resistance also contained mutations F219Y in benA, G143A in cytB or H270Y in sdhB. All TR mutants had the mutation for benA, 15 isolates had mutations for cytB, and three isolates had mutations associated with SDHI. Interestingly, SDHI was launched in 2002 and mutation in sdhB conferring resistance to SDHI was only contained in isolates isolated after 2010. This finding supports that antifungal resistance is acquired in the environment and there's something about this clade which makes them more prone to develop resistance to lots of different fungicides.

No established protocol exists for susceptibility testing against agricultural fungicides in *A. fumigatus*; therefore, we decided to perform a quick susceptibility assay by streaking dilute conidial

solution of eAF222, eAF233, eAF234, and eAF513 predicted to carry mutations conferring resistance to agricultural fungicides onto SDA plates supplemented with benzimidazole, azoxystrobin, or boscalid. To rule out the possibility of a secondary mutation conferring resistance, we selected closely related isolates eAF095, eAF537, eAF128, and eAF609 as our negative control. Reference isolates Af293 and CEA10/A1163 were also included in the assay. 48 hrs of incubation showed significant difference in growth between isolates predicted to carry mutations conferring resistance and isolates without mutations (Figure 2.4).

Discussion

Even though the earliest known clinical isolate carrying the TR_{46}/Y121F/T289A mutation was identified in the United States[5], we do not believe that the origin of this isolate is the United States due to its genetic relationship with isolates from Europe. We also did not identify TR_{34}/L98H azole resistant isolates in this study. This was due in part to our preliminary selection on SDA supplemented with tebuconazole; therefore, we cannot rule out that TR_{34}/L98H azole resistant isolates are not present in the environment. In further surveillance and studies we will have to be more strategic in our preliminary screens.

For the first time we identified TR_{46}/Y121F/T289A azole resistant *A. fumigatus* isolates in an agricultural setting in the USA. In addition, we identified genetic markers for other agricultural fungicide resistance in environmental isolates in this study and in clinical isolates. Together for the first time we have been able to show that environmental use of fungicides is driving resistance in *A. fumigatus*. We also show that isolates with single site mutations conferring resistance to agricultural fungicides share a genetic lineage. Included in this population is one of our reference isolates Af293 which is very different from our other reference isolate CEA10/A1163 and isolates with unknown mechanisms of azole resistance.

Interestingly, resistant isolates in this study were not isolated from sites known to have recent heavy exposure to fungicides. Site A17-20 was a rich compost pile of composted food scraps and landscape trimmings from the University of Georgia and site A17-22 was twigs and leaves collected from

inside a pecan processing facility. The two sites were separated by almost 200 miles or ~320 kilometers, and no cyp51A resistant isolates were recovered from sites located between the two sites. The lack of correlation between genetic relationship and geographic structure is not surprising. Based on the phylogeny of environmental isolates in this study, we observed a diverse mix of isolates in a site and rarely sequenced clones from a site.

Acknowledgments

We wish to acknowledge Tina Melie and Brandon Mangum in Brewer lab at the University of Georgia for their laboratory assistance on this project. We would like to thank Bob Kemerait, Bhabesh Dutta, Elizabeth Little, and Tim Brenneman at the University of Georgia and Katia Xavier at the University of Florida Gulf Coast Research & Education Center for assistance in obtaining samples. We would also like to thank Elizabeth Berkow, Kizee Etienne, Anastasia Litvintseva, and Shawn Lockhart at the Center for Disease Control and Prevention for support and wonderful discussions.

Table 2.1 Sampling of *Aspergillus fumigatus* strains from agricultural sites

Site ID	County, State – Crop (Substrate sampled)	# Isolated	# Grew on Teb	# of MIC values	WGS isolate ID (* TR_{46} /Y121F/T289A mutation)
A17-01	Crisp County, GA – Watermelon (Soil)	3	0	1	eAF001
A17-02	Crisp County, GA – Watermelon (Plant debris)	-	-	-	-
A17-03	Crisp County, GA – Watermelon (Plant debris)	18	7	9	eAF006, eAF010, eAF015, eAF016, eAF017
A17-04	Union County, GA – Grapevine (Soil)	14	7	9	eAF021, eAF022, eAF061, eAF067, eAF072
A17-05	Union County, GA – Apple (Soil)	9	4	5	eAF076, eAF077
A17-06	Crisp County, GA – Watermelon (Plant debris)	34	24	25	eAF039, eAF043
A17-07	Tift County, GA – Peanut (Plant debris)	8	5	6	eAF081, eAF105
A17-08	Tift County, GA – Peanut (Soil)	3	2	2	-
A17-09	Tift County, GA – Peanut (Soil)	13	8	9	eAF090, eAF111, eAF113
A17-10	Tift County, GA – Peanut (Soil)	2	2	2	eAF091
A17-11	Tift County, GA – Peanut (Soil)	6	3	4	eAF144, eAF152
A17-12	Tift County, GA – Peanut (Soil)	2	1	2	eAF153, eAF154
A17-13	Tift County, GA – Peanut (Soil)	3	2	3	eAF094, eAF095, eAF148
A17-14	Tift County, GA – Peanut (Plant debris)	14	4	6	eAF116, eAF122, eAF155, eAF158
A17-15	Tift County, GA – Peanut (Plant debris)	12	2	3	eAF128, eAF163
A17-16	Tift County, GA – Peanut (Plant debris)	25	16	18	eAF098, eAF146, eAF170, eAF170, eAF177
A17-17	Turner County, GA – Peanut (Plant debris)	4	2	3	eAF100, eAF147
A17-18	Clarke County, GA – Cucurbits (Soil)	28	0	1	-
A17-19	Clarke County, GA – Brassica (Soil)	16	0	1	eAF237
A17-20	Clarke County, GA – Mixed (Compost)	22	12	13	eAF222*, eAF223, eAF227, eAF233*, eAF234*
A17-21	Dougherty County, GA – Processing facility (Plant debris)	51	2	4	eAF263, eAF265, eAF365, eAF500
A17-22	Dougherty County, GA – Processing facility (Plant debris)	45	1	3	eAF272, eAF379, eAF513*
A17-23	Dougherty County, GA – Pecan (Compost)	6	0	3	eAF288, eAF514
A17-24	Dougherty County, GA – Pecan (Soil)	11	0	1	eAF294
A17-25	Dougherty County, GA – Pecan (Plant debris)	13	0	1	eAF406
A17-26	Dougherty County, GA – Pecan (Compost)	52	0	0	-
A17-27	Dougherty County, GA – Pecan (Plant debris)	35	1	2	eAF537, eAF544
A17-28	Dougherty County, GA – Pecan (Plant debris)	15	0	1	eAF321
A17-29	Dougherty County, GA – Pecan (Plant debris)	10	0	1	eAF325
A17-30	Dougherty County, GA – Pecan (Soil)	17	0	1	eAF335
A17-31	Dougherty County, GA – Pecan (Compost)	29	2	3	eAF549, eAF554, eAF560

Table 2.1 Sampling of *Aspergillus fumigatus* strains from agricultural sites (*continued*)

Site ID	County, State – Crop (Substrate sampled)	# Isolated	# Grew on Teb	# of MIC values	WGS isolate ID (* TR_{46} /Y121F/T289A mutation)
A17-32	Dougherty County, GA – Pecan (Plant debris)	19	0	1	eAF477
A17-33	Dougherty County, GA – Pecan (Plant debris)	22	0	1	eAF490
A17-34	Crisp County, GA – Watermelon (Compost)	-	-	-	-
A17-35	Crisp County, GA – Watermelon (Compost)	-	-	-	-
A17-36	Tift County, GA – Watermelon (Compost)	-	-	-	-
A17-37	Turner County, GA – Watermelon (Compost)	-	-	-	-
A17-38	Turner County, GA – Watermelon (Compost)	-	-	-	-
A17-39	Clinch County, GA – Blueberry (Soil)	-	-	-	-
A17-40	Clinch County, GA – Blueberry (Soil)	1	0	1	-
A17-41	Clinch County, GA – Blackberry (Soil)	-	-	-	-
A17-42	Bacon County, GA – Blueberry (Soil)	14	0	1	-
A17-43	Bacon County, GA – Blueberry (Soil)	2	0	1	eAF584
A17-44	Hillsborough County, FL – Strawberry (Soil)	25	3	6	eAF586, eAF587, eAF589, eAF591, eAF609, eAF610
A17-45	Hillsborough County, FL – Tomato (Soil)	12	1	2	eAF620, eAF621
A17-46	Hillsborough County, FL – Tomato (Soil)	21	2	3	eAF623, eAF624, eAF625
A17-47	Hillsborough County, FL – Tomato (Soil)	2	0	2	eAF645, eAF647
A17-48	Hillsborough County, FL – Watermelon (Soil)	2	2	1	eAF740
A17-49	Polk County, FL – Citrus (Soil)	6	2	3	eAF735, eAF743, eAF749
A17-50	Polk County, FL – Citrus (Soil)	3	0	0	-
A17-51	Polk County, FL – Citrus (Soil)	13	0	0	-
A17-52	Polk County, FL – Citrus (Soil)	4	0	0	-
A17-53	Polk County, FL – Citrus (Soil)	4	0	0	-
A17-54	Polk County, FL – Citrus (Soil)	5	1	2	eAF768, eAF770
A17-55	Polk County, FL – Citrus (Soil)	7	2	3	eAF773, eAF776, eAF777
A17-56	Polk County, FL – Citrus (Soil)	4	0	0	-
A17-57	Polk County, FL – Citrus (Soil)	4	0	0	-
A17-58	Polk County, FL – Citrus (Soil)	7	3	3	eAF790, eAF792
A17-59	Polk County, FL – Citrus (Soil)	2	0	0	-
A17-60	Polk County, FL – Citrus (Soil)	2	0	0	-
A17-61	Polk County, FL – Citrus (Soil)	3	0	0	-

Table 2.2 Minimum inhibitory concentrations (MIC) for *Asperigllus fumigatus* strains (*n* = 172) isolated from agricultural sites in the Georgia and Florida where azole fungicides were applied

Azole	Minimum inhibitory concentration (µg/mL)[a]								
	>16	**16**	**8**	**4**	**2**	**1**	**0.5**	**0.25**	**<0.25**
Tebuconazole	11	1		1	85	68	6		
Itraconazole					11	140	21		
Voriconazole	12					1	81	72	6
Posaconazole						15	93	58	6

[a] Strains were assayed for MIC twice. Most often, there was no variation between replicates, but if there was a difference the greater MIC is presented here.

Table 2.3 Minimum inhibitory concentrations (MIC) of *A. fumigatus* isolates with Cyp51A mutations

Isolate ID	Cyp51A mutations [a]	MIC Ranges (μg/mL) [b]			
		TEB	ITC	VRC	POS
A1163	WT	1.0	1.0	0.25	0.25
eAF221	TR_{46}/Y121F/T289A	>16	1.0-2.0	>16	1.0
eAF222	TR_{46}/Y121F/T289A	>16	2.0	>16	1.0
eAF228	TR_{46}/Y121F/T289A	>16	1.0-2.0	>16	1.0
eAF229	TR_{46}/Y121F/T289A	>16	1.0-2.0	>16	1.0
eAF230	TR_{46}/Y121F/T289A	>16	1.0-2.0	>16	1.0
eAF231	TR_{46}/Y121F/T289A	>16	1.0-2.0	>16	1.0
eAF232	TR_{46}/Y121F/T289A	>16	1.0-2.0	>16	1.0
eAF233	TR_{46}/Y121F/T289A	>16	1.0-2.0	>16	1.0
eAF234	TR_{46}/Y121F/T289A	>16	1.0-2.0	>16	1.0
eAF235	TR_{46}/Y121F/T289A	16	1.0	$\geq$16	0.5-1.0
eAF236	TR_{46}/Y121F/T289A	>16	1.0-2.0	>16	1.0
eAF513	TR_{46}/Y121F/T289A	>16	1.0	>16	1.0
eAF010	I242V	1.0-2.0	1.0	0.5	0.5-1.0
eAF175	I242V	2.0	1.0	0.25-0.5	0.5
eAF263	I242V	2.0	1.0	0.5	0.5
eAF265	I242V	2.0	1.0	0.5	0.5
eAF406	I242V	2.0	1.0	0.5	0.25
eAF500	I242V	2.0	1.0	0.5	05
eAF589	I242V	2.0	1.0	0.25-0.5	0.25-0.5
eAF621	I242V	2.0	1.0	0.5	0.5
eAF647	I242V	2.0	1.0	0.25	0.25
eAF773	I242V	2.0	1.0	0.5	0.5
eAF792	I242V	1.0-2.0	0.5-1.0	0.25-0.5	0.25-0.5
eAF016	Y46F/V172M/T248N/ E255D/K427E	1.0-2.0	1.0	0.25-0.5	0.5
eAF082	Y46F/V172M/T248N/ E255D/K427E	1.0-2.0	1.0	0.25-0.5	0.25-0.5
eAF128	Y46F/V172M/T248N/ E255D/K427E	2.0	1.0	0.5	0.5
eAF163	Y46F/V172M/T248N/ E255D/K427E	1.0-2.0	1.0	0.25-0.5	0.5
eAF609	Y46F/V172M/T248N/ E255D/K427E	2.0-4.0	1.0	0.5-1.0	0.25-0.5

[a] Cyp51A protein GenBank accession number EDP50065.1 used as reference. [b] MICs; TEB, tebuconazole; ITC, itraconazole; VRC, voriconazole; POS, posaconazole. Each assay was conducted twice.

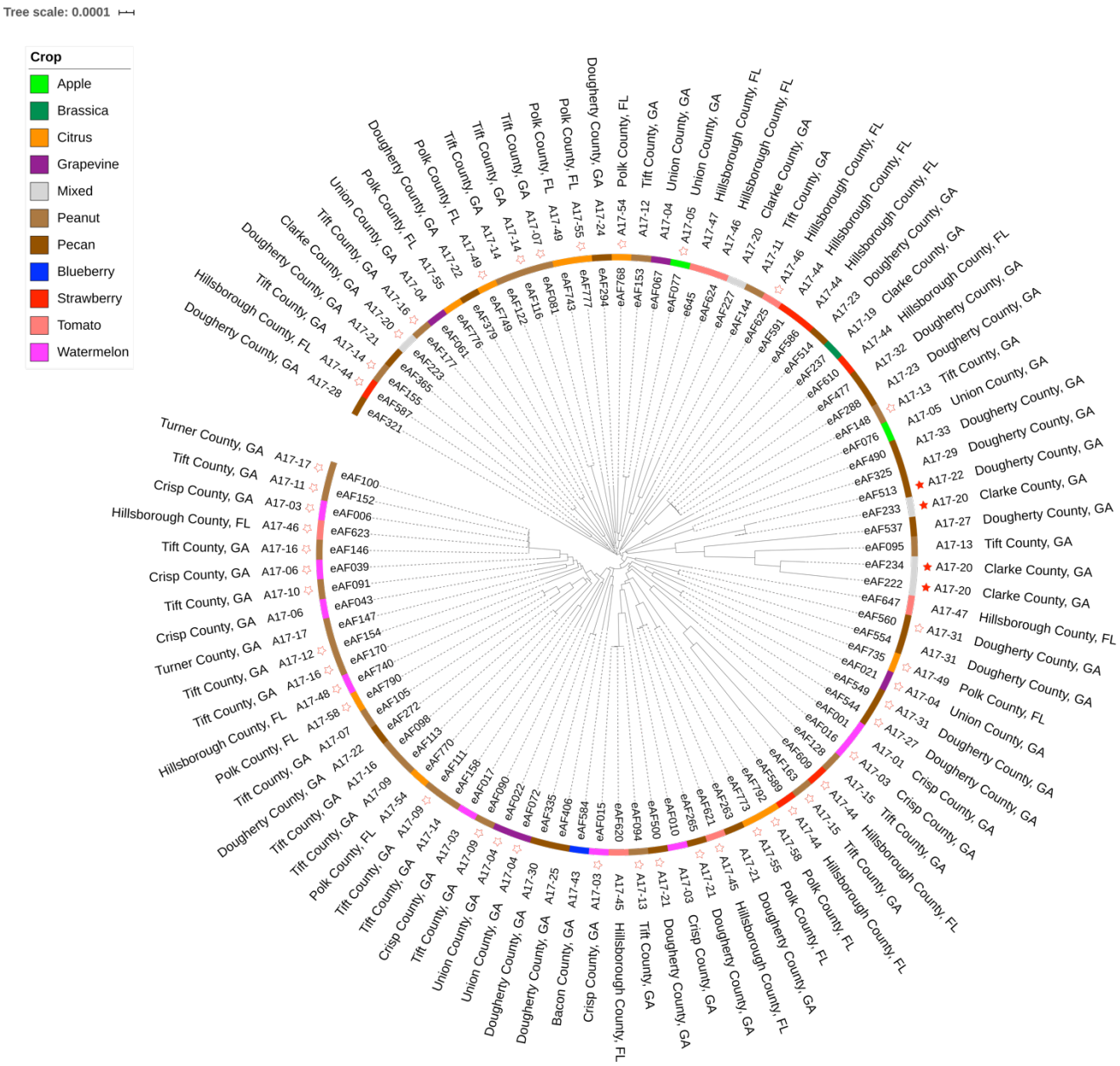

Figure 2.1 Relatedness of environmental *Aspergillus fumigatus* Cladogram of unrooted NJ tree representing the genetic relations of environmental isolates in this study. Isolates with TR_{46}/Y121F/T289A mutations cluster together (solid star). Isolates that grew on SDA supplemented with tebuconazole are distributed across the tree (open star). Colored bars represent crops sampled as indicated in the ledged. Site ID and County information are on the outer circle.

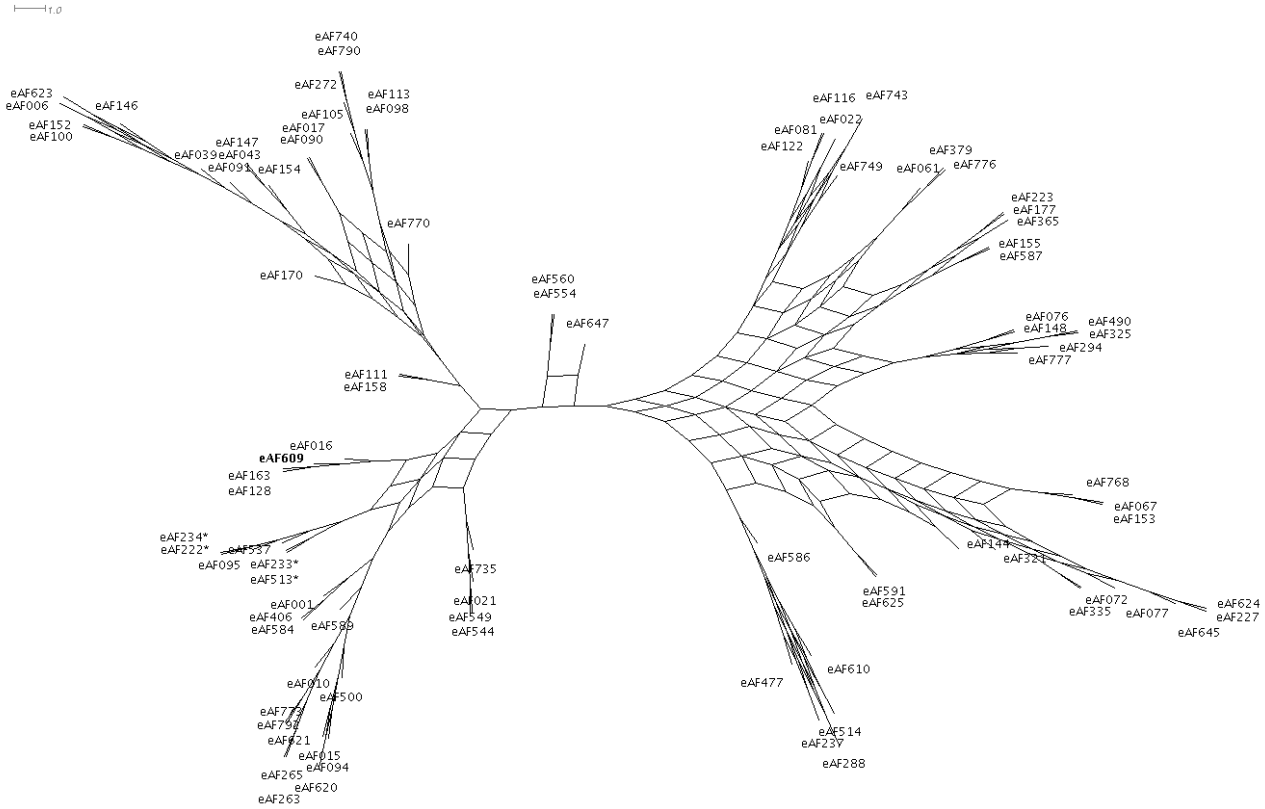

Figure 2.2 SplitsTree analysis of genetic relatedness Environmental isolates of *Aspergillus fumigatus* fall into four recombining populations. Scale bar represents the portion of nucleotide sites at which two sequences that were being compared were different. Cyp51A resistant isolates are marked (*) and clusters with eAF609 (in bold) which is shown to be near isogenic with Af293.

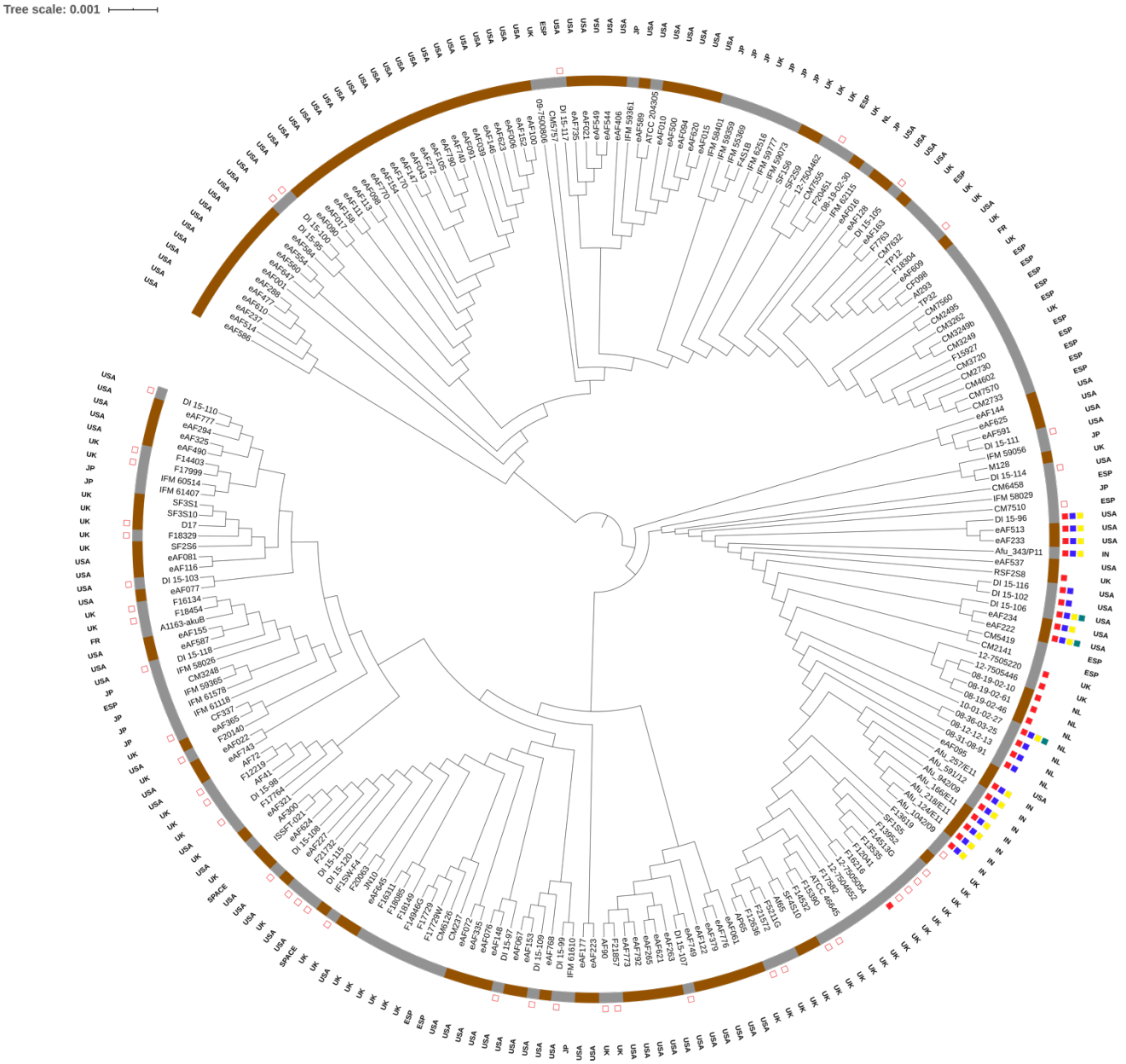

Figure 2.3 Relationship between environmental and clinical isolates Cladogram of unrooted NJ tree representing the genetic relations of clinical resistant isolates (grey bars) and environmental isolates (brown bars) in this study. Azole resistant isolates with cyp51A mutations cluster together (solid red square). Azole resistant isolates of unknown mechanism are distributed across the tree (open red square). Isolates with mutations in genes associated with resistance to agricultural fungicides benzimidazole, QoI, and SDHI (blue, yellow, and teal solid squares) also correlate with azole resistant isolates with cyp51A mutations. County of isolation information is on the outer circle. Reference isolates Af293 and A1163 was included in this analysis and highlighted to give the reader a frame of reference.

Table 2.4 Mutations associated with resistance to agricultural fungicides

Isolate	Source, year isolated Location	Benomyl resistance – BenA [a]	Carboxamide resistance – SdhB [b]	QoI resistance – Cyt B [c]	Azole resistance – Cyp51A [d]
A1163	Clinical	WT	WT	WT	WT
eAF222	Environmental, 2018 USA, Georgia	**F219Y**	**H270Y**	V13I/I119V/ **G143A**	**TR$_{46}$/Y121F/ T289A**
eAF233	Environmental, 2018 USA, Georgia	**F219Y**	WT	V13I/I119V/ **G143A**	**TR$_{46}$/Y121F/ T289A**
eAF234	Environmental, 2018 USA, Georgia	**F219Y**	WT	V13I/I119V/ **G143A**	**TR$_{46}$/Y121F/ T289A**
eAF513	Environmental, 2018 USA, Georgia	**F219Y**	WT	V13I/I119V/ **G143A**	**TR$_{46}$/Y121F/ T289A**
08-12-12-13	Clinical, 2003 Netherlands, Nijmegen	**F219Y**	WT	V13I/I119V	**TR$_{34}$/L98H/** S297T/F495I
08-19-02-10	Environmental, 2008 Netherlands, Nijmegen	WT	WT	WT	**TR$_{34}$/L98H**
08-19-02-46	Environmental, 2008 Netherlands, Nijmegen	WT	WT	WT	**TR$_{34}$/L98H**
08-19-02-61	Environmental, 2008 Netherlands, Berghem	WT	WT	WT	**TR$_{34}$/L98H**
08-31-08-91	Clinical, 2004 Netherlands, Nijmegen	**F219Y**	WT	V13I/I119V	**TR$_{34}$/L98H**
08-36-03-25	Clinical, 2005 Netherlands, Nijmegen	**F219Y**	WT	V13I/I119V	**TR$_{34}$/L98H/** S297T/F495I
10-01-02-27	Clinical, 2010 Netherlands, Nijmegen	**F219Y**	**H270Y**	V13I/I119V/ **G143A**	**TR$_{34}$/L98H**
12-7505220	Clinical, 2012 UK, Leeds	WT	WT	WT	**TR$_{34}$/L98H**
12-7505446	Clinical, 2012 UK, Leeds	WT	WT	WT	**TR$_{34}$/L98H**
F16216	Clinical, 2007 UK, Manchester	WT	WT	WT	**TR$_{34}$/L98H**
RSF2S8	Environmental, 2011 UK, Manchester	WT	WT	WT	**TR$_{34}$/L98H**
Afu 942/09	Clinical, 2009 India, Delhi	**F219Y**	WT	V13I/I119V/ **G143A**	**TR$_{34}$/L98H**
Afu 1042/09	Clinical, 2009 India, Delhi	**F219Y**	WT	V13I/I119V/ **G143A**	**TR$_{34}$/L98H**
Afu 124/E11	Environmental, 2011 India, Delhi	**F219Y**	WT	V13I/I119V/ **G143A**	**TR$_{34}$/L98H**
Afu 166/E11	Environmental, 2011 India, Bihar	**F219Y**	WT	V13I/I119V/ **G143A**	**TR$_{34}$/L98H**
Afu 218/E11	Environmental, 2011 India, Delhi	**F219Y**	WT	V13I/I119V/ **G143A**	**TR$_{34}$/L98H**
Afu 257/E11	Environmental, 2011 India, Bihar	**F219Y**	WT	V13I/I119V/ **G143A**	**TR$_{34}$/L98H**
Afu 343/P11	Clinical, 2011 India, Delhi	**F219Y**	WT	V13I/I119V/ **G143A**	**TR$_{34}$/L98H**
Afu 591/12	Clinical, 2012 India, Delhi	**F219Y**	WT	V13I/I119V/ **G143A**	**TR$_{34}$/L98H**
DI 15-96	Clinical, 2008 USA, Arizona	**F219Y**	WT	V13I/I119V/ **G143A**	**TR$_{46}$/Y121F/ T289A**
DI 15-102	Clinical, 2010 USA, Pennsylvania	**F219Y**	WT	V13I/I119V	**TR$_{34}$/L98H**
DI 15-106	Clinical, 2012 USA, Reference Lab	**F219Y**	**H270Y**	V13I/I119V/ **G143A**	**TR$_{46}$/Y121F/ T289A**
DI 15-116	Clinical, 2014 USA, Pennsylvania	**F219Y**	WT	V13I/I119V	**TR$_{34}$/L98H**

[a] BenA protein GenBank accession number EDP56324 was used as reference. [b] SdhB protein GenBank accession number EDP51777 was used as reference. [c] Cytochrome B protein GenBank accession number YP_005353050 was used as reference. [d] Cyp51A protein GenBank accession number EDP50065 was used as reference.

Figure 2.4 Agricultural fungicide resistance drug assay

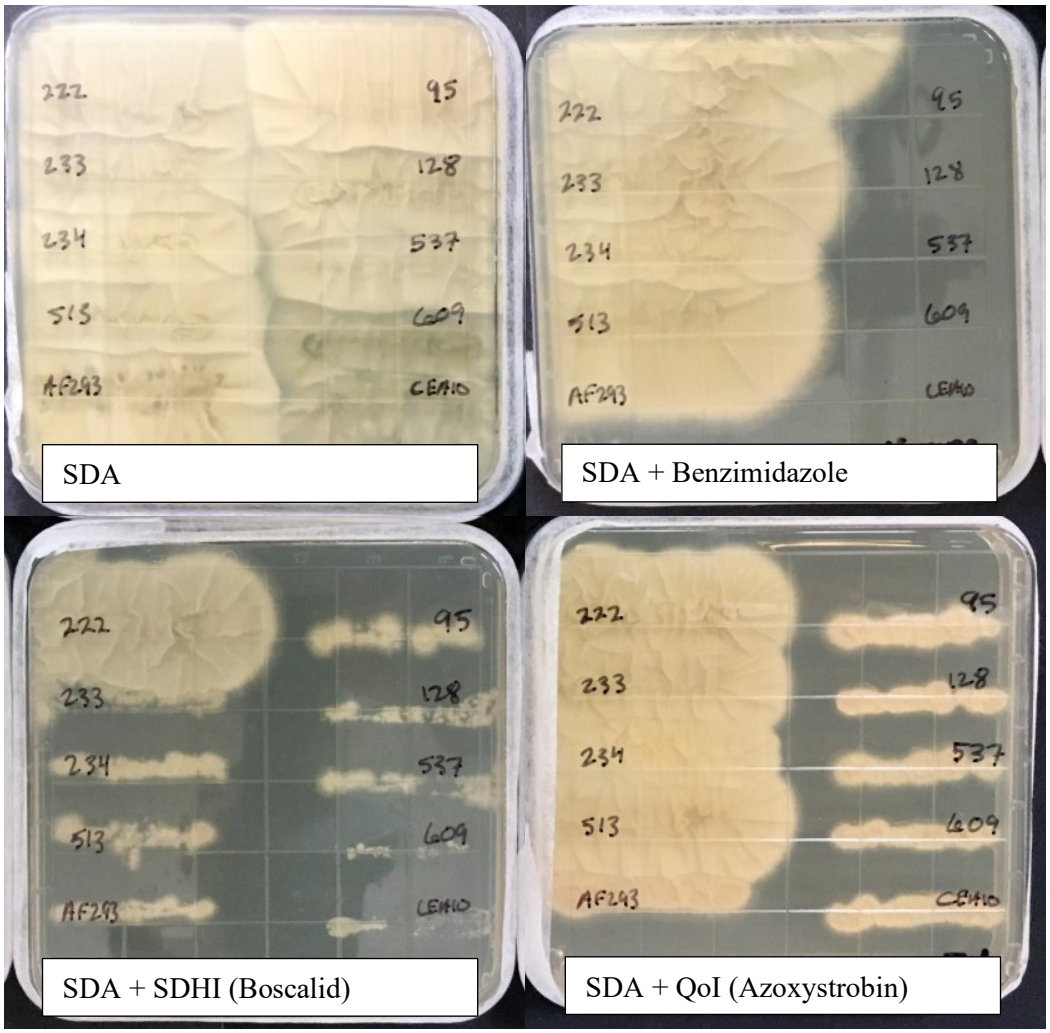

Figure 2.4 Agricultural fungicide resistance assay against benazimidazole, SDHI, and QoI was performed by streaking out a dilution of conidia of environmental isolates eAF222, eAF233, eAF234, and eAF513 containing mutations in cyp51A, benA, sdhB, and/or cytB onto SDA supplemented with drug plates. Negative control included genetically related isolates with no known mutations in cyp51A, benA, sdhB, or cytB along with reference isolates Af293 and CEA10/A1163.

References

1. Bongomin, F., Gago, S., Oladele, R.O. & Denning, D.W. Global and Multi-National Prevalence of Fungal Diseases-Estimate Precision. *J Fungi (Basel)* **3**, (2017).
2. Brown, G.D.*, et al.* Hidden killers: human fungal infections. *Sci Transl Med* **4**, 165rv13 (2012).
3. Patterson, T.F.*, et al.* Executive Summary: Practice Guidelines for the Diagnosis and Management of Aspergillosis: 2016 Update by the Infectious Diseases Society of America. *Clin Infect Dis* **63**, 433-42 (2016).
4. Verweij, P.E., Chowdhary, A., Melchers, W.J. & Meis, J.F. Azole Resistance in Aspergillus fumigatus: Can We Retain the Clinical Use of Mold-Active Antifungal Azoles? *Clin Infect Dis* **62**, 362-8 (2016).
5. Wiederhold, N.P.*, et al.* First Detection of TR34 L98H and TR46 Y121F T289A Cyp51 Mutations in Aspergillus fumigatus Isolates in the United States. *J Clin Microbiol* **54**, 168-71 (2016).
6. Vazquez, J.A. & Manavathu, E.K. Molecular Characterization of a Voriconazole-Resistant, Posaconazole-Susceptible Aspergillus fumigatus Isolate in a Lung Transplant Recipient in the United States. *Antimicrob Agents Chemother* **60**, 1129-33 (2016).
7. Hurst, S.F.*, et al.* Isolation of azole-resistant Aspergillus fumigatus from the environment in the south-eastern USA. *J Antimicrob Chemother* **72**, 2443-2446 (2017).
8. Pitkin, J.W., Panaccione, D.G. & Walton, J.D. A putative cyclic peptide efflux pump encoded by the TOXA gene of the plant-pathogenic fungus Cochliobolus carbonum. *Microbiology* **142 (Pt 6)**, 1557-65 (1996).
9. Momany, M., Westfall, P.J. & Abramowsky, G. Aspergillus nidulans swo mutants show defects in polarity establishment, polarity maintenance and hyphal morphogenesis. *Genetics* **151**, 557-567 (1999).

10. Nguyen, L.T., Schmidt, H.A., von Haeseler, A. & Minh, B.Q. IQ-TREE: a fast and effective stochastic algorithm for estimating maximum-likelihood phylogenies. *Mol Biol Evol* **32**, 268-74 (2015).

11. Hoang, D.T.*, et al.* UFBoot2: Improving the Ultrafast Bootstrap Approximation. *Mol Biol Evol* **35**, 518-522 (2018).

12. Huson, D.H. & Bryant, D. Application of phylogenetic networks in evolutionary studies. *Mol Biol Evol* **23**, 254-67 (2006).

13. Nurk, S.*, et al.* Assembling single-cell genomes and mini-metagenomes from chimeric MDA products. *J Comput Biol* **20**, 714-37 (2013).

14. van der Linden, J.W.*, et al.* Aspergillosis due to voriconazole highly resistant Aspergillus fumigatus and recovery of genetically related resistant isolates from domiciles. *Clin Infect Dis* **57**, 513-20 (2013).

15. Buil, J.B.*, et al.* Trends in Azole Resistance in Aspergillus fumigatus, the Netherlands, 1994-2016. *Emerg Infect Dis* **25**, 176-178 (2019).

16. Lucas, J.A., Hawkins, N.J. & Fraaije, B.A. The evolution of fungicide resistance. *Adv Appl Microbiol* **90**, 29-92 (2015).

17. Mair, W.*, et al.* Proposal for a unified nomenclature for target-site mutations associated with resistance to fungicides. *Pest Manag Sci* **72**, 1449-59 (2016).

CHAPTER 3

SPORULATION ENVIRONMENT DRIVES PHENOTYPIC VARIATION IN THE PATHOGEN *ASPERGILLUS FUMIGATUS*[1]

[1] Kang, S.E., Momany, M. Submitted to *BioRxiv*. doi: https://doi.org/10.1101/797076

Abstract

Aspergillus fumigatus causes more than 300,000 life-threatening infections annually and is widespread across varied environments with a single colony producing thousands of conidia, genetically-identical dormant spores. Conidia are easily wind-dispersed to new environments where they can germinate and, if inhaled by susceptible hosts, cause disease. Using high-throughput, single-cell analysis we show that germination phenotypes vary among genetically-identical individuals and that the environment of spore production determines the degree of germination heterogeneity.

Introduction

Fungal diseases kill over 1.5 million people each year[1, 2]. Rather than spreading patient-to-patient, fungal diseases are acquired from the environment or normal flora. Nine of the ten most common agents of fungal disease can be spread via spores[2, 3]. Breaking dormancy, or germinating, is arguably the most important step in pathogenesis for these fungi. Historically studies have focused on the germination environment, addressing factors such as temperature, inoculum density, carbon source, nitrogen source, and pH[4-8]. However, despite the wide range of environments in which fungal spores are produced and their importance as disease agents, the impact of sporulation environment on germination has been largely ignored. We hypothesized that exposure to specific stresses during sporulation might lead to better germination in the same or related conditions. To test this hypothesis, we performed single-cell analysis experiments in which *A. fumigatus* was sporulated under nine environmentally- and medically-relevant conditions[9-12] and the resulting conidia were transferred to all nine conditions for germination (Table 3.1). To avoid induction or selection of mutations during sporulation, we did not use serial passaging; rather, identical aliquots of inoculum were incubated for 72 h on nine types of solid medium for production of conidia and identical aliquots of conidia from each condition were transferred directly to nine types of liquid medium for germination (Figure 3.1).

Materials and Methods

Fungal strains, cultivation and preparation of conidia *Aspergillus fumigatus* CEA10 was cultivated on 1.5% agar solid complete media (CM) or minimal media (MM) as previously described[20] with modifications as described in Table 3.1. For conidial stock preparation, conidia were produced on complete media, harvested in sterile water, and $1x10^6$ conidia in 500 µl of ddH2O was plated in a homogenous layer on 25ml of solid 1% glucose *Aspergillus* minimal media with modifications described in Table 3.1 in 90mm plates in 3 technical replicates. Plates were incubated in the dark, stored upside down at 37°C or 50°C for 72hrs. *A. fumigatus* conidia from 3 plates were harvested by overlaying plates with 25ml sterile ddH2O, combining conidia and filtering through 22-25 µm Miracloth (MilliporeSigma, St. Louis, MO, USA). Conidia were washed twice in ddH2O and counted using a hemocytometer.

Germination assay Conidia from 3 plates were pooled and identical aliquots of 3-5 x 10^5 C/ml were added to liquid germination conditions described in Table 3.1[7]. Cultures were incubated for 6hrs at 37C or 50°C @ 250 rpm in dark, then fixed with 2.5% formaldehyde. 81 conditions were analyzed in total. Controls included conidia fixed at 0hr in liquid germination conditions.

Analysis of germination / Flow cytometry Flow cytometry was performed at the Center for Tropical and Emerging Global Diseases Cytometry Shared Resource Laboratory at the University of Georgia on a CyAn ADP using Summit, version 4.3 (Beckman Coulter, Fullerton, CA, USA). Between 20,000 – 25,0000 events (cells) were analyzed in four replicates for each fixed pre- and post- germination sample. Due to the sensitivity of flow cytometry and small particulates in the germinated samples, forward scatter and side scatter values smaller than fixed ungerminated conidia were filtered from the analysis. FlowJo flow cytometry analysis software, version 10 (Tree Star, Ashland, OR, USA) was used for analysis and histogram. Histogram represents the linear scaled forward scatter data to better visualize the variation in germination. Morphologies were verified using Amnis ImageStream (Amnis MerckMillipore Sigma, Seattle, WA, USA).

Viability assay - Live / dead staining For viability assays, two replicates of unfixed cells (conidia and germlings) were co-stained with 10 ug/ml fluorescein diacetate (FDA) and 2 ug/ml propidium iodine (PI) for 5 minutes in the dark, then 20,000 events were analyzed immediately using flow cytometry to measure size (forward scatter) and fluorescence. Controls included unstained and fluorescein diacetate (FDA), propidium iodine (PI), and FDA+PI stained live and dead (ethanol-killed) cells.

Statistical analysis Forward scatter scaled linear or log data was combined for each condition from all replicates. Linear and log data were checked for normality using D'Agostino-Pearson test [21]. Due to nonparametric distribution, comparison between multiple groups were analyzed by Kruskal-Wallis test followed by one-sided Dunn's multiple comparison test[22] using GraphPad Prism version 8 (GraphPad Software, La Jolla, CA, USA). Robust coefficient of variance (rCV) was calculated using 100 * 1/2 (Intensity [at 84.13 percentile] – Intensity [at 15.87 percentile]) / Median using FlowJo v10 (Tree Star, Ashland, OR, USA). Pearson correlation analysis followed by a two-tailed test was performed to assess the relationship between median log forward scatter (growth) and rCV (variation) in a given germination condition using GraphPad Prism version 8 (GraphPad Software, La Jolla, CA, USA).

Results

After 6 h incubation we used flow cytometry to detect any increase in cell size, a clear indication that germination has been initiated. The entire 9 by 9 sporulation/germination swap experiment was repeated four times. We recorded forward scatter for approximately 20,000 conidia and germlings for each condition in each replicate. For each condition, data from all replicates were concatenated and analyzed as a single population (Figure 3.2, Table 3.2).

Dormant conidia produced in all sporulation environments showed very similar forward scatter profiles except for conidia produced at 50°C, in which the forward scatter peak shifted slightly to the right, suggesting a larger size. Microscopic examination showed that conidia produced at 37°C were

approximately 2-3 μm in diameter, while those produced at 50°C were approximately 1.5 times larger (Figure 3.3).

Not surprisingly, the rate at which conidia broke dormancy and grew varied depending on germination conditions. Conidia germinated in standard media containing sufficient metals (CM, MM) at optimal temperature (37°C) showed larger median forward scatter values than conidia germinated in media with metal limitation (-Zn, -Fe), at elevated temperature (50°C), or subjected to stressors (+Cu, +Fe, NaCl, H_2O_2) (Figure 3.2, Table 3.2, Table 3.3). Across all sporulation environments, conidia broke dormancy and grew more quickly in CM germination medium than in any other germination condition. Conidia germinated in 0.5M NaCl (osmotic stress) generally broke dormancy and grew more slowly than those in other germination conditions. These results are consistent with previous work showing that rich medium and non-stressful conditions during germination favor more rapid dormancy breaking and growth[13,14,15].

In addition to the expected contribution of germination conditions, the rate at which conidia broke dormancy and grew varied depending on sporulation environment. The sporulation environments that favored rapid dormancy breaking and growth were not the same as the germination conditions that favored it. As discussed above, 0.5M NaCl during germination resulted in reduced dormancy breaking and growth. In contrast, osmotic stress imposed by 0.5M NaCl during sporulation resulted in conidia that broke dormancy and grew more quickly across germination conditions. In addition to NaCl medium, sporulation on MM or +Fe medium generally improved dormancy breaking and growth when compared to conidia from all other sporulation environments. Conidia from +Cu, -Fe, and -Zn sporulation environments generally performed significantly worse when compared to conidia from MM condition (Table 3.4) suggesting that proper metal homeostasis is necessary during sporulation as well as germination. These results show for the first time that the sporulation environment impacts the ability of a medically-important fungus to break dormancy and grow across multiple germination environments.

While we predicted that forward scatter peaks might shift left or right with changes in germination or sporulation conditions, we were surprised to see striking differences in the widths and shapes of peaks depending on sporulation environment. *A. fumigatus* conidia are clonal, with each conidium in a colony containing a single genetically-identical nucleus produced by mitosis. Previous work has shown that conidia remain dormant until they are exposed to a carbon source and water[6], at which time individuals in the population synchronously break dormancy and start growth, with rough synchrony maintained through at least the first 12 hours[16]. Thus, we expected that individual conidia produced in the same sporulation environment would break dormancy and grow synchronously, giving rise to relatively narrow peaks. The observed wide peaks show that genetically-identical conidia within the same population break dormancy and grow at different rates. The dramatic leftward shift of post-germination peaks for sporulation conditions such as -Zn medium could be explained if Zn deficiency during sporulation killed conidia. However, viability assays with fluorescein diacetate and propidium iodide showed that conidia sporulated on MM and on -Zn media contained very similar, low numbers of propidium iodide stained cells and that most of the conidia that did not enlarge during germination were not dead (Table 3.5).

To better understand the range of individual variation within genetically-identical clonal populations of conidia, we compared the robust coefficient of variation (rCV, the normalized standard deviation of the median) for forward scatter of each sporulation/germination pair (Table 3.2, Table 3.4). Conidia that were produced on NaCl, +Fe, 50ºC, and MM sporulation media showed lower rCV values and narrower forward scatter peaks across germination conditions, indicating less variation among individuals in those populations. Conidia from -Zn, -Fe, CM, +Cu, and H_2O_2 sporulation medium showed higher rCV values and wider forward scatter peaks across germination conditions, indicating more variation among individuals in those populations (Figure 3.2, Table 3.4). Taken together with median forward scatter values this shows that conidia that germinate faster tend to germinate more synchronously. Indeed, there was a negative correlation between median growth and variation in growth across most conditions (Table 3.2). The correlation between sporulation medium and variation was much

stronger than the correlation between germination medium and variation (Table 3.3, Table 3.4) consistent with the idea that the environment of sporulation drives germination variation.

Discussion

Our results show for the first time that the environment of spore production impacts the germination of *A. fumigatus* conidia and that genetically-identical conidia within a population vary in the rate of breaking dormancy and growth. That genetically-identical individuals show phenotypic variation that is increased by environmental stress suggests *A. fumigatus* might employ a bet-hedging strategy to ensure survival of progeny in varied hostile environments, including the lungs of susceptible human hosts. Previous work showed that the surface layer of dormant *A. fumigatus* conidia mask recognition by the host immune system. It is only when dormancy is broken and germination occurs that this surface layer is breached and host defenses are activated[17]. Other studies in immunosuppressed mice showed that an *A. fumigatus* isolate with slower germination survived in macrophages and was more virulent than an isolate with faster germination[18,19]. A bet-hedging strategy built on variation in germination rate could allow slow germinators within a population of *A. fumigatus* conidia to avoid the host immune system and initiate infection. It seems likely that this bet-hedging strategy would also be used by the many other fungal pathogens that produce large quantities of wind-dispersed spores.

Acknowledgments

We thank Julie Nelson at the UGA CTEGD Cytometry Shared Resource Laboratory for assistance with flow analysis, Douda Bensasson (UGA) for assistance with statistical analysis, and the UGA Department of Plant Biology and Franklin College of Arts and Sciences for funding.

Table 3.1 Sporulation and Germination Conditions

Abbreviation	Description	Medium	Temperature (ºC)
CM	Complete medium	Nutrient-rich undefined medium containing yeast extract, glucose, nitrogen, and vitamins.	37
MM	Minimal medium	Nutrient-rich defined synthetic medium containing glucose, nitrogen and vitamins.	37
50ºC	High temperature stress	MM	50
+ Cu	Copper stress	MM with 1mM CuSO4	37
+ Fe	Excessive iron stress	MM with 10mM FeSO4	37
- Fe	Iron limiting stress	MM without FeSO4	37
NaCl	Osmotic or salt stress	MM with 0.5M NaCl	37
H_2O_2	Reactive oxygen species (ROS) stress	MM with 2mM H2O2	37
- Zn	Zinc limiting stress	MM without ZnSO4	37

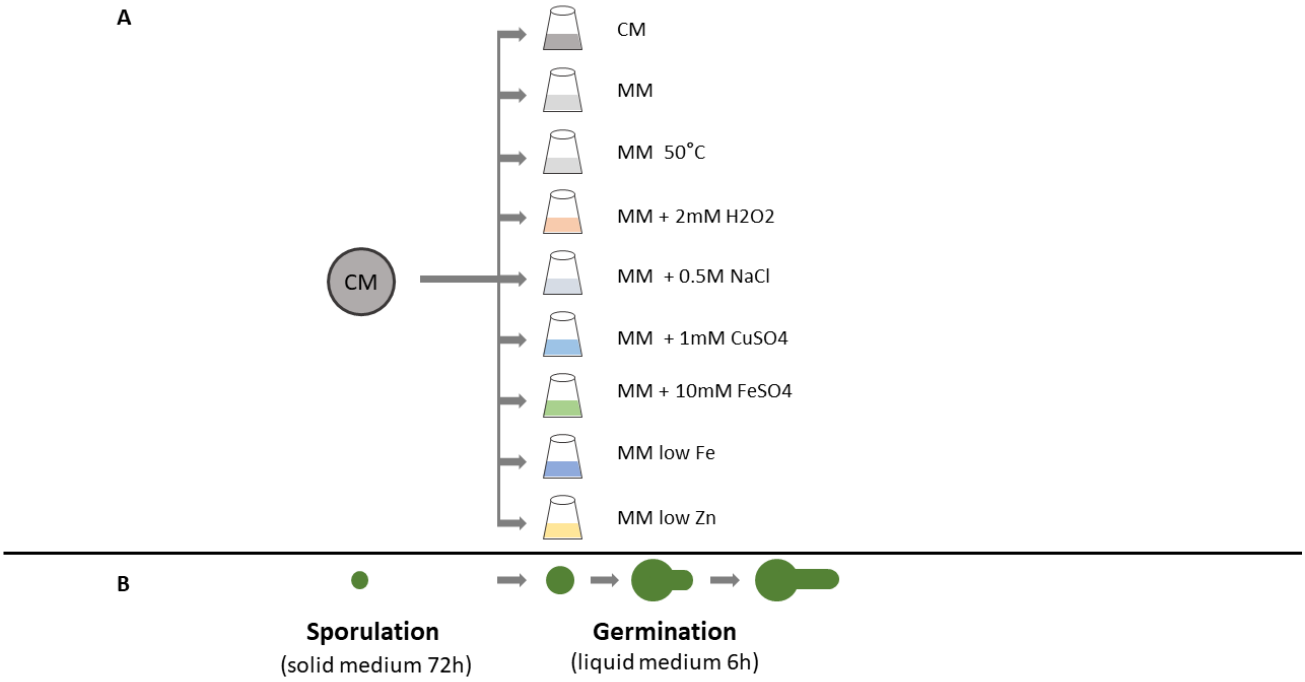

Figure 3.1 Sporulation/Germination swap assay. (A) Conidia isolated from a single sporulation condition on solid medium (CM, indicted by circle) were aliquoted into all germination conditions in liquid medium (indicated by flask shapes). The same process was repeated with conidia from each of the nine sporulation conditions being transferred to all nine germination conditions. Different colors represent different sporulation or germination conditions as indicated. (B) Diagram of relative conidium size and shape after sporulation, during germination, and for the first 6 h of growth. Dormant conidia are 2-3 microns in diameter. Upon exposure to carbon and water they break dormancy and begin to increase in size with swelling and germ tube emergence.

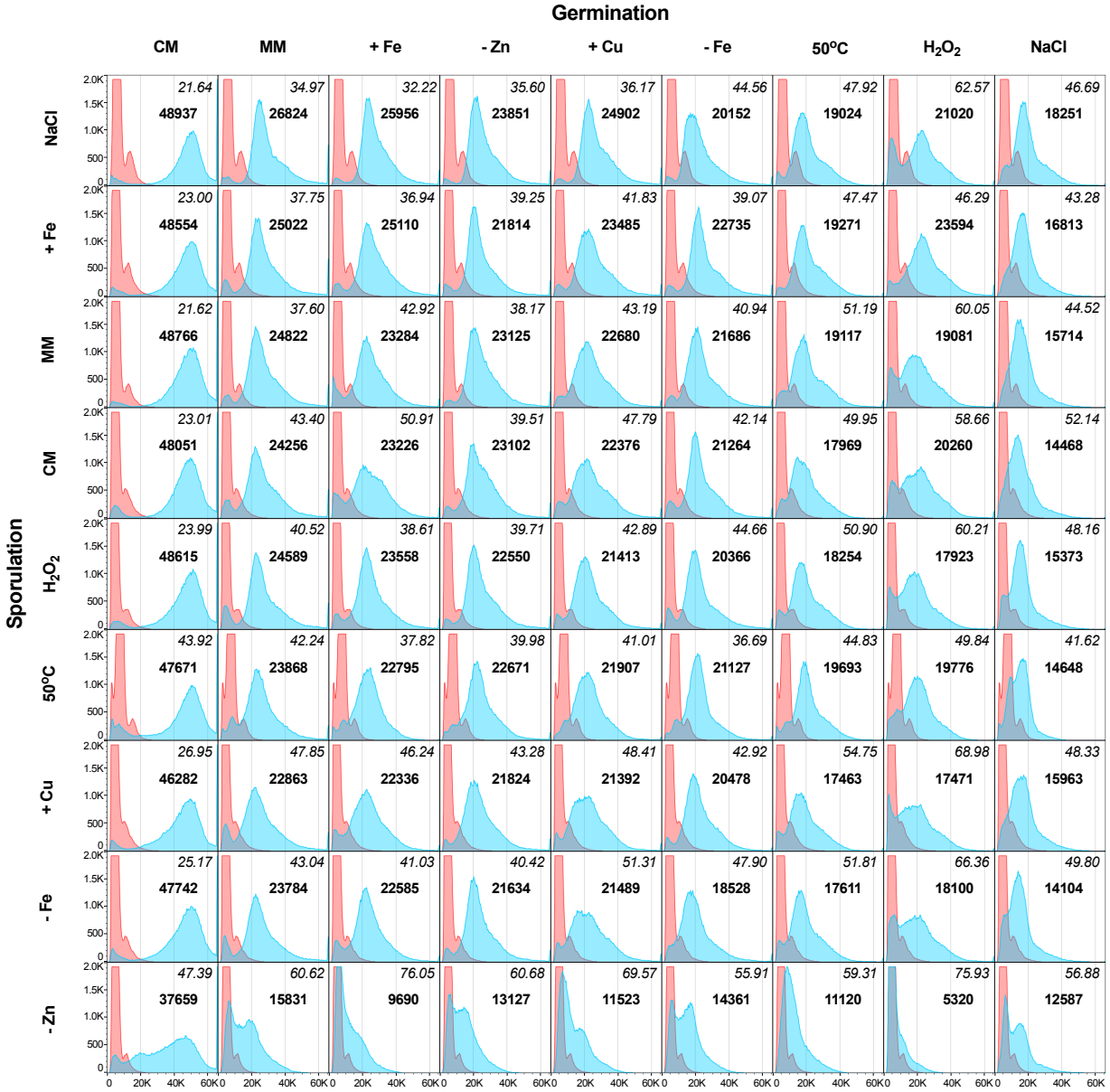

Figure 3.2 Sporulation conditions impact germination of *A. fumigatus* conidia. Conidia produced in one of nine sporulation environments were transferred to all nine conditions for germination. The X-axis shows the linear forward scatter, an indication of relative size. The Y-axis shows the number of events (cells) counted. Red peaks show forward scatter of dormant conidia from each sporulation condition measured before germination. Blue peaks show forward scatter after 6 h incubation in each germination condition. Bold values are the median of linear forward scatter values after germination. Italicized values are the robust coefficient of variation (normalized standard deviation around the median) of linear forward scatter values after germination.

Table 3.2 Statistical analysis of all sporulation/germination combinations grouped by germination condition

Condition[a]	Count[b]	Median FS log	rCV[c] FS log	Correla-tion[d]	Kruskal-Wallis test[e]	Mean rank[f]	Dunn's test mean rank difference[g]	Adjusted p value[h]
MM_CM	95144	2478.79	21.52	r = -0.76	H = 40024	459001	17078	<0.0001
NaCl_CM	78242	2486.04	21.64	$r^2 = 0.58$	$p < 0.0001$	455501	13578	<0.0001
H_2O_2_CM	96383	2469.32	24.06	$p = 0.0172$		450746	8823	<0.0001
+Fe_CM	87260	2469.32	22.89		df = 8	448703	6779	<0.0001
CM_CM	97042	2441.72	22.98		N = 838458	441923	0	0
-Fe_CM	96369	2425.30	25.15			430911	-11012	<0.0001
50ºC_CM	96476	2419.85	44.02			413821	-28102	<0.0001
+Cu_CM	92402	2350.14	27.02			402131	-39792	<0.0001
-Zn_CM	99140	1915.25	47.38			283485	-158438	<0.0001
NaCl_MM	97795	1363.85	34.91	r = -0.97	H = 73623	536218	59912	<0.0001
+Fe_MM	97356	1272.01	37.77	$r^2 = 0.95$	$p < 0.0001$	479074	2768	0.1241
MM_MM	99618	1260.63	37.61	$p < 0.0001$		476306	0	0
H_2O_2_MM	95216	1249.34	40.55		df = 8	465652	-10655	<0.0001
CM_MM	99510	1232.59	43.35		N = 879122	476306	-22296	<0.0001
-Fe_MM	90478	1207.90	42.98			441512	-34795	<0.0001
50ºC_MM	99738	1213.35	42.27			436620	-39687	<0.0001
+Cu_MM	99607	1162.60	47.85			416017	-60289	<0.0001
-Zn_MM	99804	804.03	60.56			255003	-221303	<0.0001
50ºC_50ºC	92197	1000.00	44.83	r = -0.88	H = 66136	476370	0	0
+Fe_50ºC	93361	979.97	47.46	$r^2 = 0.78$	$p < 0.0001$	475620	-750	>0.9999
NaCl_50ºC	97933	966.83	47.85	$p = 0.0017$		465563	-10807	<0.0001
MM_50ºC	98523	971.19	51.17		df = 8	465089	-11281	<0.0001
H_2O_2_50ºC	93272	926.75	50.92		N = 850884	441059	-35311	<0.0001
CM_50ºC	91169	912.60	49.92			428297	-48074	<0.0001
-Fe_50ºC	96623	895.67	51.71			422887	-53483	<0.0001
+Cu_50ºC	88024	887.65	54.69			415224	-61146	<0.0001
-Zn_50ºC	99782	564.88	59.37			247198	-229173	<0.0001
NaCl_+Cu	99651	1266.31	36.19	r = -0.95	H = 98530	556718	117224	<0.0001
+Fe_+Cu	99094	1194.40	41.89	$r^2 = 0.90$	$p < 0.0001$	503498	64005	<0.0001
MM_+Cu	99743	1152.19	43.20	$p = 0.0001$		480441	40948	<0.0001
CM_+Cu	99349	1136.75	47.76		df = 8	470876	31382	<0.0001
50ºC_+Cu	99816	1113.97	41.02		N = 893961	453197	13704	<0.0001
H_2O_2_+Cu	99627	1087.44	42.88			449469	9976	<0.0001
-Fe_+Cu	96996	1091.66	51.24			443675	4182	0.0026
+Cu_+Cu	99783	1086.76	48.48			439493	0	0
-Zn_+Cu	99902	585.57	69.49			226287	-213206	<0.0001
NaCl_+Fe	99228	1318.61	32.21	r = -0.95	H = 134734	561372	36469	<0.0001
+Fe_+Fe	98019	1274.88	37.02	$r^2 = 0.90$	$p < 0.0001$	524903	0	0
H_2O_2_+Fe	99528	1197.09	38.63	$p < 0.0001$		485785	-39118	<0.0001
MM_+Fe	99685	1183.70	42.89		df = 8	467293	-57611	<0.0001
CM_+Fe	99399	1181.04	50.89		N = 894027	461779	-63125	<0.0001
-Fe_+Fe	99426	1147.02	41.04			452230	-72673	<0.0001
50ºC_+Fe	99750	1157.38	37.79			445125	-79779	<0.0001
+Cu_+Fe	99206	1134.19	46.32			442087	-82817	<0.0001
-Zn_+Fe	99786	492.47	76.08			184738	-340165	<0.0001

+Fe_-Fe	98514	1154.78	39.07	r = -0.94	H = 69575	532146	130798	<0.0001
MM_-Fe	99623	1101.52	40.90	$r^2 = 0.88$	$p < 0.0001$	496886	95539	<0.0001
CM_-Fe	99585	1079.45	42.11	$p = 0.0002$		486759	85411	<0.0001
50ºC_-Fe	99744	1074.45	36.64		df = 8	467520	66172	<0.0001
+Cu_-Fe	99288	1041.31	42.96		N = 894698	460698	59350	<0.0001
H_2O_2_-Fe	99614	1034.30	44.61			457644	56296	<0.0001
NaCl_-Fe	99005	1023.42	44.62			457306	55958	<0.0001
-Fe_-Fe	99739	941.09	47.82			401348	0	0
-Zn_-Fe	99586	729.93	55.89			266867	-134481	<0.0001
NaCl_NaCl	96262	926.40	46.76	r = -0.61	H = 38350	521519	0	0
+Fe_NaCl	94649	854.36	43.24	$r^2 = 0.37$	$p < 0.0001$	471595	-49924	<0.0001
MM_NaCl	98676	798.63	44.48	$p = 0.0810$		439242	-82277	<0.0001
+Cu_NaCl	98386	811.30	48.34		df = 8	438109	-83410	<0.0001
H_2O_2_NaCl	95905	780.87	48.13		N = 844639	422261	-99258	<0.0001
CM_NaCl	98280	734.87	52.18			399070	-122449	<0.0001
-Fe_NaCl	98810	716.92	49.76			378681	-142838	<0.0001
50ºC_NaCl	90919	744.85	41.54			377304	-144215	<0.0001
-Zn_NaCl	72752	639.24	56.88			329666	-191853	<0.0001
+Fe_H_2O_2	98665	1199.78	46.21	r = -0.79	H = 157131	574968	126910	<0.0001
CM_H_2O_2	99912	1029.66	58.63	$r^2 = 0.63$	$p < 0.0001$	496227	48169	<0.0001
NaCl_H_2O_2	99461	1067.38	62.65	$p = 0.0107$		493134	45076	<0.0001
50ºC_H_2O_2	99781	1004.51	49.88		df = 8	488352	40294	<0.0001
MM_H_2O_2	99818	969.01	60.11		N = 895339	476862	28804	<0.0001
-Fe_H_2O_2	99275	920.17	66.37			453240	5182	<0.0001
H_2O_2_H_2O_2	99386	909.88	60.18			448058	0	0
+Cu_H_2O_2	99514	887.65	69.01			438229	-9830	<0.0001
-Zn_H_2O_2	99527	270.17	76.08			160729	-287330	<0.0001
NaCl_-Zn	99601	1210.62	35.68	r = -0.99	H = 897081	525981	310313	<0.0001
MM_-Zn	99801	1175.74	38.20	$r^2 = 0.97$	$p < 0.0001$	498613	282945	<0.0001
CM_-Zn	99818	1173.10	39.53	$p < 0.0001$		487019	271350	<0.0001
H_2O_2_-Zn	99767	1144.79	39.64		df = 8	483843	268175	<0.0001
50ºC_-Zn	99821	1152.19	40.04		N = 897081	470437	254769	<0.0001
+Fe_-Zn	98771	1108.98	39.27			456940	241272	<0.0001
+Cu_-Zn	99836	1108.98	43.28			449778	234109	<0.0001
-Fe_-Zn	99757	1099.05	40.47			449086	233418	<0.0001
-Zn_-Zn	99909	667.14	60.62			215668	0	0

[a] Sporulation_Germination denotes conidia transferred from solid medium sporulation environment into liquid medium germination conditions as described in Table 1.

[b] Number of events (cells) analyzed by flow cytometry.

[c] rCV = normalized standard deviation of the median, an indication of variance in the population.

[d] Pearson correlation analysis between median forward scatter and observed variation (rCV) within a germination group. r = correlation coefficient.

[e] The Kruskall-Wallis test determines whether there is a difference in distribution between multiple groups and is performed on ranked data. H = the Kruskall-Wallis statistic, an indication of the difference between groups; df = degrees of freedom. The p values indicate significance of differences among sporulation environments in the germination condition.

[f] Mean rank from Kruskal-Wallis test indicates which sporulation conditions tend to have the greatest values in the germination group.

[g] Dunn's multiple comparison test. Mean rank for each sporulation environment in the same germination condition was compared to the mean rank of the same sporulation and germination conditions. Dunn's test compares the difference in the sum of ranks between two samples with the expected average difference (based on the number of the groups and size).

[h] Significance: $p > 0.05$ (ns), $p \leq 0.05$ (*), $p \leq 0.01$ (**), $p \leq 0.001$ (***), $p \leq 0.0001$ (****) was determined using Dunn's test comparing the difference in the mean ranks between each sporulation condition and matching sporulation and germination conditions.

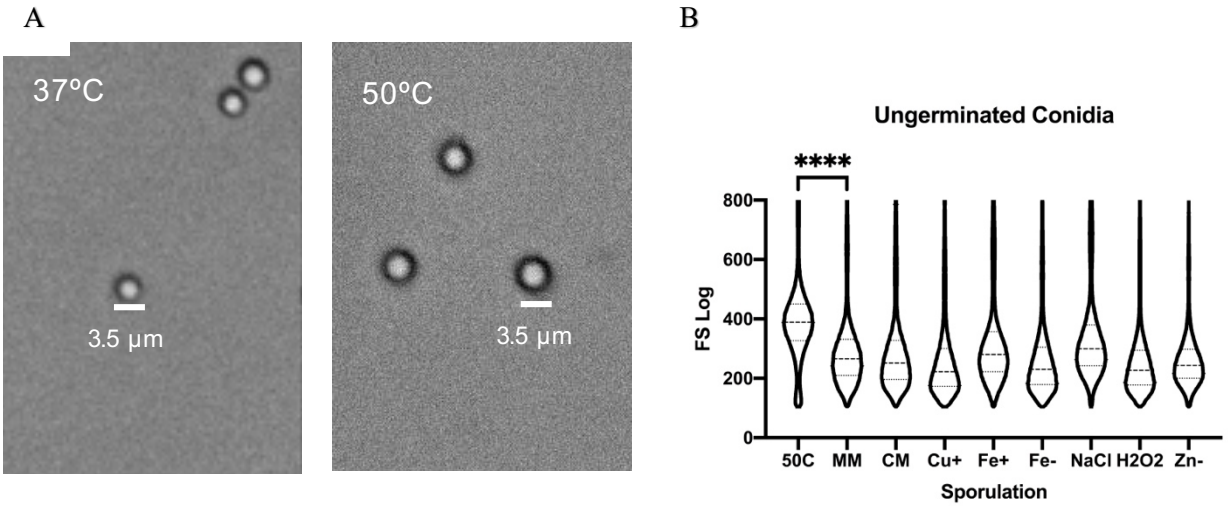

Figure 3.3 Conidia produced at 50°C are larger. (A) Light microscopy of conidia sporulated at 37°C and 50°C on minimal medium, 1,000X magnification. (B) Violin plot of forward scatter log scaled values of dormant (ungerminated) conidia from all sporulation environments. Dashed line represents median. Dotted line represents quantile at 25% and 75%. Kruskal-Wallis test followed by one-sided Dunn's multiple comparison tests. Significance: $p \leq 0.0001$ (****)

Table 3.3. Statistical analysis of germination conditions

Germ Condition[a]	Counts[b]	Median FS log	rCV[c] FS log	Correlation[d]	Kruskal-Wallis test[e]	Mean rank[f]	Dunn's test mean rank difference[g]	Adjusted p value[h]
_CM	838458	2404	28.58	r = -0.77	H = 1578766	6496947	2135891	<0.0001
_MM	879122	1213	45.10	$r^2 = 0.59$	df = 8	4361056	0	0
_+Fe	894027	1152	48.64	$p = 0.0159$	$p < 0.0001$	4049783	-311274	<0.0001
_-Zn	897081	1106	43.18			4027523	-333533	<0.0001
_+Cu	893961	1102	48.76		N = 7888209	3926138	-434873	<0.0001
_-Fe	894698	1030	44.98			3705829	-655228	<0.0001
_50°C	850884	907.8	53.52			3205174	-1155883	<0.0001
_H2O2	895339	926.4	67.61			3171735	-1189321	<0.0001
_NaCl	844639	784.4	48.86			2610009	-1751048	<0.0001

[a] _Germination denotes concatenated data of all conidia transferred from each of the nine solid medium sporulation environments into the designated liquid medium germination condition as described in Table 1.
[b] Number of events (cells) analyzed by flow cytometry.
[c] rCV = normalized standard deviation of the median, an indication of variance in the population.
[d] Pearson correlation analysis between median forward scatter and observed variation (rCV) between germination groups. r = correlation coefficient.
[e] The Kriskall-Wallis test determines whether there is a difference in distribution between multiple groups and is performed on ranked data. H = the Kruskall-Wallis statistic, an indication of the difference between groups; df = degrees of freedom. The p values indicate significance of differences between germination conditions.
[f] Mean rank from Kruskal-Wallis test indicates which germination conditions tend to have the greatest values.
[g] Dunn's multiple comparison test. Mean rank for each germination condition was compared to the mean rank of germination in MM (the base medium for all conditions). Dunn's test compares the difference in the sum of ranks between two samples with the expected average difference (based on the number of the groups and size).
[h] Significance: $p > 0.05$ (ns), $p \leq 0.05$ (*), $p \leq 0.01$ (**), $p \leq 0.001$ (***), $p \leq 0.0001$ (****) was determined using Dunn's test comparing the difference in the mean ranks between each germination condition and MM (the base medium).

Table 3.4 Statistical analysis of sporulation environments

Spor Condition[a]	Counts[b]	Median FS log	rCV[c] FS log	Correlation[d]	Kruskal-Wallis test[e]	Mean rank[f]	Dunn's test mean rank difference[g]	Adjusted p value[h]
NaCl_	867178	1207.90	50.91	r = -0.96	H = 507181	4452790	226289	<0.0001
+Fe_	865689	1186.37	52.66	$r^2 = 0.93$	df = 8	4395261	168760	<0.0001
MM_	865689	1141.87	56.42	$p < 0.0001$	$p < 0.0001$	4226501	0	0
CM_	884064	1124.04	60.77			4115234	-111266	<0.0001
H2O2_	878698	1108.98	58.51		N=7888209	4097254	-129247	<0.0001
50ºC_	878242	1096.58	54.50			3991188	-235313	<0.0001
+Cu_	876046	1074.61	59.74			3824987	-301514	<0.0001
-Fe_	877473	1062.59	62.59			3899258	-327243	<0.0001
-Zn_	870188	634.94	79.93			2387773	-1838727	<0.0001

[a] Sporulation_ denotes concatenated data of all conidia from the designated solid medium sporulation environment into each of the nine liquid medium germination conditions as described in Table 1.
[b] Number of events (cells) analyzed by flow cytometry.
[c] rCV = normalized standard deviation of the median, an indication of variance in the population.
[d] Pearson correlation analysis between median forward scatter and observed variation (rCV) between sporulation groups. r = correlation coefficient.
[e] The Kriskall-Wallis test determines whether there is a difference in distribution between multiple groups and is performed on ranked data. H = Kruskall-Wallis statistic, an indication of the difference between groups; df = degrees of freedom. The p values indicate significance of differences among sporulation environments compared to MM (the base medium).
[f] Mean rank from Kruskal-Wallis test indicates which sporulation environments tend to have the greatest values.
[g] Dunn's multiple comparison test. Mean rank for each sporulation environment compared to the mean rank of sporulation on MM (the base medium). Dunn's test compares the difference in the sum of ranks between two samples with the expected average difference (based on the number of the groups and size).
[h] Significance: $p > 0.05$ (ns), $p \leq 0.05$ (*), $p \leq 0.01$ (**), $p \leq 0.001$ (***), $p \leq 0.0001$ (****) was determined using Dunn's test comparing the difference in the mean ranks between each sporulation environment and MM (the base medium).

Table 3.5 Viability Assay[a]

Sporulation Environment	Signal in conidia that did not enlarge (%)			
	Pre-germination (Dormant)	CM germination condition	H_2O_2 germination condition	-Zn germination condition
MM sporulation	N = 43274	N = 648	N = 2665	N = 2212
FDA signal (Live)	81.75	93.85	77.75	80.30
PI signal (Dead)	3.84	8.68	8.76	5.37
-Zn sporulation	N = 43128	N = 626	N = 12525	N = 13487
FDA signal (Live)	83.90	100.00	74.55	95.30
PI signal (Dead)	1.25	12.90	3.96	1.83

[a] Conidia were produced on sporulation media, harvested and introduced to germination media for 6 h incubation exactly as described for Figure 1. Unfixed conidia and germlings were co-stained with fluorescein diacetate (FDA) and propidium iodine (PI) and fluorescence and size were analyzed immediately using flow cytometry. 20,000 events were analyzed and experiments were performed in duplicate.

References

1. Bongomin, F., Gago, S., Oladele, R.O. & Denning, D.W. Global and Multi-National Prevalence of Fungal Diseases-Estimate Precision. *J Fungi (Basel)* **3**, (2017).
2. Brown, G.D*., et al.* Hidden killers: human fungal infections. *Sci Transl Med* **4**, 165rv13 (2012).
3. Botts, M.R. & Hull, C.M. Dueling in the lung: how Cryptococcus spores race the host for survival. *Curr Opin Microbiol* **13**, 437-42 (2010).
4. Brown, W. On the germination and growth of fungi at various temperatures and in various concentrations of oxygen and of carbon dioxide. *Ann Bot-London* **36**, 257-283 (1922).
5. Loo, M. Some required events in conidial germination of Neurospora crassa. *Dev Biol* **54**, 201-13 (1976).
6. Osherov, N. & May, G.S. The molecular mechanisms of conidial germination. *Fems Microbiol Lett* **199**, 153-60 (2001).
7. Araujo, R. & Rodrigues, A.G. Variability of germinative potential among pathogenic species of Aspergillus. *J Clin Microbiol* **42**, 4335-7 (2004).
8. Wang, Z*., et al.* Metabolism and Development during Conidial Germination in Response to a Carbon-Nitrogen-Rich Synthetic or a Natural Source of Nutrition in Neurospora crassa. *MBio* **10**, (2019).
9. Errasquin, E.L., Patino, B., Fernandez, R.M. & Vazquez, C. Occurrence of Aspergillus fumigatus in a compost polluted with heavy metals. *Microbiology of Composting* 487-494 (2002).
10. Tepsic, K., Gunde-Cimerman, N. & Frisvad, J.C. Growth and mycotoxin production by Aspergillus fumigatus strains isolated from a saltern. *Fems Microbiol Lett* **157**, 9-12 (1997).
11. Haas, H. Iron - A Key Nexus in the Virulence of Aspergillus fumigatus. *Front Microbiol* **3**, 28 (2012).
12. Amich, J. & Calera, J.A. Zinc acquisition: a key aspect in Aspergillus fumigatus virulence. *Mycopathologia* **178**, 379-85 (2014).

13. Schmit J.C. & Brody, S. Biochemical genetics of Neurospora crassa conidial germination. *Bacteriological Reviews* **40**, 1-41 (1976).

14. Meletiadis, J., Meis, J.F., Mouton, J.W., Verweij, P.E. Analysis of growth characteristics of filamentous fungi in different nutrient media. *Journal of Clinical Microbiology* **39**, (2001).

15. Osherov, N., Conidial Germination in Aspergillus fumigatus, in *Aspergillus Fumigatus and Aspergillosis* (eds Latgé, J.P., Steinbach, W.J.) 131-142 (ASM Press: Washington, D.C., 2009).

16. Momany, M. & Taylor, I. Landmarks in the early duplication cycles of Aspergillus fumigatus and Aspergillus nidulans: polarity, germ tube emergence and septation. *Microbiology* **146 Pt 12**, 3279-84 (2000).

17. Aimanianda, V.*, et al.* Surface hydrophobin prevents immune recognition of airborne fungal spores. *Nature* **460**, 1117-21 (2009).

18. Amarsaikhan, N.*, et al.* Isolate-dependent growth, virulence, and cell wall composition in the human pathogen Aspergillus fumigatus. *PLoS One* **9**, e100430 (2014).

19. Rosowski, E.E.*, et al.* Macrophages inhibit Aspergillus fumigatus germination and neutrophil-mediated fungal killing. *PLoS Pathog* **14**, e1007229 (2018).

20. Momany, M., Westfall, P.J. & Abramowsky, G. Aspergillus nidulans swo mutants show defects in polarity establishment, polarity maintenance and hyphal morphogenesis. *Genetics* **151**, 557-567 (1999).

21. Dagostino, R.B., Belanger, A. & Dagostino, R.B. A Suggestion for Using Powerful and Informative Tests of Normality. *American Statistician* **44**, 316-321 (1990).

22. Dunn, O.J. Multiple Comparisons Using Rank Sums. *Technometrics* **6**, 241-252 (1964).

CHAPTER 4

CONIDIAL TRANSCRIPTOME OF *ASPERGILLUS FUMIGATUS* [1]

[1] Kang, S.E., Upadhyay, S., Lin, X., Momany, M. To be submitted to G3: Genes, Genomes, Genetics

Abstract

Conidia, asexual spores, of *Aspergillus fumigatus* are the infectious propagules which affect over 8,000,000 people globally. Regulation of proper spore formation and germination is essential for infection. In this chapter, we used RNAseq to analyze conidia exhibiting slow and fast germination phenotypes to identify genes associated with a germinating phenotype. We identified transmembrane proteins that may be important for signaling and rapid nutrient assimilation in germinating conidia. Then we compared the conidial transcriptomes to multiple hyphal developmental transcriptomes to understand the spore biology. We identified novel "master" regulators for processes important for proper spore biology. Identification of these genes involved in spore formation and germination could lead to novel drug discovery.

Introduction

Conidia are the asexual propagules of *A. fumigatus* and are abundantly produced in long chains under nutrient deficient conditions and/or exposure to oxidative stress[1]. Disturbances to the environment by rain or wind can disperse conidia over long distances[2-4]. Conidia can withstand UV, extreme temperatures and desiccation due to their highly organized rodlet layer and melanized cell wall[5, 6]. When inhaled the 2-3 um conidia are able to get deep into the lung where they can initiate germination in the presence of water and glucose. During the swelling process it releases proteins such as proteases into the environment. It is able to sense its environment and rapidly modulate its transcriptome to prepare for successful germination and growth.

As a ubiquitous saprophytic fungus that plays an essential role in recycling environmental carbon and nitrogen[6] , *A. fumigatus* is able to utilize a wide variety of carbon and nitrogen sources. Its genome encodes a high number of efflux pumps and transporters. Its genome also encodes a high number of catalases, superoxide dismutases, and glutathione transferases for the detoxification of reactive oxygen species (ROS)[7-9] that are considered important virulence mechanisms. The ability to detoxify ROS allows for survival of phagocytosis and intracellular germination which leads to lethal disruption of the host cell

and eventually infection. Recent studies have shown that survival of phagocytosis resembles that of amoeba predation[10, 11], and there is much speculation regarding the evolution of these virulence mechanisms.

Previous transcriptomics studies during early stages of germination have shown that the conidia switches from fermentative metabolism to respiratory metabolism[12, 13], dormant conidia are stress-tolerant structures due to regulation of oxidative stress adaptation[14], and conidia are full of secondary metabolite transcripts[15]. These studies have correlated with conidial proteomic studies[16-19]. While a few regulators of these processes have been identified and characterized we have yet to identify global master regulators of the conidia.

Materials and Methods

Fungal strain and growth condition *A. fumigatus* isolate CEA10 was used for this study. Isolate was stored in 20% glycerol at -80C and maintained on 1.5% agar solid complete media (CM) or minimal media (MM) as previously described[20].

Conidia preparation Fresh conidia were produced by spreading 1x10^6 conidia in 500 ul of ddH2O in a homogenous layer on 25ml of solid 1% glucose *Aspergillus* minimal media with modifications (Table 4.1) in 90mm plates in 3 technical replicates. Plates were incubated in the dark, stored upside down at 37C or 50C for 72hrs. *A. fumigatus* conidia were pooled from 3 technical replicates harvested by overlaying plates with 25ml sterile ddH2O and filtered through 22-25 um miracloth. Conidia suspensions were washed twice in ddH2O and counted using a haemocytometer.

Hyphae preparation Hyphae were produced by diluting 1x10^9 conidia in 10 ml of CM in 50 ml Falcon tubes. Cultures were incubated in the dark at 37C, shaking at 250 rpm for 8 hr and 24 hr. At respected timepoint, cultures were strained, washed twice with PBS, and snap frozen in liquid nitrogen. Conidiophore/hyphae were produced by spreading hyphae grown in CM liquid culture for 24hr onto CM plates and the entire sample was harvested at 5 hr, 9 hr, and 24 hr post hyphal transfer (ht). Samples were

washed twice with PBS and snap frozen in liquid nitrogen[21]. Diagram of hyphal development is shown in Figure 4.1.

RNA isolation, mRNA library construction and Illumina sequencing Total RNA was isolated from samples using a modified TRIzol (Thermo Fisher Scientific) protocol with RNeasy Plant Mini Kit (Qiagen, Hilden, Germany) and treated with Qiagen RNase-free DNase. Briefly, ~100 mg of samples were harvested, washed, then lyophilized in 2 ml tubes containing 0.5 mm disruption glass beads (RPI, catalog #9831). Lyophilized samples were homogenized using GeneGrinder at 1750 rpm for 30 sec, twice. 1 ml of TRIzol was added to the samples and incubated for 5 min at RT. 0.2 ml of chloroform was added to the mix and incubated for 1 min at RT. Samples were centrifuged at 15,000 *g* for 10 min at 4C to separate phases. 200 ul of top layer was added to 500 ul of βME/RLT buffer from RNeasy Plant Mini Kit and samples were processes according to manufacturer's specifications.

RNA quality (RNA Integrity Number (RIN) > 6.5) was assessed using an Agilent Bioanalyzer RNA nanochip (Agilent, Wilmington, DE, USA). Conidia sequencing libraries were prepared using KAPA Stranded mRNA-Seq Kit (Roche, Indianapolis, IN, USA), according to the manufacturer's specifications. Sequencing libraries were qPCR quantified, pooled in equimolar concentrations and analyzed on an Illumina NextSeq, producing 2 x 75-nucleotide paired-end reads at University of Georgia Genomics and Bioinformatics Core. Hyphal sequencing libraries were prepared using TruSeq Stranded mRNA Library Prep Kit (Illumina, San Diego, CA, USA), according to the manufacturer's specifications. Sequencing libraries were qPCR quantified, pooled in equimolar concentrations and analyzed on an Illumina NextSeq, producing 2 x 75-nucleotide paired-end reads at Texas A&M Genomics Core.

Transcriptome data analysis After removing low quality reads and adapter sequences, the raw reads were aligned to the reference genome A1163 (CADRE 43) using the new tuxedo suite[22]: HISAT v2.1.0 (`--dta --max-intronlen 2000 -I 100 --rna-strandness RF`). StringTie v1.3.4d was used to estimate gene abundance in FPKM (fragments per kilobase of exon and million mapped reads) and TPM (transcripts per million). Venn diagram comparison (http://bioinformatics.psb.ugent.be/webtools/Venn/) was performed using TPM values. Transcripts were

considered absent in log2 normalized TPM analysis when abundance was zero. FungiDB was used for Gene Ontology Slim term enrichment analysis with $p < 0.05$[23].

To identify genes associated with phenotypic differences in germination, we performed groupwise gene expression of conidia from 50C and zinc limiting conditions with conidia from NaCl and excessive Fe conditions. Significant DEGs were selected using Bioconductor R package Ballgown[24] by comparing FPKM values with $p \leq 0.05$, FDR ≤ 0.05, and log2fold change > 1. To identify genes enriched in the conidia, we performed groupwise gene expression of conidia from all conditions with gene expression of hyphae from different developmental states. Hierarchical clustering heatmaps were performed using the heatmap.2 function from the gplots package (R software).

microProtein annotation To identify novel regulators of germination, miPFinder[25] was used to predict microProteins for *A. fumigatus* isolate Af293using default settings. Syntenic orthologues were identified for A1163 using FungiDB.

Results

Transcriptomes were analyzed following the new Tuxedo suite pipeline. Quality control summary of RNA-seq data are shown in Table 4.1.

To get a quick overview of the conidial transcriptomes we removed genes with low expression values (TPM < 1) and compared them with one another (Table 4.2). Conidia from different sporulation environments contained varying numbers of transcripts including sporulation environment specific gene expression. We identified over 8600 different transcripts in conidia, of which approximately 7100 transcripts were shared between conidia regardless of sporulation environment (Figure 4.2a). The analysis was repeated for hyphal transcriptomes from different timepoints and we identified 9074 different transcripts in hyphae of which approximately 6900 were shared between hyphae regardless of timepoint. (Figure 4.2b) The transcripts found in both conidia and hyphae were compared with each other (Figure 4.2c). Almost 90% of genes expressed in conidia were also expressed in hyphae. Conidia of

other fungi have also been shown to contain transcripts representing 60-75% of all possible ORFS in the genome[26, 27].

Principle component analysis (PCA) of all the genes was used to visually compare the transcriptomes. PCA analysis of raw TPM+0.01 values showed there are small differences in genes expressed between conidia from different sporulation environments (Figure 4.3a) while analysis of log2 normalized TPM+0.01 values show that there is a larger difference in genes expressed between conidia and hyphae (Figure 4.3b). Interestingly, when the TPM+0.01 values were log2 normalized, conidia raised under minimal media are shown to be different from conidia raised under stress conditions which cluster together. This suggests that regardless of the stress imposed on the conidia, there are similarities in gene expression.

Differential expression (DE) was performed using Ballgown. Initially, standard pairwise comparison between each sample according to developmental stage was performed, then DE genes identified in each comparison were compared between conidia and hyphae. However, this resulted in a list of genes that was not meaningful to understanding the processes occurring in the conidia. Therefore, we decided to group the transcriptomes based on phenotype and perform DE analysis.

To identify genes differentially expressed between conidia with fast and slow germination phenotypes, conidia from NaCl and high Fe were grouped and compared to conidia from 50C and Zn limiting conditions. 7978 genes were differentially expressed between conidia with fast and slow germination phenotypes. However, using the cutoff thresholds of log2 fc > 1 and confidence values $p<0.05$ and FDR < 0.05 we identified only 379 DE genes that were significantly upregulated in conidia and 397 DE genes that were significantly downregulated in conidia with fast germination phenotype (Figure 4.4a).

GO slim analysis was performed. Enriched GO slim terms of DE genes associated with fast germination included: biological processes involved in metabolism, transmembrane transport, and oxidoreductase activity. A previous study in *Saccharomyces cerevisiae* has shown that higher gene expression of plasma membrane transporters in a population contributes to faster adaptation under

suboptimal environments[28]. Therefore, we can speculate that conidia the fast germination phenotype was due to a higher expression of a set of transmembrane transporters allowing for adaptation to a wide variety of germination environments. GO slim terms of DE genes associated with slow germinating conidia included carbohydrate metabolism for cell well organization or biogenesis, secondary metabolic process and again oxidoreductase activity (Figure 4.5a,b). This suggests that conidia with slow germinating phenotype are putting more resources towards building a cell wall, and could explain the enlarged size of conidia from 50C. Whether or not the cell wall was affected in conidia from Zn limiting condition remains to be analyzed.

Transmembrane proteins are associated with fast germination. GO slim enrichment analysis showed an enrichment of 52 transmembrane transport. Manual annotation of the transcriptome revealed that there are an additional 91 genes with transmembrane domains that are enriched in fast germinating conidia that were not part of the GO slim. The 143 transmembrane domain containing genes enriched in fast germinating conidia were filtered by genes that were also enriched in conidia (**TABLE 4.3**).

Nitrogen assimilation is essential for life and important during early germination. MepA (AFUB_0588590), an ammonium transporter shown to play a role in scavenging ammonium under nitrogen starvation conditions[29] was enriched in fast germinating conidia. During germination in an environment where nitrogen is not readily available this may be essential. There were nine putative amino acid permeases. Putative amino acid permeases AFUB_089830 (gap1 orthologue) and AFUB_046850 (can1 orthologue) has been shown to be important for virulence in *Cryptococcus neoformans*[30, 31], stress response in *Saccharomyces cerevisiae*[32-34], and conidiation in *Fusarium verticillioides*[35]. There was a putative amino acid permease, AFUB_033460, that showed 22.45 fold-increase in conidia and warrants future examination in its roles in germination and possibly virulence.

Carbon assimilation is essential for life and important during early germination. AFUB_032610, a putative succinate:fumarate antiporter (Acr1), shown to be essential for growth on ethanol or acetate[36] was enriched in fast germinating conidia. This may be important for utilizing fermentative metabolic reserves during the earliest stages of germination prior to transporting carbons from the environment into

the cell. There were six sugar transporters. Not included in the table was a putative MFS sugar transporter (AFUB_010470) which showed 67.67 fold increase in conidia compared to hyphae and a 2.38 fold-increase with $p < 0.05$ and FDR = 0.11. The role of this gene has not been studied; however, due to the high enrichment in the conidia makes me wonder about its role in germination.

Transmembrane proteins involved in signaling are important for germination and for drug targets[37]. Being able to sense and respond appropriately to the germination environment is necessary for successful growth. AFUB_013620, a putative integral membrane protein Pth11-like, was enriched in fast germinating conidia. In *Neurospora crassa* Pth11-like proteins are a class of seven transmembrane domain G protein coupled receptors shown to play a role in asexual development and hyphal growth as well as response to oxidative stress, antifungals, and nutrients[38]. In addition to AFUB_031620, AFUB_099510, a specific seven transmembrane protein integral membrane protein, was found to be always highly upregulated in conidia regardless of sporulation condition or isolate genotype. The role of these transmembrane proteins as signaling or adhesion related proteins should be investigated[39].

Interestingly, in the list of transmembrane proteins enriched in both conidia and fast germinating conidia were erg4A (AFUB_062080) shown to be necessary for conidiation and resistance to oxidative stress and cell wall perturbing agents[40] and atrF (AFUB_093930) an ABC drug exporter shown to be upregulated in the presence of azoles[41-43]. These genes have been studied extensively for their role in azole resistance; however, their role in normal biological function has yet to be fully realized.

A set of 35 transmembrane proteins were upregulated in conidia and in slow germinating conidia (Table 4.4). There were 12 uncharacterized proteins. AFUB_073200 and AFUB_086860 syntenic orthologues of were not identified in Af293. AFUB_059070, AFUB_05810, and AFUB_057800 were always enriched in conidia regardless of sporulation condition and were also enriched in conidia of isolates from Ireland[15] therefore proper regulation of these genes may be significant in conidia.

Zinc homeostasis has been shown to be important for virulence[44] and may also be important for germination. Two zinc ion transporters, zrfA (AFUB_079250) and AFUB_024650, were upregulated in conidia with the slow germination phenotype. ZrfA was induced under zinc limiting conditions[45].

Conidia enriched AFUB_024650 has not been reported to be involved in zinc ion accumulation in hyphae, and may play a role in zinc accumulation during early stages of germination. The differential expression of these genes was primarily driven by the expression level in conidia from zinc limiting conditions.

Signaling molecules that may regulate germination. AFUB_087610, a calcium-transporting ATPase, has been previously characterized as being an essential gene in *A. fumigatus*[46]. Its orthologue has been shown to play a role in oxidative stress response and conidiation in *Beauveria bassiana*[47]. AFUB_052070, plasma membrane ATPase, is an orthologue of *S. cerevisiae* PMA1 which has been shown to be regulated by glucose levels and play a role in environmental sensing[48, 49]. In addition, there was a transmembrane bound transcription factor AFUB_074510 that may regulate expression of several genes in response to the germination environment. Transmembrane bound transcription factors remain inactivated until activated by an external or internal stimuli[50].

Due to the extreme stressful conditions under which slow germinating conidia were raised we can speculate that these genes may be necessary for rapid compensation of elements lacking in the conidia necessary for germination and growth and/or for either ensuring that the germination environment is properly suited for survival. To study the effects of these transmembrane proteins, overexpressing them and measuring changes in germination may be more interesting than generating null mutants.

To identify genes differentially expressed between conidia and hyphae, conidia from all conditions were grouped and compared to hyphae of all developmental stages. 6529 genes were differentially expressed between conidia and hyphae. We used a cutoff threshold of log2 fc > 1 and confidence values $p<0.05$ and FDR < 0.05. We identified 2182 differentially expressed genes that were significantly upregulated in the conidia and 2251 DE genes that were significantly downregulated in the conidia (**Figure 4.4b**).

Enriched GO slim terms of DE genes upregulated in conidia included: autophagy, catabolic process, response to stress, signal transduction, DNA binding, ion binding and organelles. These results are similar to what had been previously observed in conidia of *Aspergillus* spp.[13, 14, 51] Whereas, GO slim

terms of DE genes downregulated in conidia included: translation, metabolic processes, cell cycle, cytoskeleton organizations, etc (**Figure 4.6a,b**). These processes are expected in cells that are actively growing.

Transcription factors (TF) are upregulated in conidia. Since transcription factors can regulate multiple genes they are considered "master regulators" and indicators of potential processes they regulate. Go Slim analysis showed that 149/326 TFs were upregulated in conidia. Manual annotation using data from FungiDB, UniProt, and CIS-BP database[52] resulted in 487 potential transcription factors, 210 of which were upregulated in conidia (**Table 4.5)**. We used a generous cut off of log2fc > 1, $p < 0.05$ and FDR < 0.05 to examine as many differentially expressed transcription factors since small changes in expression level can cause huge changes.

Transcription factors involved in carbon and nitrogen metabolism were highly upregulated in conidia. As previously described in *Aspergillus* spp*,* conidia are undergoing fermentative metabolism[16, 53]. Indeed, alcR (AFUB_055060) an ethanol response TF was 17.62 upregulated in conidia. Transcripts of three alcohol dehydrogenases were either abundantly present or enriched in the conidia: alcC (AFUB_053780), AFUB_052430, and AFUB_090070. In addition, aldehyde dehydrogenases necessary for ethanol metabolism were also enriched in conidia: aldA (AFUB_077440) and AFUB_070420.

The FacB (AFUB_013000) transcription factor involved in acetate metabolism, gluconeogenesis and glyoxylate cycle was 6.58 upregulated in conidia. Genes involved in acetate metabolism were abundant or enriched in conidia: facA (AFUB_068120) acetyl-coenzyme A synthetase role in acetate metabolism and sulfur compound metabolic process, acuD (AFUB_070430 and AFUB_095430) an isocitrate lyase, acuE (AFUB_094750) malate synthase, and acuF (AFUB_073680) a phophoenolpyruvate carboxykinase which is induced only when acetate is present[54]. AcuF is also regulated by acuK (AFUB_022860) a transcriptional activator of gluconeogenesis and iron acquisition[55]. AcuK was 4.39 upregulated in conidia.

FacB also regulates fatty acid metabolism to use fatty acids as sole carbon source[56]. Indeed, we observed a slight increase in transcription factors induced by the presence of long-chain fatty acids: FarA

(AFUB_099050) was enriched by 1.51 and farB1 (AFUB_0883430) was enriched by 3.61. *A. fumigatus* does not have a known homologue of yeast gene that is induced by the presence of short-chain fatty acids. However, there was a 2.79 enrichment of a putative C6 transcription factor AFUB_084620 which is predicted to play a role in short-chain fatty acid catabolic process. Fatty acid metabolism occurs in peroxisomes, and indeed there was 8.19 enrichment of a putative peroxisome proliferation transcriptional regulator AFUB_048940 in addition to downstream peroxisome proteins (Figure 4.7).

In addition to transcription factors regulating active carbon metabolism, conidia are upregulated in transcription factors involved in cellulose degradation clrB (AFUB_087890) and pectin metabolism pathway gaaR (AFUB_06540). To the best of our knowledge, neither cellulose nor pectin was present in the sporulation media. As a saprophytic fungus, we suspect *A. fumigatus* is anticipating germinating on decaying plant matter. Being able to utilize a wide range of substrates is what allows *A. fumigatus* to be such a ubiquitous fungus. Conidia were also enriched for transcription factors involved in utilization of a range of sugars: arabinose metabolism araR (AFUB_001990), xylose metabolism xlnR (AFUB_031270), and galactose metabolism galX (AFUB_010420).

Nitrogen metabolism is important for cell growth. Genes involved in Autophagy were GO Slim enriched in conidia. Autophagy is trigged by nutrient starvation and a way to recycle nitrogen (Figure 4.8). Regulators of nitrate reductase metabolism area (AFUB_096370) and nirA (AFUB_059600) were both upregulated in the conidia. Yet conventional pathway of nitrate assimilation by crnA permease, niaD (AFUB_012300) nitrate reductase, niiA (AFUB_012310) nitrite reductase and reactive nitrogen intermediate detoxification gene fhbA (AFUB_099700) were down regulated in conidia. Instead putative nitrate reductases (AFUB_034030, AFUB_034030) and putative nitrite reductase (AFUB_058010) all showing conidia specific gene expression were highly up regulated. Additionally, nitric oxide detoxification genes fhbB (AFUB_081400) and gnoA (AFUB_018120) previously shown to be part of the conidial proteome were upregulated in the conidia[16]. FhbB expression has previously been shown not to be induced in hyphae and gnoA was shown to be involved in detoxifying reactive nitrogen intermediates during initiation of germination[57].

KEGG analysis of the nitrogen metabolism pathway showed that conidia were enriched in carbonic anhydrases cafC (AFUB_066550) which converts CO2 to HCO_3^- (Figure 4.9). HCO_3^- is important for maintaining cellular pH homeostasis. CafC transcription could only be induced by levels of CO2 much higher than that of atmospheric gases[58] which suggests that there is a buildup of CO2 in conidia. Which supports that conidia are undergoing respiration under oxygen limiting conditions and there is a lack of gas exchange. It is interesting that note that cafC homologe cafA (AFUB_068280) was downregulated in conidia whereas in hyphae it was highly expressed and previously shown to be induced by high levels of CO2[58].

Transcription factors involved in stress response were highly upregulated in conidia. The top differentially expressed TF was srbC (AFUB_016450), a putative sterol regulatory element binding protein family (SREBP). Members of this family SrbA and SrbB have been well studied for their role in hypoxia response[59]. They also play a role in ergosterol biosynthesis, azole tolerance, iron acquisition, ethanol fermentation and nitrate assimilation[60, 61]. However, srbC had not been characterized[59] due to its low expression in hyphae (personal communications with Robert Cramer). However, abundant expression of srbC in conidia may suggest a conidia specific regulation of genes in sterol synthesis, iron regulation, metabolism, and/or stress response.

Next on the list was AFUB_087240, a putative C2H2 transcription factor. Orthologs of this in other fungal species has been annotated as “early growth response protein”; however, annotation indicates potential homology to *Sacharomyces cerevisiae* alcohol dehydrogenase II synthesis regulator, ADR1. Therefore, could play a role in regulating fermentative metabolism in conidia. To further predict the possible function of this gene, web base network analysis STRING was used[62]. Analysis showed that AFUB_087240 was coexpressed with transcription factors rum1 (AFUB_051950) and putative sin3 (AFUB_051950). Rum1 has been shown to be involved in the negative regulation of conidiation through abaA and brlA and aflatoxin biosynthesis in *A. flavus*[63]. Rum1 was 3.27 fold upregulated in conidia and abaA and brlA expression were downregulated in conidia. Sin3 plays a role in both activating and repressing genes involved in carbohydrate metabolism, heat stress, and osmotic stress[64]. AFUB_087240

has yet to be characterize; however, coexpression with rum1 and sin3 suggests that this gene may be involved in regulating genes involved in both metabolism and stress response.

Reactive oxygen species are generated by carbon and nitrogen metabolism during conidial maturation[65, 66]. Oxidative stress response bZIP Atf transcription factors were upregulated in conidia. A putative A1163 specific orthologue of atfA (AFUB_044290) was highly upregulated in conidia. AtfA (AFUB_037850) was abundantly expressed in the conidia and been previously shown to be essential for conidial viability under heat and oxidative stress in *A. fumigatus*[14]. Expression of atfA was induced during conidiophore development and continued to increase in conidia. Both atfB and atfC were among the top ten differentially expressed TF in conidia. AtfB has been shown to participate in a regulatory network that induces aflatoxin biosynthesis as part of the cellular response to oxidative stress in *A. parasiticus*[67]. AtfB was shown to regulate both yap1 and skn7 in *A. parasiticus.* Indeed both transcription factors were upregulated in conidia. Interestingly atfD was upregulated only in conidia from zinc limiting conditions. The differential coexpression and regulation of orthologues of AtfA is interesting. Identification of the regulator of orthologues of AtfA could lead to severe susceptibility to oxidative stress in conidia.

As mentioned above, skn7 aka srrA was upregulated in conidia. Skn7 is a HSF domain containing transcription factor. Analysis of this family of TFs showed that all HSF domain containing TFs were upregulated in conidia. Heat shock transcription factor hsf1 and a third HSF domain containing TF AFUB_098510 were upregulated in conidia. As their name indicates, heat shock proteins are induced by heat shock; however, they have also been found to be induced during osmotic stress, oxidative stress, and during hypoxia.

CP2 or grainy head family of TFs were upregulated in conidia. Grainy head TFs has been shown to be important in development in fungi and animals[68-70]. In *N. crassa* grainy head mutants displayed defects in conidial separation. Grainy head TF was shown to regulate processes involved in: nitrogen, sulfur and selenium metabolism; membrane transport and cellular import; metabolism of aromatic groups; carbohydrate transport; metabolism of amino acids; and disease, virulence, and defense related genes[70].

The conidial separation defect phenotype resembled that of *A. fumigatus* exoß(1-3)glucanase GH55 mutant *Δexg5,6,7,8,9,10*. GH55 mutants showed defects in conidial wall formation, maturation, and separation. Furthermore, germination was delayed regardless of media[71].

While we expect conidia to experience osmotic stress during maturation and desiccation, conidia from this study were analyzed within 48hrs of sporogenesis and based on ultrastructural characterization of *A. fumigatus* conidia, we can assume that conidia are in an early stage of maturation and have yet to undergo desiccation. Combined with expression of Atf transcription factors we can assume reactive oxygen species are accumulating within conidia. Detoxification of reactive oxygen species is carried out by catalases, superoxide dismutases, glutathione reductases, and antioxidants[72-75].

Important conidial processes may be regulated by microProteins (miPs). In addition to transcription factors, a set of microProtein (miP) predicted using miPFinder[25] (Table 4.6) were upregulated in conidia, and, if translated, would allow for additional regulation of the processes above. A miP is generally a small protein with no catalytic activity that is able to bind to a larger protein of shared ancestor to inhibit the proper function of the larger protein. These larger proteins are likely to form multimers with themselves for proper function.

The top differentially expressed miP was a thioredoxin domain-containing protein AFUB_079630 and in the same group AFUB_034260 was also enriched in conidia. Thioredoxins are small redox proteins. In this group, there were five thioredoxin microproteins predicted to interact with seven larger thioredoxin proteins, which suggests developmental specific regulation of thioredoxin proteins. Of the seven possible interactors disulfide-isomerase AFUB_023230 and AFUB_066190 were previously identified ithe conidial proteome and, therefore, could be potential targets of these miP. There was also a thioredoxin-like fold domain-containing protein AFUB_091140 predicted to interact with a protein of unknown function AFUB_071650. AFUB_071650 was also previously identified in conidial proteome.

Additionally, there were three miPs whose levels were upregulated in conidia and are probably also important to proper conidial function. A putative sterigmatocystin biosynthesis cytochrome P450 AFUB_046710 which was predicted to interact with 12 different cytochrome P450s in various secondary

metabolite clusters. A cytochrome b5 AFUB_061970 predicted to interact with acyl-coA dehydrogenases reductases, desaturases and chitin synthases. A LysM domain protein AFUB_096750 predicted to interact with six different chitinases. A Really Interesting New Gene (RING) finger protein AFUB_062320 was upregulated in conidia. There were three potential miP in this group predicted to interact with 18 different RING proteins which are involved in a wide range of cellular processes through ubiquitin ligase activity[76]. None of the potential interactors had been previously identified in conidial proteomics study. However, transcript levels of two potential interactors AFUB_011550 and AFUB_013410 were enriched in conidia.

Discussion

Transcriptomic studies of *A. fumigatus* conidia have been done using different isolates on rich media[12, 14, 15] without account for the heterogeneity of conidia due to spatial and temporal heterogeneity in colonies[77]. In our study, we compared synchronized conidia displaying different germination phenotypes to identify genes associated with each phenotype. Then we compared conidia from reference isolate A1163 to hyphae from different developmental stages to identify conidia enriched genes. By introducing controlled noise into our dataset we attempted to identify genes that would be true to conidia regardless of environmental and developmental variation.

Analysis of the global transcriptome of conidia shows that synchronized conidia from different sporulation environments contain transcripts from ~70% of the annotated genome. Abundant transcripts are enriched in processes such as translation, nitrogen metabolism, response to stress, and signal transduction. Lamarre et al hypothesized that some of these transcripts may be necessary for exit from dormancy; however, recent proteomic analysis and transmission electron microscopy of conidia at days 3, 15, and 30 by Anjo et al showed that the conidia are actively translating and undergoing physical changes until between 15 and 30 days[18].

Comparison between conidia transcriptome data presented in this study and the 729 proteins from publicly available proteome datasets[16-18, 78] show that 621 proteins have transcripts found in the conidia

and 292 proteins matched abundant transcripts. Additionally, 106 proteins without matching transcripts in the conidia had transcripts in samples containing conidiophores 24hrs after hyphal transfer, which suggests that conidia are transcriptionally born during early stages of sporogenesis. Teertstra et al has shown that the transcriptome can change as conidia age from day 2 to 8 (ref). Further experiments are necessary to understand when transcription stops in conidia and what the transcriptome looks like in fully dormant conidia.

We have confirmed the processes previous studies have shown and have added to the story. Conidia are indeed undergoing fermentative metabolism during maturation; however, they are also utilizing alternative carbon sources such as fatty acids. Fatty acid metabolism in conidia may be regulated through novel transcription factors not found in yeast. Conidia are undergoing autophagy to utilize intracellular stores of nitrate and convert it into ammonia using alternate pathways. These processes are occurring in a cell where gas exchange is not occurring determined by the increased expression of cafC. In a completely enclosed structure the cell cannot readily secrete reactive species; therefore, it is likely to be producing thioredoxins and secondary metabolites which act as antioxidants to detoxify the cell of reactive species. There is an increasing level of evidence that reactive species and secondary metabolism production correlate with developmental changes.

Interestingly, one of the highest differentially expressed transcription factors was srbC, which seems to be a conidia specific SREBP. SrbA and SrbB are members of this family of TFs and are known to play a role in hypoxia response by either interacting with themselves or with one another. Comparison of transcripts upregulated in conidia with a list of genes always found to be upregulated during hypoxia[79] growth conditions showed a large overlap (55 of the 62 genes). One can speculate that hypoxia resistance is not a mechanism adapted in the environment, rather part of a developmental state in conidia.

Acknowledgements

We would like to thank Alex Harkess and Karolina Heyduk of the Leebens-mack lab for teaching me how to do library preps on a budget and Zhuofei Hou and Shan-Ho Tsai of the Georgia Advanced Computing Resource Center at University of Georgia for their sustained help troubleshooting every program I tried to run. We would like to thank the generosity of the Department of Plant Biology, Plant Biology Graduate Student Association, and funders on Experiment.com (DOI: 10.18258/8345) for funding this project.

Table 4.1 Overview of samples for transcriptome analysis

Sample ID	Developmental Stage	Growth Condition	Raw Reads	Total mapped (%)
MM	Conidia	Minimal media, 37C	11,239,814	97.05
			27,602,415	97.13
			22,389,272	97.51
50C	Conidia	Minimal media, 50C	13,809,650	97.24
		(high temperature of	26,787,185	96.87
		compost)	21,292,042	97.22
- Zn	Conidia	Minimal media, 37C	24,440,787	97.19
		w/o zinc	25,186,310	97.32
		(zinc limiting condition)	15,454,294	97.93
+ Fe	Conidia	Minimal media, 37C	14,365,181	97.48
		w/ 10mM FeSO4	31,555,194	94.18
		(excessive iron)	23,208,461	97.15
NaCl	Conidia	Minimal media, 37C	20,510,038	97.21
		w/ 0.5M NaCl	38,081,689	97.23
		(osmotic/salt)	21,818,765	97.49
8hr	Hyphae	Complete media, liquid,	13,281,883	99.29
	First septation	37C, 250 rpm, 8 hr	17,045,238	99.34
		incubation		
24hr	Hyphae	Complete media, liquid,	15,714,591	99.17
	Sexual competence	37C, 250 rpm, 24 hr	13,483,468	99.33
		incubation		
5ht	Hyphae	Complete media, 37C,	15,093,260	98.95
	Conidiophore development	24 hr incubation + 5 hr post	28,603,460	99.16
		hyphal transfer		
9ht	Hyphae	Complete media, 37C,	15,565,936	99.15
	Conidiophore development	24 hr incuabtion + 9 hr post	53,598,325	99.07
		hyphal transfer		
24ht	Hyphae	Complete media, 37C,	12,266,146	99.14
	Conidiophore development	24 hr incubation + 24 hr	40,765,857	99.16
	Early sporogenesis	post hyphal transfer		

Table 4.2 Summary of conidial transcriptome

	MM	NaCl	+ Fe	50°C	- Zn	Overall Unique
# of Genes TPM > 1	7440	8100	7836	8240	7946	8617
Up Regulated †	457	146	82	640	508	1718
Down Regulated †	365	126	30	418	334	1184

† # of Differentially Expressed (DE) genes: fold-change > 2, p-value < 0.05, q-val < 0.05. Conidia from a sporulation condition was compared to conidia from all other conditions for DE analysis.

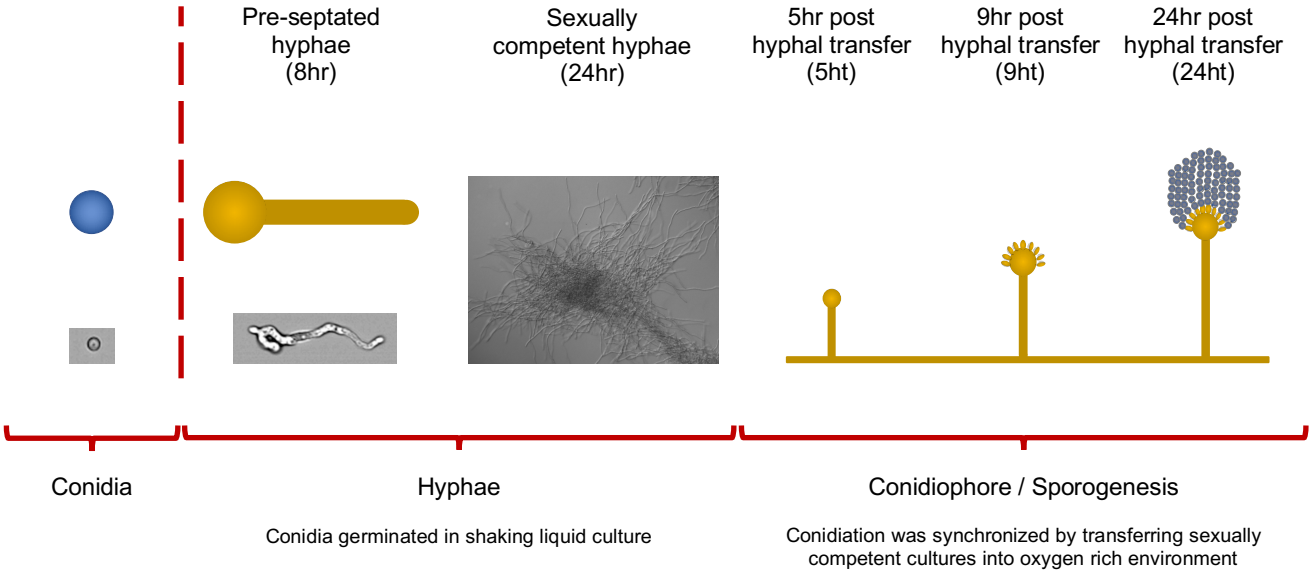

Figure 4.1 Diagram of developmental stages in *Aspergillus fumigatus*

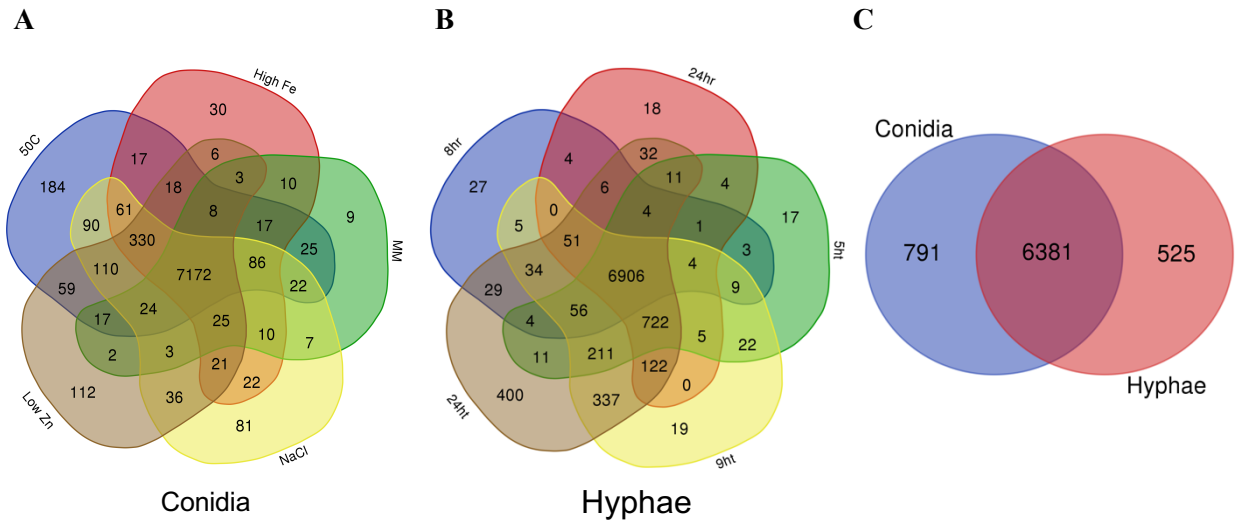

Figure 4.2 Comparison of conidial and hyphal transcriptomes Venn Diagram of # genes with average TPM > 1 from each conidial condition (A). Venn Diagram of # genes with average TPM > 1 from each hyphal condition (B). Comparison of # genes with average TPM > 1 found in all conidial and all hyphal datasets (C).

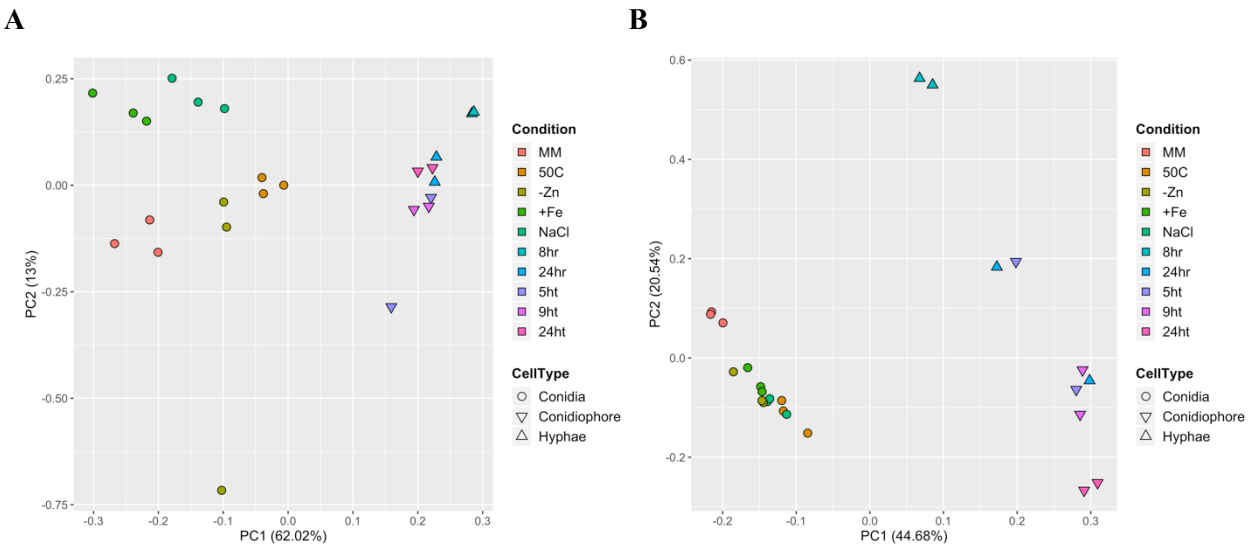

Figure 4.3 Principle component analysis PCA is based on raw TPM+0.01 values (A) and log2 normalized TPM+0.01 values (B) for all 10109 annotated genes. Conidia raised under different sporulation environments (circles), conidiophore (inverted triangles) and hyphae from planktonic cultures at 8hrs and 24hrs (triangles) as indicated by the legend.

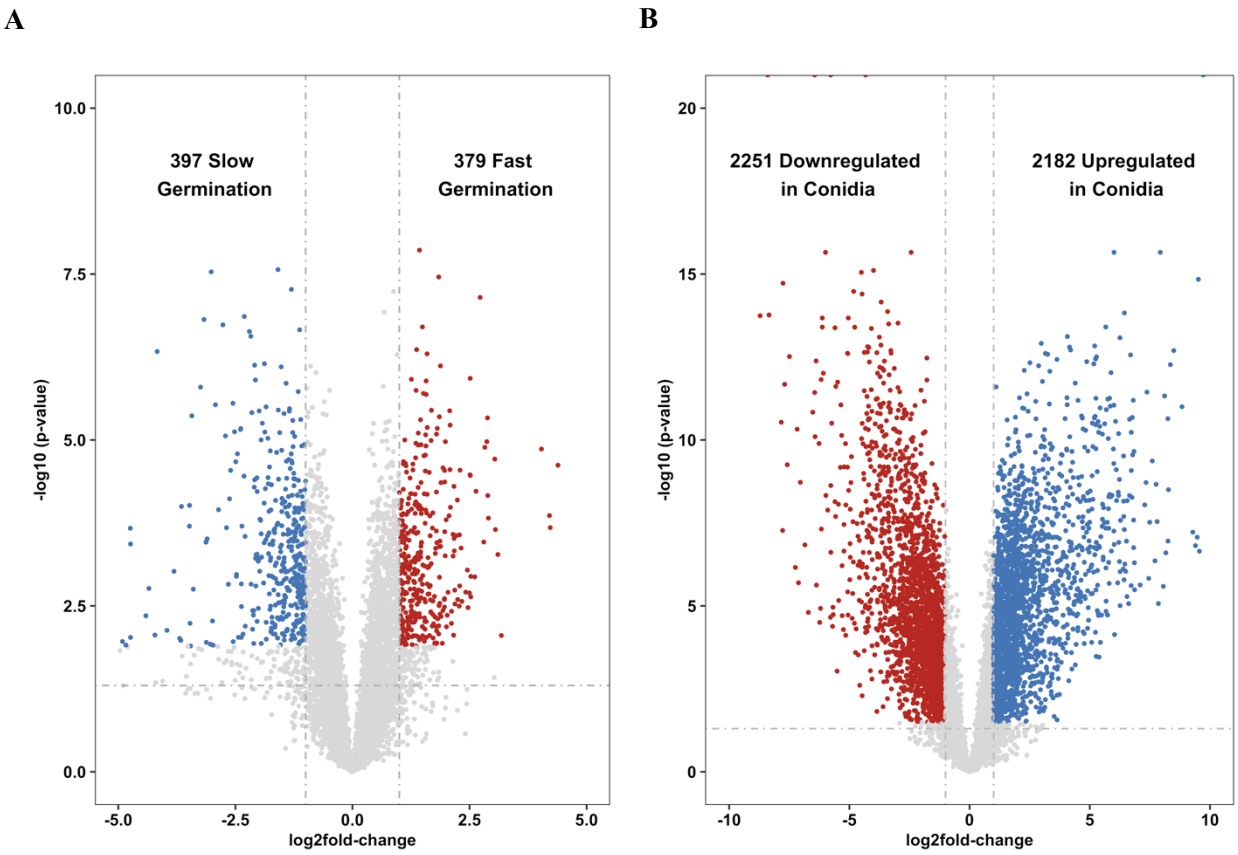

Figure 4.4 Differential expression analysis Volcano plot of differentially expressed genes between conidia with fast and slow germination phenotype (A). Volcano plot of differentially expressed genes between conidia and hyphae (B). Threshold for calling significant DE genes were fold-change > 2 (or log2fc > 1), p-value < 0.05, and FDR < 0.05.

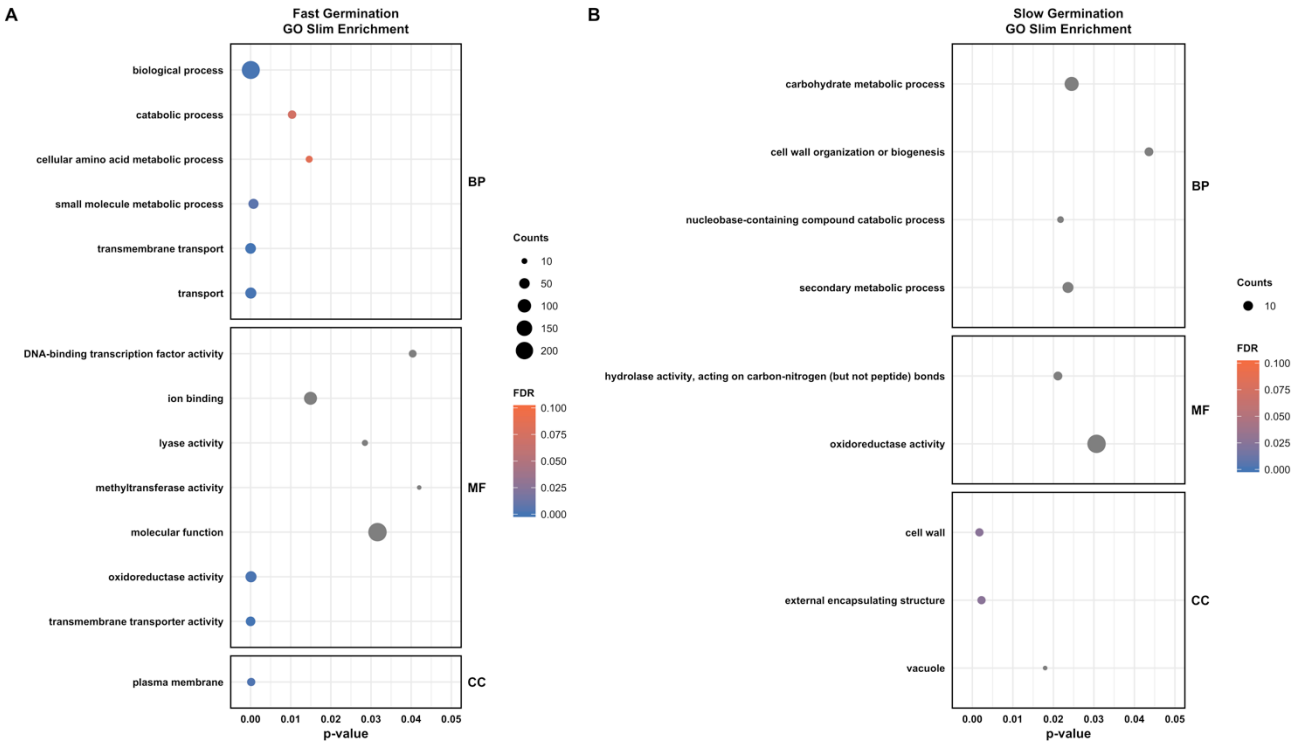

Figure 4.5 GO Slim analysis of differentially expressed genes in fast and slow germinating conidia
GO slim terms are on the y-axis, p-value is on the x-axis. Size of circles represent the number of genes in each GO slim term. Color scale represents the Benjamini-Hochberg false discovery rate (FDR). GO slim enrichment is categorized by biological processes (BP), molecular function (MF) and cellular components (CC).

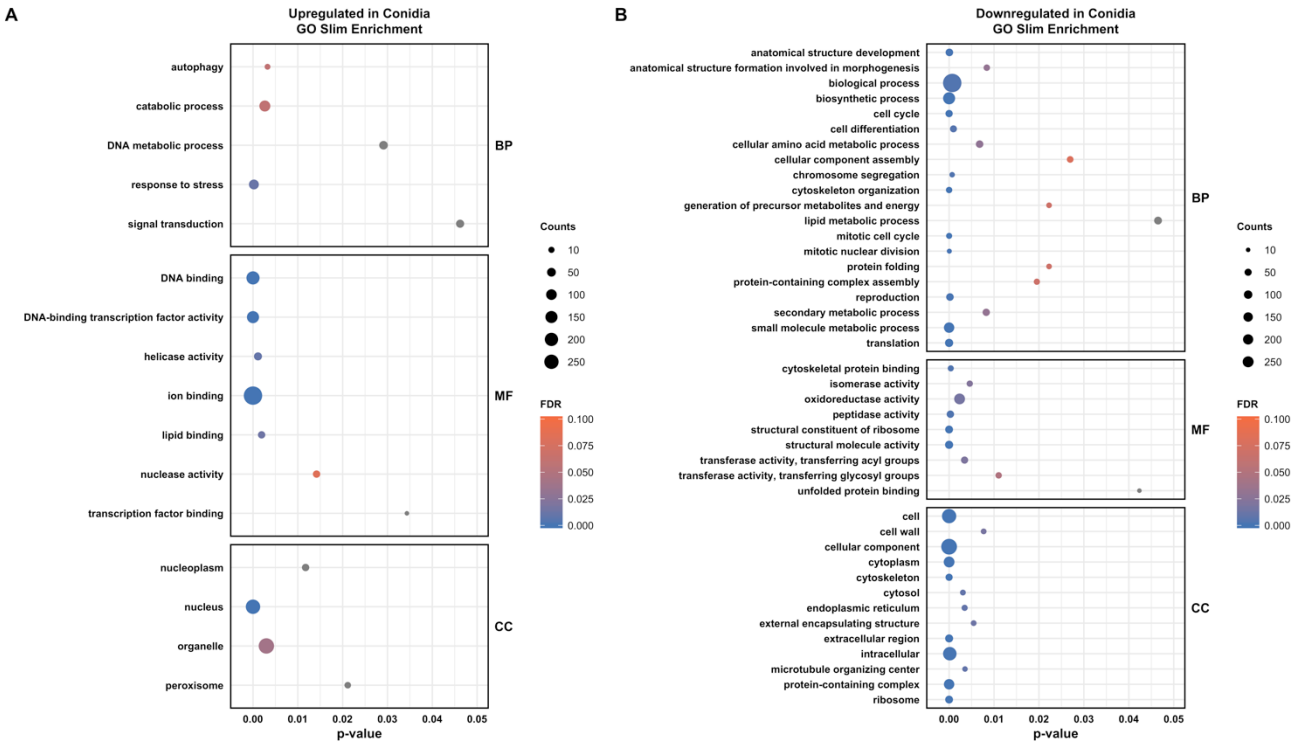

Figure 4.6 GO Slim analysis of differentially expressed genes in conidia and hyphae GO slim terms are on the y-axis, p-value is on the x-axis. Size of circles represent the number of genes in each GO slim term. Color scale represents the Benjamini-Hochberg false discovery rate (FDR). GO slim enrichment is categorized by biological processes (BP), molecular function (MF) and cellular components (CC).

Table 4.3 Transmembrane proteins enriched in both conidia and fast germinating conidia

Gene_ID A1163 Af293 Orthologue	UniProt Annotation	# TM domains	Fast / Slow fc	C / H fc
AFUB_037400 AFUA_3G11790	Galactose-proton symport, putative	12	16.39	7.75
AFUB_094010 AFUA_6G04280	Integral membrane protein	4	7.31	20.22
AFUB_003160 AFUA_1G02770	Uncharacterized protein	1	5.65	7.49
AFUB_033180 AFUA_2G17490	Flavin-binding monooxygenase, putative	1	4.72	6.82
AFUB_094900 AFUA_6G03380	Uncharacterized protein	1	4.55	2.39
AFUB_017190 AFUA_2G00110	MFS transporter, putative	9	4.33	3.29
AFUB_094970 AFUA_6G03320	MFS multidrug transporter, putative	13	3.58	2.22
AFUB_021590 AFUA_2G04540	Uncharacterized protein	5	3.51	3.23
AFUB_013620 AFUA_1G14080	Integral membrane protein Pth11-like, putative	7	3.49	4.68
AFUB_095940 AFUA_6G02400	MFS drug efflux pump, putative	14	3.48	8.98
AFUB_048950 #N/A	Uncharacterized protein	2	3.47	3.63
AFUB_062080 AFUA_5G14350	C-24(28) sterol reductase erg4A	9	3.26	2.23
AFUB_032610 AFUA_2G16930	Succinate:fumarate antiporter (Acr1), putative	0	3.21	24.44
AFUB_050050 AFUA_5G01510	Amino acid permease, putative	12	3.17	4.71
AFUB_033460 AFUA_2G17790	Amino acid transporter, putative	11	3.12	22.45
AFUB_048030 AFUA_3G00430	High-affinity glucose transporter, putative	12	3.12	3.56
AFUB_093930 AFUA_6G04360	ABC drug exporter AtrF	12	3.04	3.58
AFUB_017060 AFUA_1G17680	MFS transporter, putative	12	3.02	6.96
AFUB_101820 AFUA_4G01340	MFS monosaccharide transporter, putative	11	2.98	5.13

Gene_ID in **bold** were always enriched in conidia regardless of sporulation condition. Fold change values have $p < 0.05$ and FDR < 0.05

Table 4.3 Transmembrane proteins enriched in both conidia and fast germinating conidia (*continued*)

Gene_ID A1163 Af293 Orthologue	UniProt Annotation	# TM domains	Fast / Slow fc	C / H fc
AFUB_089830 AFUA_7G04290	Amino acid permease (Gap1), putative	11	2.94	5.93
AFUB_085310 AFUA_8G01300	Uncharacterized protein	6	2.88	3.33
AFUB_048730 AFUA_5G00280	MFS sugar transporter, putative	11	2.76	4.63
AFUB_085850 AFUA_8G00720	Amino acid transporter, putative	11	2.71	3.82
AFUB_022290 AFUA_2G05260	Salicylate hydroxylase, putative	1	2.70	2.87
AFUB_058590 AFUA_5G11020	Ammonium transporter MepA	11	2.64	2.78
AFUB_099620 AFUA_4G03435	Uncharacterized protein	6	2.63	2.13
AFUB_048220 AFUA_3G00220	MFS sugar transporter, putative	9	2.55	4.24
AFUB_017260 AFUA_2G00180	Neutral amino acid permease	11	2.44	2.43
AFUB_023930 AFUA_2G07910	Myo-inositol transporter	12	2.42	5.86
AFUB_099510 AFUA_4G03540	Integral membrane protein, putative	7	2.34	29.42
AFUB_084350 AFUA_8G02260	Neutral amino acid permease	11	2.28	8.82
AFUB_076100 AFUA_6G10050	Small oligopeptide transporter, OPT family	12	2.18	2.05
AFUB_024820 AFUA_2G08910	MFS transporter, putative	12	2.17	4.45
AFUB_077580 AFUA_6G11560	Integral membrane protein, putative	6	2.09	4.64
AFUB_100240 AFUA_4G02880	Uncharacterized protein	6	2.06	4.02
AFUB_049370 AFUA_5G00930	Amino acid permease, putative	12	2.03	10.20
AFUB_082430 AFUA_8G05070	Neutral amino acid permease	11	2.03	2.36
AFUB_046850 AFUA_3G01560	Amino acid permease (Can1), putative	10	2.01	2.23

Gene_ID in **bold** were always enriched in conidia regardless of sporulation condition. Fold change values have $p < 0.05$ and FDR < 0.05

Table 4.4 Transmembrane proteins enriched in both conidia and slow germinating conidia

Gene_ID A1163 Af293 Orthologue	UniProt Annotation	# TM domains	Slow / Fast fc	C / H fc
AFUB_079250 AFUA_1G01550	High affinity zinc ion transporter, putative	8	8.18	2.91
AFUB_086830 AFUA_7G00270	FAD binding monooxygenase, putative	1	7.94	13.90
AFUB_052070 AFUA_5G03550	Plasma membrane ATPase (EC 7.1.2.1)	9	6.28	14.73
AFUB_071030 #N/A	Metalloreductase, putative	6	5.49	2.53
AFUB_099080 AFUA_4G03940	Ferric-chelate reductase, putative	7	5.17	4.15
AFUB_097200 AFUA_6G00320	Integral membrane protein	6	4.98	11.17
AFUB_086860 #N/A	Uncharacterized protein	7	4.90	2.42
AFUB_075490 #N/A	LamGL domain-containing protein	2	4.21	4.88
AFUB_096730 AFUA_6G00740	Fatty acid hydroxylase domain-containing protein	1	4.10	4.09
AFUB_073200 #N/A	Uncharacterized protein	7	3.84	15.24
AFUB_081680 AFUA_8G05860	Aromatic amino acid and leucine permease	11	3.24	5.43
AFUB_092410 AFUA_7G06830	MFS tranporter, putative	11	3.20	5.09
AFUB_096740 AFUA_6G00730	Uncharacterized protein	1	3.14	3.14
AFUB_073220 AFUA_6G07260	Purine-cytosine permease, putative	12	2.91	4.82
AFUB_047370 AFUA_3G01030	RTA1 domain protein, putative	5	2.82	2.13
AFUB_047950 AFUA_3G00500	Integral membrane protein	4	2.81	14.95
AFUB_049050 AFUA_5G00580	CAP10 domain-containing protein	1	2.75	2.28
AFUB_057830 AFUA_5G10240	Uncharacterized protein	1	2.73	6.72
AFUB_024130 AFUA_2G08120	MFS monosaccharide transporter (Hxt8), putative	11	2.67	4.43

Gene_ID in **bold** were always enriched in conidia regardless of sporulation condition. Fold change values have $p < 0.05$ and FDR < 0.05

Table 4.4 Transmembrane proteins enriched in both conidia and slow germinating conidia (*continued*)

Gene_ID A1163 Af293 Orthologue	UniProt Annotation	# TM domains	Slow / Fast fc	C / H fc
AFUB_085490 AFUA_8G01110	Integral membrane protein, putative	4	2.64	35.51
AFUB_080590 AFUA_8G07190	Uncharacterized protein	2	2.58	18.14
AFUB_056580 AFUA_5G09040	Uncharacterized protein	1	2.55	2.60
AFUB_036540 AFUA_3G12630	Cytochrome b561, putative	5	2.46	3.34
AFUB_018660 AFUA_2G01590	Non-classical export protein Nce2, putative	4	2.42	42.33
AFUB_000470 AFUA_6G14280	Uncharacterized protein	2	2.42	3.83
AFUB_009130 AFUA_1G09680	Protein transport protein SFT2	4	2.33	2.55
AFUB_059070 AFUA_5G11500	Uncharacterized protein	1	2.31	15.05
AFUB_026270 AFUA_2G10470	ATP-dependent protease (CrgA), putative	1	2.27	3.34
AFUB_000890 AFUA_6G13840	Uncharacterized protein	2	2.25	3.12
AFUB_057810 AFUA_5G10210	Uncharacterized protein	1	2.24	29.13
AFUB_087610 AFUA_7G01030	Calcium-transporting ATPase (EC 7.2.2.10)	8	2.24	5.03
AFUB_077880 AFUA_6G11880	Uncharacterized protein	1	2.22	3.02
AFUB_074510 AFUA_6G08550	C6 transcription factor, putative	1	2.12	2.94
AFUB_024650 AFUA_2G08740	ZIP metal ion transporter, putative	6	2.05	8.48
AFUB_057800 AFUA_5G10200	Uncharacterized protein	1	2.03	30.02

Gene_ID in **bold** were always enriched in conidia regardless of sporulation condition. Fold change values have $p < 0.05$ and FDR < 0.05

Table 4.5 Conidia enriched transcription factors

Gene_ID A1163 Af293 Orthologue	Annotation	TF Family	C / H fc
AFUB_016450 AFUA_1G17060	HLH DNA binding domain protein (SrbC), putative	BHLH	164.55
AFUB_087240 AFUA_7G00652	C2H2 transcription factor, putative	C2H2	71.64
AFUB_044290 #N/A	BZIP transcription factor; Putative bZip-type transcription factor with similarity to atfA	BZIP	65.46
AFUB_016730 AFUA_1G17360	BZIP transcription factor (AtfC), putative; Putative bZip-type transcription factor with similarity to atfA	BZIP	44.13
AFUB_017530 AFUA_2G00470	C6 transcription factor, putative	Zn(2)-C6	30.58
AFUB_088380 AFUA_7G01810	C6 transcription factor, putative	Zn(2)-C6	23.75
AFUB_101990 AFUA_4G01510	C6 transcription factor, putative; 1 TM domain; Ortholog(s) have role in sporocarp development involved in sexual reproduction	Zn(2)-C6	23.36
AFUB_055060 AFUA_5G07510	C6 transcription factor (AlcR)	Zn(2)-C6	17.62
AFUB_060680 AFUA_5G12960	BZIP transcription factor (AtfB), putative; Putative bZip-type transcription factor with similarity to atfA	BZIP	16.82
AFUB_063540 AFUA_4G06420	Fungal specific transcription factor (GaaR), putative	Fungal specific	12.75
AFUB_085820 AFUA_8G00750	C2H2 transcription factor, putative	C2H2 Zn(2)-C6	12.69
AFUB_084330 AFUA_8G02280	C6 transcription factor, putative	Zn(2)-C6	12.53
AFUB_076360 AFUA_6G10310	Uncharacterized protein	Zn(2)-C6	11.70
AFUB_067900 AFUA_4G10820	HMG box transcriptional regulator, putative	HMG box	10.60
AFUB_051400 AFUA_5G02880	C6 transcription factor, putative	Zn(2)-C6	10.30
AFUB_086770 AFUA_7G00210	C6 transcription factor, putative	Zn(2)-C6	10.20
AFUB_016720 AFUA_1G17350	CP2 transcription factor, putative	CP2 / Grainyhead	10.19
AFUB_048380 #N/A	C6 transcription factor, putative	Zn(2)-C6	9.96
AFUB_015380 AFUA_1G15850	C6 transcription factor, putative	Zn(2)-C6	9.78
AFUB_055470 AFUA_5G07940	Myb-like domain-containing protein; Has domain(s) with predicted chromatin binding activity	Myb	9.53
AFUB_097380 AFUA_6G00120	C6 transcription factor, putative; 1 TM domain; Ortholog(s) have role in hyphal growth	Zn(2)-C6	9.28
AFUB_084440 AFUA_8G02170	C6 finger domain protein, putative	Zn(2)-C6	8.99
AFUB_013410 AFUA_1G13920	RING zinc finger protein, putative	RING	8.64
AFUB_048940 AFUA_5G00495	Uncharacterized protein	Zn(2)-C6	8.19

Gene_ID in **bold** were always enriched in conidia regardless of sporulation condition. Fold change values have $p < 0.05$ and FDR < 0.05

Table 4.5 Conidia enriched transcription factors (*continued)*

Gene_ID A1163 Af293 Orthologue	Annotation	TF Family	C / H fc
AFUB_037220 AFUA_3G11960	Forkhead transcription factor Fkh1/2, putative	Forkhead	8.14
AFUB_075680 AFUA_6G09630	C6 finger domain protein (GliZ)	Zn(2)-C6	8.07
AFUB_035590 AFUA_3G13600	C6 transcription factor, putative	Zn(2)-C6	7.62
AFUB_039350 AFUA_3G09820	C2H2 transcription factor (DvrA), putative	C2H2	7.61
AFUB_048740 AFUA_5G00290	C6 transcription factor, putative	Zn(2)-C6	7.45
AFUB_044300 #N/A	CP2 transcription factor, putative	CP2 / Grainyhead	7.42
AFUB_045780 #N/A	PUT3-like fungal specific transcription factor, putative	Fungal specific	7.24
AFUB_010420 AFUA_1G11000	C6 transcription factor (GalX), putative; Ortholog(s) have role in galactose catabolic process	Zn(2)-C6	7.21
AFUB_051220 AFUA_5G02690	Zn(2)-C6 fungal-type domain-containing protein; Ortholog(s) have role in conidiophore development	Zn(2)-C6	7.16
AFUB_095290 AFUA_6G03010	C2H2 finger domain protein (Zms1), putative	C2H2	7.14
AFUB_087890 AFUA_7G01310	C6 transcription factor (ClrB), putative	Zn(2)-C6	6.97
AFUB_037970 AFUA_3G11170	CP2 domain-containing protein; Ortholog(s) have sequence-specific DNA binding activity and role in carotenoid biosynthetic process, circadian rhythm, conidiophore development	CP2 / Grainyhead	6.88
AFUB_015440 AFUA_1G15910	C6 transcription factor RosA-like, putative; Ortholog(s) have role in conidiophore development	Zn(2)-C6	6.67
AFUB_013000 AFUA_1G13510	C6 transcription factor (FacB); Putative C6 transcription factor with a predicted role in acetate metabolism	Zn(2)-C6	6.58
AFUB_024400 AFUA_2G08450	Transcription factor TFIIE complex alpha subunit, putative	-	6.51
AFUB_049545 AFUA_5G01065	C6 transcription factor, putative	Zn(2)-C6	6.44
AFUB_048990 AFUA_5G00520	C6 transcription factor, putative	Zn(2)-C6	6.28
AFUB_022340 AFUA_2G05310	C6 transcription factor, putative	Zn(2)-C6	5.86
AFUB_088460 AFUA_7G01890	C6 transcription factor, putative	Zn(2)-C6	5.72
AFUB_099630 AFUA_4G03430	C6 transcription factor, putative	Zn(2)-C6	5.68
AFUB_000960 AFUA_6G13770	C6 finger domain protein, putative	Zn(2)-C6	5.50
AFUB_002240 AFUA_1G01850	C6 finger domain protein, putative	Zn(2)-C6	5.39
AFUB_016220 AFUA_1G16830	C6 transcription factor, putative	Zn(2)-C6	5.34

Gene_ID in **bold** were always enriched in conidia regardless of sporulation condition. Fold change values have $p < 0.05$ and FDR < 0.05

Table 4.5 Conidia enriched transcription factors (*continued)*

Gene_ID A1163 Af293 Orthologue	Annotation	TF Family	C / H fc
AFUB_021320 AFUA_2G04262	C6 transcription factor, putative	Zn(2)-C6	5.23
AFUB_092490 AFUA_7G06940	Fungal specific transcription factor, putative	Fungal specific	5.14
AFUB_020250 AFUA_2G03180	C6 finger domain protein, putative	Zn(2)-C6	5.00
AFUB_016820 AFUA_1G17460	C6 transcription factor, putative	Zn(2)-C6	4.89
AFUB_096370 AFUA_6G01970	GATA transcriptional activator (AreA)	GATA	4.82
AFUB_014910 AFUA_1G15370	C6 transcription factor, putative	Zn(2)-C6	4.71
AFUB_079860 #N/A	Fungal specific transcription factor, putative	Fungal specific	4.64
AFUB_037850 AFUA_3G11330	BZIP transcription factor (AtfA), putative	BZIP	4.64
AFUB_037210 AFUA_3G11970	C2H2 transcription factor (PacC), putative	C2H2	4.61
AFUB_015560 AFUA_1G16220	C6 transcription factor, putative	Zn(2)-C6	4.60
AFUB_001990 AFUA_1G01590	C6 transcription factor (AraR), putative	Zn(2)-C6	4.56
AFUB_038290 AFUA_3G10840	Zinc knuckle transcription factor/splicing factor MSL5/ZFM1, putative	CCHC finger	4.53
AFUB_029870 AFUA_2G14250	CBF/NF-Y family transcription factor, putative	CBF/NF-Y	4.52
AFUB_044060 AFUA_3G03900	C6 transcription factor, putative	Zn(2)-C6	4.51
AFUB_087340 AFUA_7G00770	C6 transcription factor, putative	Zn(2)-C6	4.50
AFUB_014300 AFUA_1G14750	C2H2 transcription factor (Sfp1), putative; Ortholog(s) have role in positive regulation of ribosomal protein gene transcription from RNA polymerase II promoter, regulation of cell size and cytoplasm, nucleus localization	C2H2	4.45
AFUB_013550 AFUA_1G14060	C2H2 finger domain protein, putative; Ortholog(s) have role in mRNA splicing, via spliceosome and U4/U6 x U5 tri-snRNP complex localization	C2H2	4.41
AFUB_071380 AFUA_4G14220	C6 finger domain protein, putative	Zn(2)-C6	4.40
AFUB_022860 AFUA_2G05830	Putative transcription factor involved in regulation of gluconeogenesis and acquisition of iron (acuK)	Zn(2)-C6	4.39
AFUB_096500 AFUA_6G01840	C6 transcription factor, putative	Zn(2)-C6	4.35
AFUB_005170 AFUA_1G04830	Transcription factor (AbaA)	TEA	4.33
AFUB_083600 AFUA_8G03970	C6 finger domain protein, putative	Zn(2)-C6	4.26

Gene_ID in **bold** were always enriched in conidia regardless of sporulation condition. Fold change values have $p < 0.05$ and FDR < 0.05

Table 4.5 Conidia enriched transcription factors (*continued)*

Gene_ID A1163 Af293 Orthologue	Annotation	TF Family	C / H fc
AFUB_032220 AFUA_2G16540	C2H2 finger domain protein, putative	C2H2	4.20
AFUB_085380 AFUA_8G01240	C6 transcription factor, putative; Ortholog(s) have role in secondary metabolite biosynthetic process	Zn(2)-C6	4.17
AFUB_099770 AFUA_4G03310	C6 finger domain protein, putative	Zn(2)-C6	4.16
AFUB_044670 AFUA_3G03550	Fungal specific transcription factor, putative	Fungal specific	4.16
AFUB_075990 AFUA_6G09930	BZIP transcription factor (Yap1 / NapA), putative	BZIP	4.14
AFUB_022280 AFUA_2G05250	Transcription factor (RfeD), putative	Rpap1	4.13
AFUB_080380 AFUA_8G07360	C6 transcription factor, putative	Zn(2)-C6	4.11
AFUB_051080 AFUA_5G02550	RNA polymerase III transcription factor subunit, putative	-	4.11
AFUB_017020 AFUA_1G17640	C6 transcription factor (RegA)	C2H2 Zn(2)-C6	4.10
AFUB_101810 AFUA_4G01322	Zn(2)-C6 fungal-type domain-containing protein	Zn(2)-C6	4.05
AFUB_046330 AFUA_3G02070	C2H2 transcription factor, putative	C2H2	4.03
AFUB_088210 AFUA_7G01640	C6 transcription factor, putative	Zn(2)-C6	4.03
AFUB_078010 AFUA_6G12020	C2H2 finger domain protein, putative	C2H2	4.00
AFUB_031270 AFUA_2G15620	Xylanolytic transcriptional activator (XlnR)	Zn(2)-C6	3.98
AFUB_036440 AFUA_3G12730	Transcription factor TFIIIB complex subunit Brf1, putative	Cyclin	3.91
AFUB_019790 AFUA_2G02690	Fungal specific transcription factor (AtrR), putative	Fungal specific	3.90
AFUB_030440 AFUA_2G14800	HLH transcription factor (Hpa3), putative; acetyltransferases	BHLH	3.89
AFUB_039150 AFUA_3G10030	Forkhead domain protein	Forkhead	3.87
AFUB_051340 AFUA_5G02800	C6 transcription factor, putative	Zn(2)-C6	3.86
AFUB_027530 AFUA_2G11780	Probable DNA-binding protein (CreA)	C2H2	3.82
AFUB_004470 AFUA_1G04110	C2H2 transcription factor, putative; 3 TM domain	C2H2	3.74
AFUB_027970 AFUA_2G12310	HLH transcription factor, putative	BHLH	3.72
AFUB_098510 AFUA_4G04502	HSF_DOMAIN domain-containing protein; Ortholog(s) have role in conidium formation, response to heat	HSF	3.72
AFUB_037000 AFUA_3G12180	C6 transcription factor, putative	Zn(2)-C6	3.67

Gene_ID in **bold** were always enriched in conidia regardless of sporulation condition. Fold change values have $p < 0.05$ and FDR < 0.05

Table 4.5 Conidia enriched transcription factors (*continued)*

Gene_ID A1163 Af293 Orthologue	Annotation	TF Family	C / H fc
AFUB_048230 AFUA_3G00210	C6 finger domain protein, putative	Zn(2)-C6	3.62
AFUB_083430 AFUA_8G04130	C6 transcription factor (FarB1), putative; Putative C6 transcription factor with a predicted role in beta oxidation of fatty acids	Zn(2)-C6	3.61
AFUB_089880 AFUA_7G04340	C6 transcription factor, putative	Zn(2)-C6	3.57
AFUB_037160 AFUA_3G12020	Sigma-70 region 2 family protein	Fungal specific	3.57
AFUB_077460 AFUA_6G11450	C6 transcription factor, putative	Zn(2)-C6	3.54
AFUB_039010 AFUA_3G10160	C6 transcription factor, putative	Zn(2)-C6	3.54
AFUB_055550 AFUA_5G08020	HLH DNA binding protein (Penr2), putative	BHLH	3.54
AFUB_047470 AFUA_3G00930	C6 transcription factor, putative; Ortholog(s) have role in conidiophore development, conidium formation, hyphal growth, sporocarp development involved in sexual reproduction	Zn(2)-C6	3.51
AFUB_008610 AFUA_1G09190	C6 finger domain protein, putative	Zn(2)-C6	3.49
AFUB_000110 #N/A	PrnA-like fungal specific transcription factor, putative	Fungal specific	3.49
AFUB_013910 AFUA_1G14360	C6 transcription factor, putative	Zn(2)-C6	3.44
AFUB_061020 AFUA_5G13310	C6 transcription factor, putative	Zn(2)-C6	3.43
AFUB_062110 AFUA_5G14390	C6 transcription factor, putative	Zn(2)-C6	3.42
AFUB_059600 AFUA_5G12020	C6 transcription factor (NirA), putative	Zn(2)-C6	3.42
AFUB_050430 AFUA_5G01900	Heat shock transcription factor (Hsf1), putative	HSF	3.41
AFUB_085450 AFUA_8G01150	C6 transcription factor, putative	Zn(2)-C6	3.40
AFUB_067230 AFUA_4G10110	Homeobox transcription factor (HtfA), putative	Homeobox	3.34
AFUB_076060 AFUA_6G10010	C6 transcription factor, putative	Zn(2)-C6	3.33
AFUB_050000 AFUA_5G01460	C6 finger domain protein, putative	Zn(2)-C6	3.30
AFUB_061640 AFUA_5G13930	CCCH finger DNA binding protein, putative	CCCH finger	3.30
AFUB_093890 AFUA_6G04400	Transcription factor TFIIIB component, putative	SANT	3.29
AFUB_037190 AFUA_3G11990	C6 transcription factor (Mut3), putative	Zn(2)-C6	3.28
AFUB_051950 AFUA_5G03430	PHD transcription factor (Rum1), putative	Jumonji	3.27

Gene_ID in **bold** were always enriched in conidia regardless of sporulation condition. Fold change values have $p < 0.05$ and FDR < 0.05

Table 4.5 Conidia enriched transcription factors (*continued)*

Gene_ID A1163 Af293 Orthologue	Annotation	TF Family	C / H fc
AFUB_099350 AFUA_4G03670	C6 transcription factor, putative	Zn(2)-C6	3.27
AFUB_011060 AFUA_1G11620	C6 transcription factor (QutA), putative	Zn(2)-C6	3.25
AFUB_022560 AFUA_2G05540	Cell division control protein (Cdc5), putative	HTH myb	3.21
AFUB_017410 AFUA_2G00360	Homeobox and C2H2 transcription factor, putative	Homeobox	3.18
AFUB_050260 AFUA_5G01730	MYB DNA-binding domain protein	Myb	3.16
AFUB_042180 AFUA_3G06870	MYB DNA-binding domain protein	Myb	3.16
AFUB_005770 AFUA_1G05420	Transcription factor SipA3, putative; Ortholog(s) have role in cellular response to drug	PH	3.16
AFUB_036390 AFUA_3G12780	C6 transcription factor, putative	Zn(2)-C6	3.12
AFUB_019640 AFUA_2G02540	BZIP transcription factor (RsmA), putative	BZIP	3.12
AFUB_074560 AFUA_6G08600	Transcription factor TFIID complex 145 kDa subunit, putative	-	3.08
AFUB_037920 AFUA_3G11250	C2H2 transcription factor (Ace2 / Swi5), putative; C2H2 transcription factor with a role in conidiophore development, pigment production, germination and virulence	C2H2	3.07
AFUB_046000 AFUA_3G02320	C2H2 finger domain protein (Kin17), putative	C2H2	3.06
AFUB_078520 AFUA_6G12522	Stress response regulator/HFS transcription factor (Skn7 / SrrA), putative	HFS	3.03
AFUB_005350 AFUA_1G04980	RNA polymerase III transcription factor TFIIIC subunit (Tfc4), putative	-	3.00
AFUB_101600 AFUA_4G01105	C2H2 transcription factor, putative	C2H2 Zn(2)-C6	2.95
AFUB_006120 AFUA_1G05740	C6 transcription factor, putative; Ortholog(s) have role in conidiophore development, hyphal growth and cytoplasm, nucleus localization	Zn(2)-C6	2.94
AFUB_074510 AFUA_6G08550	C6 transcription factor, putative; 1 TM domain	Zn(2)-C6	2.94
AFUB_014290 AFUA_1G14740	Transcription factor TFIIA complex subunit Toa1, putative	-	2.93
AFUB_059150 AFUA_5G11580	Transcription factor TFIIH subunit Tfb4, putative	-	2.91
AFUB_033540 AFUA_2G17860	C6 transcription factor, putative; Ortholog(s) have role in cellular response to drug, growth of symbiont in host and positive regulation of cell adhesion involved in single-species biofilm formation, more	Zn(2)-C6	2.91
AFUB_090250 AFUA_7G04710	NF-X1 finger transcription factor, putative	NF-X1 finger	2.89
AFUB_043110 AFUA_3G05940	Transcription factor Rba50, putative; Ortholog(s) have role in transcription from RNA polymerase II promoter and cytosol, nucleus localization	Rpap1	2.87

Gene_ID in **bold** were always enriched in conidia regardless of sporulation condition. Fold change values have $p < 0.05$ and FDR < 0.05

Table 4.5 Conidia enriched transcription factors (*continued)*

Gene_ID A1163 Af293 Orthologue	Annotation	TF Family	C / H fc
AFUB_058830 AFUA_5G11260	Siderophore transcription factor (SreA)	GATA	2.86
AFUB_101870 AFUA_4G01392	Zn(2)-C6 fungal-type domain-containing protein	Zn(2)-C6	2.86
AFUB_021650 AFUA_2G04600	C6 transcription factor, putative	Zn(2)-C6	2.84
AFUB_009970 AFUA_1G10550	CBF/NF-Y family transcription factor, putative; Ortholog(s) have role in filamentous growth	CBF/NF-Y	2.82
AFUB_084620 AFUA_8G01990	C6 transcription factor, putative; Ortholog(s) have role in short-chain fatty acid catabolic process	Zn(2)-C6	2.79
AFUB_073070 AFUA_6G07130	C6 transcription factor, putative	Zn(2)-C6	2.79
AFUB_071830 AFUA_4G14590	C6 transcription factor, putative	Zn(2)-C6	2.78
AFUB_063310 AFUA_4G06190	Fungal specific transcription factor, putative	Fungal specific	2.77
AFUB_049390 AFUA_5G00950	C6 transcription factor, putative	Zn(2)-C6	2.77
AFUB_069160 #N/A	C6 transcription factor Prf, putative (Fragment)	Zn(2)-C6	2.77
AFUB_077740 AFUA_6G11750	C6 transcription factor, putative	Zn(2)-C6	2.73
AFUB_085170 AFUA_8G01440	C6 finger domain protein, putative	Zn(2)-C6	2.72
AFUB_025190 AFUA_2G09330	C6 finger domain protein, putative	Zn(2)-C6	2.71
AFUB_039050 AFUA_3G10120	RNA polymerase I and III transcription factor complex component Tbp, putative; 2 TM domain	TBP	2.71
AFUB_101950 AFUA_4G01470	C6 finger domain protein, putative	Zn(2)-C6	2.70
AFUB_030930 AFUA_2G15255	C6 transcription factor (Leu3), putative	Zn(2)-C6	2.70
AFUB_082260 AFUA_8G05270	C6 transcription factor, putative	Zn(2)-C6	2.70
AFUB_045020 AFUA_3G03230	BZIP transcription factor, putative	BZIP	2.69
AFUB_074500 AFUA_6G08540	C6 finger domain protein, putative	Zn(2)-C6	2.67
AFUB_101510 AFUA_4G01010	C6 transcription factor, putative	Zn(2)-C6	2.66
AFUB_045330 AFUA_3G02920	C6 transcription factor, putative	Zn(2)-C6	2.65
AFUB_038770 AFUA_3G10380	Transcription factor TFIIIC complex subunit Tfc6, putative	-	2.64
AFUB_100190 AFUA_4G02940	BZIP transcription factor, putative	BZIP	2.63
AFUB_071660 AFUA_4G14400	C2H2 finger domain protein, putative	C2H2	2.61

Gene_ID in **bold** were always enriched in conidia regardless of sporulation condition. Fold change values have $p < 0.05$ and FDR < 0.05

Table 4.5 Conidia enriched transcription factors (*continued)*

Gene_ID A1163 Af293 Orthologue	Annotation	TF Family	C / H fc
AFUB_021220 AFUA_2G04150	C6 transcription factor, putative; 2 TM domain	Zn(2)-C6	2.61
AFUB_016630 AFUA_1G17240	C6 transcription factor, putative	Zn(2)-C6	2.59
AFUB_069500 AFUA_4G12560	C6 transcription factor, putative; Ortholog(s) have role in hyphal growth	Zn(2)-C6	2.57
AFUB_007280 AFUA_1G06900	C2H2 transcription factor (CrzA), putative; C2H2-type zinc finger transcription factor involved in calcium ion homeostasis	C2H2	2.57
AFUB_015750 AFUA_1G16410	C6 transcription factor, putative	Zn(2)-C6	2.55
AFUB_036250 AFUA_3G12940	C6 transcription factor (HasF), putative	Zn(2)-C6	2.54
AFUB_064650 AFUA_4G07560	MYB DNA-binding domain protein and HSA domain protein	HSA Myb	2.53
AFUB_089710 AFUA_7G04170	C6 transcription factor, putative; Ortholog(s) have role in growth of symbiont in host, nitrogen utilization	Zn(2)-C6	2.52
AFUB_092720 AFUA_6G09356	MADS-box domain-containing protein	MADS-box	2.52
AFUB_011800 AFUA_1G12332	Jumonji family transcription factor, putative	Jumonji	2.50
AFUB_083880 AFUA_8G02710	C6 transcription factor, putative	Zn(2)-C6	2.49
AFUB_020500 AFUA_2G03430	C6 transcription factor, putative	Zn(2)-C6	2.49
AFUB_056710 AFUA_5G09170	C2H2 finger domain protein, putative	C2H2	2.46
AFUB_089440 AFUA_7G03910	C2H2 zinc finger protein; Ortholog(s) have role in conidium formation, negative regulation of conidium formation and positive regulation of sexual sporulation resulting in formation of a cellular spore, more	C2H2	2.44
AFUB_032870 AFUA_2G17220	C2H2 transcription factor (AmdX), putative	C2H2	2.42
AFUB_094410 AFUA_6G03880	Uncharacterized protein	C2H2 ZF	2.40
AFUB_012800 AFUA_1G13310	BZIP transcription factor, putative	BZIP	2.40
AFUB_000400 AFUA_6G14350	C6 transcription factor, putative	Zn(2)-C6	2.39
AFUB_036510 AFUA_3G12660	C6 finger domain protein Acr-2, putative	Zn(2)-C6	2.39
AFUB_075870 AFUA_6G09820	Transcription factor AATF/Che-1, putative; Ortholog(s) have role in maturation of SSU-rRNA from tricistronic rRNA transcript (SSU-rRNA, 5.8S rRNA, LSU-rRNA) and 90S preribosome, nucleolus, small-subunit processome localization	AATF	2.37
AFUB_009490 AFUA_1G10080	C2H2 transcription factor (ZafA), putative	C2H2	2.37

Gene_ID in **bold** were always enriched in conidia regardless of sporulation condition. Fold change values have $p < 0.05$ and FDR < 0.05

Table 4.5 Conidia enriched transcription factors (*continued)*

Gene_ID A1163 Af293 Orthologue	Annotation	TF Family	C / H fc
AFUB_076200 AFUA_6G10140	C6 transcription factor, putative	Zn(2)-C6	2.35
AFUB_082950 AFUA_8G04540	C6 transcription factor, putative; 2 TM domain; Ortholog(s) have role in cellular response to biotic stimulus, cellular response to starvation and conidiophore development, more	Zn(2)-C6	2.34
AFUB_079560 AFUA_1G01240	C6 transcription factor, putative	Zn(2)-C6	2.34
AFUB_043270 AFUA_3G05760	C6 transcription factor (Fcr1), putative	Zn(2)-C6	2.33
AFUB_009120 AFUA_1G09670	HLH transcription factor (GlcD), putative	BHLH	2.33
AFUB_069900 AFUA_4G13000	Flavin-containing amine oxidase, putative	HMG box	2.32
AFUB_029740 AFUA_2G14120	C6 finger domain protein, putative	Zn(2)-C6	2.31
AFUB_081700 AFUA_8G05840	Fungal specific transcription factor, putative	Fungal specific	2.31
AFUB_044040 AFUA_3G03920	C6 transcription factor, putative	Zn(2)-C6	2.30
AFUB_079450 AFUA_1G01340	C6 transcription factor, putative	Zn(2)-C6	2.24
AFUB_002740 AFUA_1G02360	Fungal_trans domain-containing protein	Fungal specific	2.23
AFUB_013830 AFUA_1G14280	C6 finger domain protein, putative	Zn(2)-C6	2.23
AFUB_073760 AFUA_6G07800	C6 finger domain protein, putative	Zn(2)-C6	2.17
AFUB_073490 AFUA_6G07530	BZIP transcription factor (MetR), putative; Putative bZIP transcription factor with a role in sulfur amino acid metabolism	BZIP	2.17
AFUB_001960 AFUA_1G01560	C6 finger domain protein, putative	Zn(2)-C6	2.16
AFUB_015020 AFUA_1G15470	C6 transcription factor (UaY), putative	Zn(2)-C6	2.14
AFUB_069670 AFUA_4G12750	Transcription factor, putative; Ortholog(s) have role in deadenylation-dependent decapping of nuclear-transcribed mRNA and cytosol, nucleus localization	-	2.12
AFUB_022410 AFUA_2G05380	C6 transcription factor, putative	Zn(2)-C6	2.11
AFUB_052710 AFUA_5G04190	HLH transcription factor (PalcA), putative	BHLH	2.11
AFUB_062090 AFUA_5G14360	C6 transcription factor, putative; 1 TM domain	Zn(2)-C6	2.08
AFUB_024170 AFUA_2G08170	RNA polymerase II transcription factor SIII (Elongin) subunit A, putative	-	2.07
AFUB_083510 AFUA_8G04050	NDT80_PhoG domain protein XprG; regulation of extracellular proteases	NDT80	2.07

Gene_ID in **bold** were always enriched in conidia regardless of sporulation condition. Fold change values have $p < 0.05$ and FDR < 0.05

Table 4.5 Conidia enriched transcription factors (*continued)*

Gene_ID A1163 Af293 Orthologue	Annotation	TF Family	C / H fc
AFUB_003240 AFUA_1G02860	C2H2 transcription factor, putative	C2H2	2.07
AFUB_057630 AFUA_5G10040	C6 transcription factor, putative	Zn(2)-C6	2.06
AFUB_054000 AFUA_5G06460	C6 finger domain protein, putative	Zn(2)-C6	2.06
AFUB_004490 AFUA_1G04140	C6 finger domain protein, putative	Zn(2)-C6	2.02
AFUB_060790 AFUA_5G13080	Uncharacterized protein	Zn(2)-C6	2.01

Gene_ID in **bold** were always enriched in conidia regardless of sporulation condition. Fold change values have $p < 0.05$ and FDR < 0.05

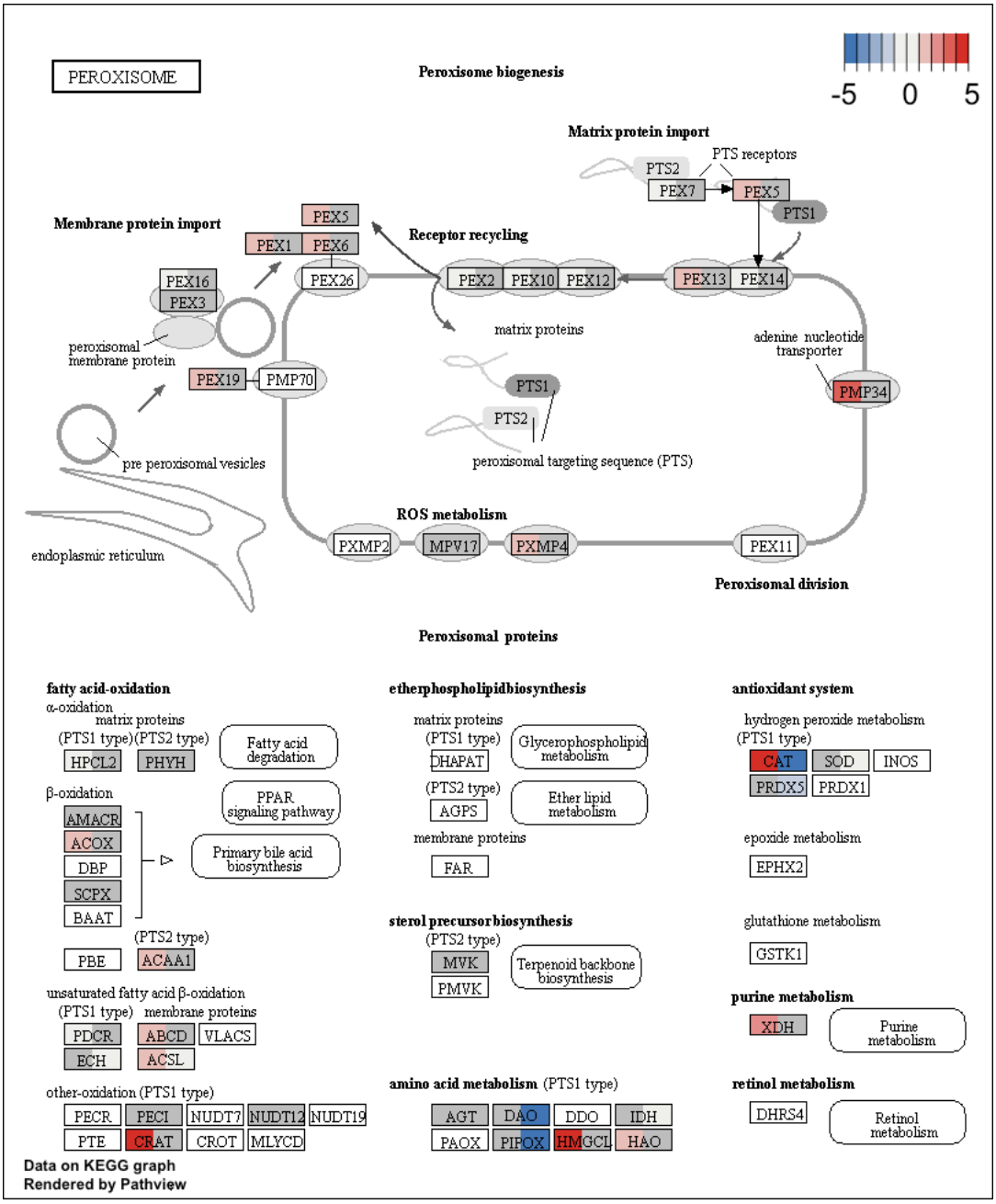

Figure 4.7 KEGG analysis of peroxisome proteins. Genes enriched in conidia (red) and in hyphae (blue). The intensity of enrichment has been scaled to +/- 5 as indicated by the scale bar. Boxes in dark gray are proteins in *A. fumigatus* genome that are not differentially expressed. Boxes in white are proteins not annotated in *A. fumigatus* genome.

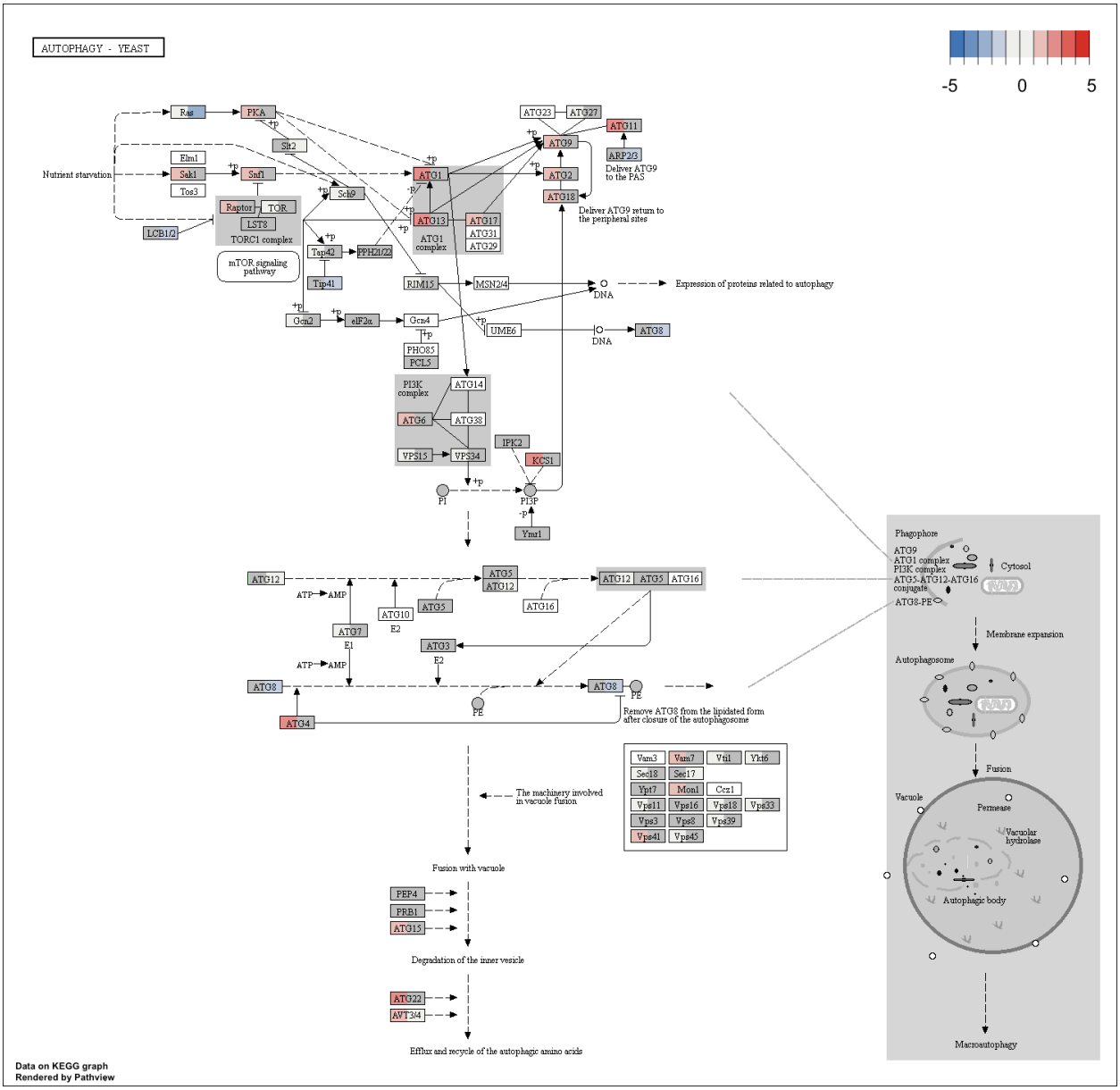

Figure 4.8 KEGG analysis of autophagy pathway Genes enriched in conidia (red) and in hyphae (blue). The intensity of enrichment has been scaled to +/- 5 as indicated by the scale bar. Boxes in dark gray are genes in *A. fumigatus* genome that are not differentially expressed. Boxes in white are genes not annotated in *A. fumigatus* genome.

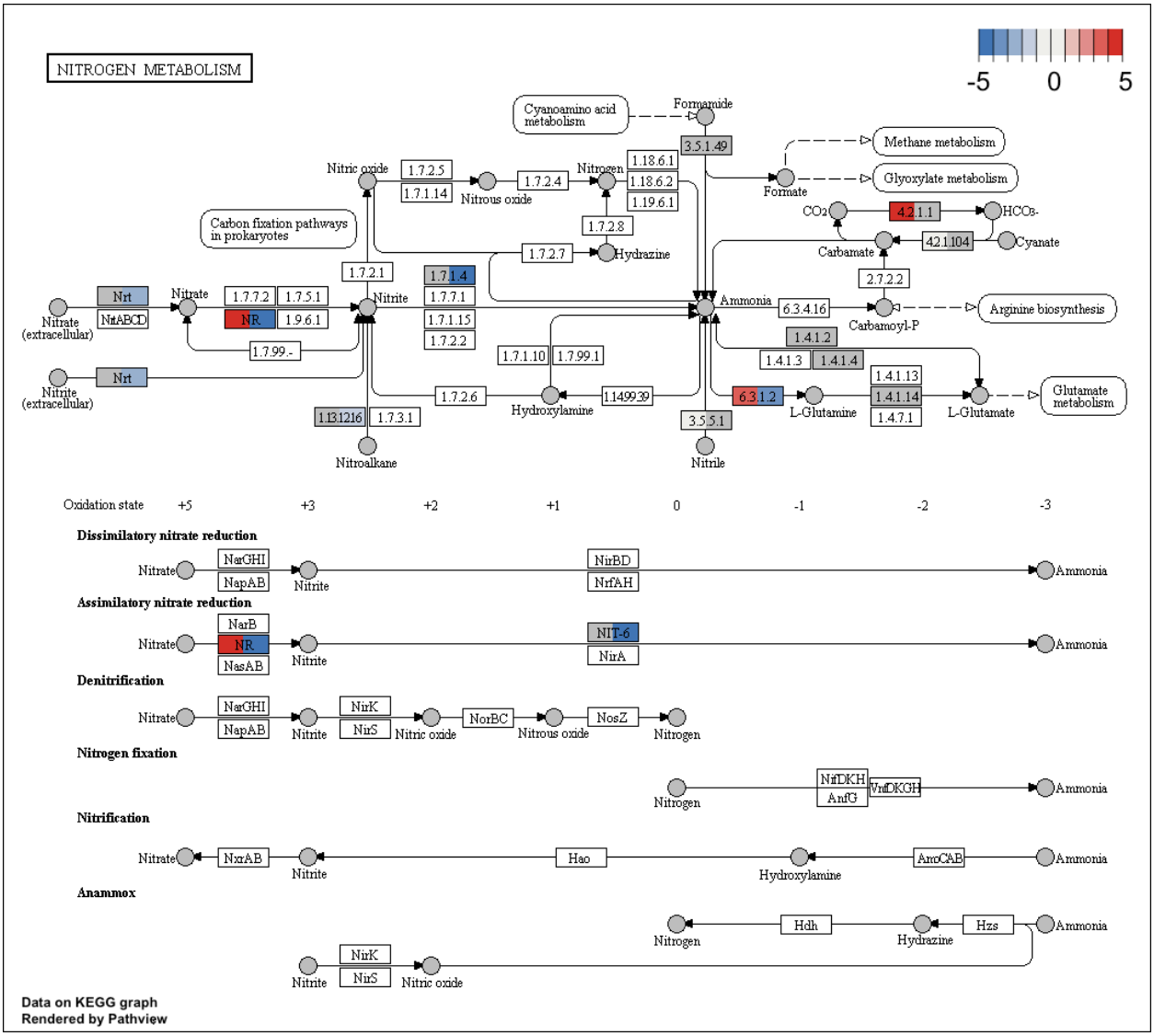

Figure 4.9 KEGG analysis of nitrogen metabolism pathway Genes enriched in conidia (red) and in hyphae (blue). The intensity of enrichment has been scaled to +/- 5 as indicated by the scale bar. Boxes in dark gray are enzymes in *A. fumigatus* genome that are not differentially expressed. Boxes in white are enzymes not annotated in *A. fumigatus* genome.

Table 4.6 *Aspergillus fumigatus* microProteins

Predicted miP_ids Gene_ID Af293 Gene_ID A1163	Protein Length Af293	Annotation	C/H fc	A1163 orthologue of predicted binding partners
XP_001481691.1 AFUA_1G01175 **AFUB_079630**	128	Thioredoxin domain-containing protein	133.49	XP_751916.1, XP_749744.1, XP_753425.1, XP_755392.2, XP_753290.1, XP_755829.1, XP_750281.1
XP_754127.1 AFUA_3G14970 **AFUB_034260**	109	Thioredoxin	4.52	
XP_753517.1 AFUA_5G11320 AFUB_058890	110	Thioredoxin	0.62	
XP_747097.1 AFUA_8G01090 AFUB_085510	116	Thioredoxin, putative	0.45	
XP_750918.1 AFUA_6G10300 AFUB_076350	108	Thioredoxin, putative	0.34	
XP_753192.1 AFUA_5G14650 **AFUB_062320**	97	RING finger protein	29.79	XP_755664.1, XP_001481667.1, XP_747197.1, XP_755297.1, XP_750209.1, XP_749382.1, XP_756024.1, XP_752576.1, XP_001481421.1, XP_751790.1, XP_752762.1, XP_753974.1, XP_749083.1, XP_748562.1, XP_747290.1, XP_747655.1, XP_754709.1, XP_750592.1
XP_751371.1 AFUA_4G14620 AFUB_071860	134	RING finger protein		
XP_001481523.1 AFUA_5G14845 AFUB_062520	99	RING-finger domain protein, putative		
XP_748490.1 AFUA_3G01690 **AFUB_046710**	129	Sterigmatocystin biosynthesis cytochrome P450 monooxygenase, putative (EC 1.14.-.-)	14.33	XP_749877.1, XP_751828.1, XP_746900.1, XP_747856.1, XP_750865.1, XP_755127.1, XP_755858.1, XP_748668.2, XP_747185.2, XP_753882.1, XP_751418.1, XP_748665.2
XP_753231.1 AFUA_5G14260 **AFUB_061970**	137	Cytochrome b5, putative	7.22	XP_751977.1, XP_750976.1, XP_747355.1, XP_750468.1, XP_748717.1, XP_752124.1, XP_746498.1, XP_753636.1, XP_752948.1, XP_753601.1, XP_752653.1, XP_748918.1, XP_749348.1, XP_749520.1, XP_755676.1, XP_747146.1
XP_755107.1 AFUA_2G07720 AFUB_023760	84	Cytochrome b5, putative		
XP_731484.2 AFUA_6G00720 **AFUB_096750**	80	LysM domain protein, putative	4.79	XP_747946.1, XP_001481468.1, XP_001481488.1, XP_752910.2, XP_001481465.1, XP_747948.2
XP_748952.1 AFUA_7G05570 AFUB_091150	106	Uncharacterized protein	3.87	XP_751394.1
XP_750982.1 AFUA_6G10960 AFUB_076980	79	Uncharacterized protein	3.75	XP_755928.2
XP_753834.1 AFUA_5G08020 AFUB_055550	139	HLH DNA binding protein (Penr2), putative	3.54	XP_752546.1
XP_752321.1 AFUA_1G09540 AFUB_008990	123	Vacuolar transporter chaperon Vtc1, putative	2.92	XP_755238.1, XP_750473.1

Gene_ID in **bold** are genes of interest. Fold change values have $p < 0.05$ and FDR < 0.05

Table 4.6 *Aspergillus fumigatus* MicroProteins (*continued*)

Predicted miP_ids Gene_ID Af293 Gene_ID A1163	Protein Length Af293	Annotation	C/H fc	A1163 orthologue of predicted binding partners
XP_748953.1 AFUA_7G05560 **AFUB_091140**	122	Thioredoxin-like_fold domain-containing protein	2.77	XP_751394.1
XP_749142.1 AFUA_7G03660 AFUB_089190	105	ABC-type ATPase Hef3-like, putative	2.75	XP_748943.1, XP_747719.1, XP_752217.1, XP_753932.1, XP_751564.1, XP_751944.1, XP_753010.1
XP_748519.2 AFUA_3G01990 AFUB_046420	137	DUF636 domain protein	2.75	XP_755597.1, XP_749096.1
XP_750068.1 AFUA_1G03180 AFUB_003600	134	DUF636 domain protein	0.38	
XP_755864.1 AFUA_2G15290 AFUB_030960	136	DUF636 domain protein		
XP_746820.1 AFUA_7G01105 AFUB_087690	112	GFA domain-containing protein		
XP_753943.2 AFUA_5G06910 AFUB_054460	137	DUF636 domain protein		
XP_750825.1 AFUA_6G09356 AFUB_092720	103	MADS-box domain-containing protein	2.52	XP_754763.1
XP_750821.1 AFUA_6G09335 AFUB_092760	130	SRF-type transcription factor family protein	0.22	
XP_746589.1 AFUA_4G04020 AFUB_098990	120	FK506-binding protein 1B (FKBP)	2.44	XP_750747.1
XP_751096.1 AFUA_6G12170 AFUB_078170	112	FK506-binding protein 1A (FKBP)	0.23	
XP_749519.1 AFUA_2G03870 AFUB_020940	134	FK506-binding protein 2 (EC 5.2.1.8)	0.14	
XP_750073.1 AFUA_1G03230 AFUB_003650	139	ABC multidrug transporter, putative	1.69	XP_754025.1, XP_751419.1, XP_747768.1, XP_747730.1, XP_748687.1, XP_748598.1, XP_748663.1, XP_749444.1, XP_752639.1, XP_746882.1, XP_751826.1, XP_751165.1, XP_751944.1, XP_751910.1, XP_753593.1, XP_753821.1, XP_753839.1, XP_753720.1, XP_752405.2, XP_753056.1, XP_749286.1, XP_754399.1, XP_750621.1, XP_748306.1, XP_754651.1, XP_753691.1, XP_752661.1, XP_748943.1, XP_750227.1, XP_755735.2, XP_753381.1, XP_752803.1, XP_752217.1, XP_753932.1, XP_747719.1, XP_753010.1, XP_746352.2

Gene_ID in **bold** are genes of interest. Fold change values have $p < 0.05$ and FDR < 0.05

Table 4.6 *Aspergillus fumigatus* MicroProteins (*continued*)

Predicted miP_ids Gene_ID Af293 Gene_ID A1163	Protein Length Af293	Annotation	C/H fc	A1163 orthologue of predicted binding partners
XP_750079.1 AFUA_1G03290 AFUB_003710	116	Myo-inositol transporter 1	1.73	XP_750516.1, XP_755126.1, XP_747117.1, XP_748444.1, XP_747770.1, XP_755791.1, XP_753005.1, XP_748611.1, XP_752216.1, XP_001481451.1, XP_750589.2, XP_748363.1, XP_749649.1, XP_751072.1, XP_755484.1, XP_752470.1, XP_754208.1, XP_746451.1, XP_746376.1, XP_752549.1, XP_001481478.1, XP_748871.1, XP_751333.1, XP_751523.1, XP_752524.1, XP_746324.1, XP_747891.1, XP_746835.1, XP_748226.1, XP_752989.1, XP_754933.1, XP_754363.1, XP_750103.2, XP_753203.1, XP_754404.1, XP_746497.1, XP_754420.2, XP_749587.1, XP_753358.1, XP_753961.1, XP_748059.1, XP_748312.1, XP_752358.1, XP_747088.1, XP_746358.1, XP_751330.1, XP_747005.1, XP_748690.1, XP_753099.1, XP_747072.1, XP_748341.2, XP_747486.1, XP_754226.2, XP_751366.1, XP_751372.1, XP_754349.1, XP_746441.1
XP_753161.1 AFUA_5G14960 AFUB_079070	100	Uncharacterized protein	1.44	XP_752972.1
XP_755534.2 AFUA_2G12020 AFUB_027730	119	U6 snRNA-associated Sm-like protein LSm4	1.29	XP_752051.1, XP_751791.1
XP_749642.2 AFUA_2G05110 AFUB_022140	120	Small nuclear ribonucleoprotein Sm D1 (snRNP core protein D1)	0.75	
XP_749081.1 AFUA_7G04280 AFUB_089820	83	U6 snRNA-associated Sm-like protein LSm5	0.73	
XP_748912.1 AFUA_7G05980 AFUB_091560	95	Small nuclear ribonucleoprotein E (snRNP-E) (Sm protein E)	0.63	
XP_751802.1 AFUA_4G10240 AFUB_067360	116	Small nuclear ribonucleoprotein Sm D3 (Sm-D3) (snRNP core protein D3)	0.57	
XP_755856.1 AFUA_2G15210 AFUB_030880	91	U6 snRNA-associated Sm-like protein LSm2	0.57	
XP_753362.1 AFUA_5G12910 AFUB_060630	122	Small nuclear ribonucleoprotein Sm D2 (Sm-D2) (snRNP core protein D2)	0.56	
XP_752799.1 AFUA_1G14290 AFUB_013840	134	Small nuclear ribonucleoprotein (LSM7), putative	0.55	
XP_753396.1 AFUA_5G12570 AFUB_060230	83	U6 small nuclear ribonucleoprotein (Lsm3), putative	0.55	

Gene_ID in **bold** are genes of interest. Fold change values have $p < 0.05$ and FDR < 0.05

Table 4.6 *Aspergillus fumigatus* MicroProteins (*continued*)

Predicted miP_ids Gene_ID Af293 Gene_ID A1163	Protein Length Af293	Annotation	C/H fc	A1163 orthologue of predicted binding partners
XP_755885.2 AFUA_2G15500 AFUB_031150	88	Small nuclear ribonucleoprotein SmF, putative	0.47	
XP_747301.1 AFUA_8G04960 AFUB_082540	78	Small nuclear ribonucleoprotein G (snRNP-G)	0.45	
XP_750522.1 AFUA_6G06325 AFUB_072210	80	U6 snRNA-associated Sm-like protein LSm6	0.44	
XP_755280.1 AFUA_2G09460 AFUB_025330	89	Potassium transporter	0.65	XP_748113.1, XP_751477.1, XP_753000.1
XP_752533.1 AFUA_1G11670 AFUB_011110	98	U6 snRNA-associated Sm-like protein LSm8	0.62	XP_752051.1
XP_746487.1 AFUA_4G03010 AFUB_100120	100	MARVEL domain-containing protein	0.61	XP_750981.1
XP_747037.1 AFUA_8G01690 AFUB_084900	124	MARVEL domain-containing protein		
XP_753607.1 AFUA_5G10350 AFUB_057920	73	Uncharacterized protein	0.57	XP_750065.1
XP_754458.1 AFUA_3G11610 AFUB_037560	104	Non-histone chromosomal protein 6	0.55	XP_751745.1, XP_750203.1
XP_751623.1 AFUA_4G12080 AFUB_069070	139	Ubiquitin conjugating enzyme (MmsB), putative (EC 6.3.2.19)	0.51	XP_753930.1, XP_755984.1
XP_749979.1 AFUA_1G02290 AFUB_002680	106	CVNH domain-containing protein	0.47	XP_749023.1
XP_001481644.1 AFUA_2G01405 AFUB_018490	111	Cyanovirin-N family protein		
XP_755186.2 AFUA_2G08520 AFUB_024460	131	50S ribosomal protein L14	0.44	XP_747063.1
XP_749473.1 AFUA_2G03380 AFUB_020450	127	Alkaline serine protease	0.28	
XP_749724.1 AFUA_2G05950 AFUB_022990	126	Ribonucloprotein	0.42	XP_752727.1, XP_751177.1
XP_755151.1 AFUA_2G08150 AFUB_024160	80	NEDD8-like protein (RubA), putative	0.42	XP_751791.1, XP_751218.1, XP_754028.1

Gene_ID in **bold** are genes of interest. Fold change values have $p < 0.05$ and FDR < 0.05

Table 4.6 *Aspergillus fumigatus* MicroProteins (*continued*)

Predicted miP_ids Gene_ID Af293 Gene_ID A1163	Protein Length Af293	Annotation	C/H fc	A1163 orthologue of predicted binding partners
XP_754563.1 AFUA_3G10560 AFUB_038600	120	C6 finger domain protein, putative	0.42	XP_754332.1, XP_750852.1, XP_753610.1, XP_752286.1, XP_755869.1, XP_750323.1, XP_749668.1, XP_747522.1, XP_755001.1, XP_748172.1, XP_750130.1, XP_748873.1, XP_748614.1, XP_749547.1, XP_748246.1, XP_746530.1, XP_752465.1, XP_748508.1, XP_748651.2, XP_753137.1, XP_753360.1, XP_748878.1, XP_755418.1, XP_751810.1, XP_753218.1, XP_748234.1, XP_001481433.1, XP_001481479.1, XP_755897.1, XP_750671.1
XP_748250.1 AFUA_5G00910 AFUB_049350	119	MBL2-like secreted peptide, putative	0.38	XP_747168.1, XP_753281.1
XP_001481581.1 AFUA_3G00175 AFUB_048260	110	Uncharacterized protein		
XP_749434.1 AFUA_2G02990 AFUB_020050	119	MYB DNA-binding domain protein	0.35	XP_748793.1, XP_749437.1
XP_754205.1 AFUA_3G14200 **AFUB_035020**	134	Uncharacterized protein	0.33	XP_750316.1
XP_755308.1 AFUA_2G09750 AFUB_025600	130	Rhodanese domain-containing protein	0.32	XP_750709.1
XP_754757.1 AFUA_3G08580 AFUB_040520	118	Glycine-rich RNA-binding protein, putative	0.29	XP_754840.1, XP_749738.1, XP_752566.1, XP_748983.1, XP_750167.1, XP_750695.1, XP_752199.1, XP_752947.1, XP_753922.1, XP_749317.1, XP_747328.1, XP_747559.1, XP_750045.2, XP_750233.1, XP_754657.1, XP_755320.1, XP_748978.2, XP_749696.1, XP_746709.1, XP_754975.1, XP_750989.1, XP_751108.1
XP_746994.1 AFUA_8G02120 AFUB_084490	103	Uncharacterized protein	0.28	XP_754769.1
XP_746494.1 AFUA_4G03080 AFUB_100050	120	C2H2 finger domain protein, putative	0.23	XP_755991.1
XP_754253.1 AFUA_3G13710 **AFUB_035480**	98	GTP cyclohydrolase I, putative (EC 3.5.4.16)	0.24	XP_748029.1
XP_754573.1 AFUA_3G10460 AFUB_038700	124	Nuclear transport factor NTF-2, putative	0.18	XP_747927.1
XP_748648.1 AFUA_3G03290 AFUB_044960	135	Uncharacterized protein	0.18	XP_754308.1
XP_001481670.1 AFUA_2G13175 AFUB_028810	136	Uncharacterized protein	0.12	XP_747409.1

Gene_ID in **bold** are genes of interest. Fold change values have $p < 0.05$ and FDR < 0.05

Table 4.6 *Aspergillus fumigatus* MicroProteins (*continued*)

Predicted miP_ids Gene_ID Af293 Gene_ID A1163	Protein Length Af293	Annotation	C/H fc	A1163 orthologue of predicted binding partners
XP_752748.1 AFUA_1G13780 AFUB_013260	103	Histone H4	0.12	XP_754973.1
XP_752255.1 AFUA_1G08880 AFUB_008300	79	Iron/copper transporter Atx1, putative	0.15	XP_751569.1
XP_755278.1 AFUA_2G09440 AFUB_025300	73	Acetyl xylan esterase		XP_747458.1
XP_747374.1 AFUA_8G05730 #N/A	122	Beta-glucosidase, putative		XP_750759.1, XP_748896.1, XP_750327.1, XP_747720.1, XP_753108.1
XP_748431.1 AFUA_3G01100 **AFUB_047310**	127	C2H2 finger domain protein, putative		XP_751682.1, XP_751788.1, XP_752374.1, XP_750264.1, XP_747561.1, XP_755510.1, XP_749117.1, XP_755710.1, XP_747808.1, XP_750439.1, XP_754494.1, XP_754013.1, XP_747886.1, XP_753026.1, XP_752394.1, XP_754424.1, XP_748527.1, XP_001481416.1, XP_755959.1, XP_753992.1, XP_001481599.1, XP_754216.1, XP_748914.1, XP_750160.2, XP_755388.1, XP_751917.1, XP_753722.1
XP_755272.1 AFUA_2G09370 AFUB_025240	83	Choline dehydrogenase family protein		XP_748276.1, XP_748478.1, XP_754807.1, XP_752502.2, XP_755835.1, XP_746395.1, XP_747216.1
XP_752004.1 AFUA_4G08220 #N/A	126	Cytochrome P450 monooxygenase, putative		XP_750704.2, XP_747180.1, XP_001481477.1
XP_751033.1 AFUA_6G11500 AFUB_077510	134	Dipeptidase (EC 3.4.13.19)		XP_750854.2
XP_749677.1 AFUA_2G05480 AFUB_022500	121	DNA-directed RNA polymerase subunit		XP_754844.1
XP_750387.1 AFUA_1G06380 AFUB_006760	#N/A	#N/A		
XP_746509.1 AFUA_4G03230 AFUB_099890	131	Extracellular guanyl-specific ribonuclease RntA (EC 3.1.27.3)		XP_746338.1
XP_747107.1 AFUA_8G00990 AFUB_085600	106	F-box domain protein		XP_748679.1, XP_749772.1, XP_748761.1, XP_750869.1
XP_748838.1 AFUA_7G06730 AFUB_092310	130	FAD monooxygenase, putative		XP_748584.1, XP_749293.1, XP_749150.1, XP_747728.1, XP_752736.1, XP_751031.1
XP_748147.1 AFUA_5G01950 AFUB_050470	138	Histone H2A.Z		XP_755065.1

Gene_ID in **bold** are genes of interest. Fold change values have $p < 0.05$ and FDR < 0.05

Table 4.6 *Aspergillus fumigatus* MicroProteins (*continued*)

Predicted miP_ids Gene_ID Af293 Gene_ID A1163	Protein Length Af293	Annotation	C/H fc	A1163 orthologue of predicted binding partners
XP_746408.1 AFUA_4G00480 AFUB_101020	113	MFS multidrug transporter, putative		XP_749713.1, XP_753975.1, XP_755490.1, XP_746343.1, XP_748207.1, XP_746349.1, XP_752750.1, XP_750393.1, XP_753662.1, XP_755582.1, XP_748243.2, XP_746906.1, XP_748179.1, XP_748072.1, XP_756023.1, XP_752219.1, XP_749943.1, XP_748433.1, XP_747772.1, XP_752403.2, XP_748509.1, XP_755474.2, XP_755968.1, XP_748525.2, XP_748600.1
XP_746409.1 AFUA_4G00470 AFUB_101010	87	MFS multidrug transporter, putative		XP_749713.1, XP_747772.1, XP_748072.1, XP_749020.1, XP_752750.1, XP_746343.1, XP_753975.1, XP_748433.1, XP_750393.1, XP_746906.1, XP_748509.1, XP_755490.1, XP_756023.1, XP_755474.2, XP_748179.1, XP_748207.1, XP_748525.2, XP_749943.1, XP_752219.1, XP_752403.2, XP_755582.1, XP_748243.2, XP_751465.1, XP_748298.1, XP_754445.1, XP_746890.1, XP_755968.1, XP_748324.2, XP_746349.1, XP_748514.1, XP_746309.2
XP_755598.1 AFUA_2G12660 AFUB_028310	65	Polyprenyl synthetase family protein (EC 2.5.1.1)		XP_750866.1, XP_746966.1, XP_752686.1, XP_748183.1
XP_747784.1 AFUA_6G02920 AFUB_095380	121	SNARE protein Snc2, putative		XP_751011.1
XP_753149.1 AFUA_5G15080 AFUB_062570	100	Rho-associated protein kinase, putative		XP_750811.1, XP_747793.1, XP_755834.1, XP_751193.1, XP_754301.1, XP_751641.1, XP_753789.1, XP_753780.1, XP_750689.1, XP_753986.1, XP_754354.1, XP_753498.1, XP_746877.2, XP_755552.1, XP_749055.1, XP_752459.1, XP_748120.1
XP_754053.1 AFUA_5G05790 AFUB_053340	120	Ubiquitin ligase subunit HrtA, putative		XP_752576.1, XP_755664.1, XP_749382.1, XP_747197.1, XP_756024.1, XP_747290.1, XP_001481667.1, XP_749423.1
XP_746794.1 AFUA_7G01380 AFUB_087950	105	Anaphase promoting complex subunit Apc11, putative		
XP_748493.1 AFUA_3G01720 AFUB_046680	53	Uncharacterized protein		XP_752405.2, XP_748306.1
XP_731536.1 AFUA_6G00196 AFUB_097330	88	Uncharacterized protein		XP_747772.1, XP_755968.1, XP_750393.1, XP_746906.1, XP_754270.1, XP_746890.1, XP_749943.1, XP_747222.1, XP_752750.1
XP_749857.1 AFUA_1G01070 #N/A	139	Uncharacterized protein		XP_749839.2
XP_746849.1 AFUA_7G00810 AFUB_087390	134	Uncharacterized protein		XP_755796.1

Gene_ID in **bold** are genes of interest. Fold change values have $p < 0.05$ and FDR < 0.05

Table 4.6 *Aspergillus fumigatus* MicroProteins (*continued*)

Predicted miP_ids Gene_ID Af293 Gene_ID A1163	Protein Length Af293	Annotation	C/H fc	A1163 orthologue of predicted binding partners
XP_748788.1 AFUA_7G08270 #N/A	103	Uncharacterized protein		XP_750817.1, XP_751392.1
XP_748242.1 AFUA_5G00990 AFUB_049430	63	Uncharacterized protein		XP_746433.2
XP_752620.1 AFUA_1G12500 AFUB_011970	101	Uncharacterized protein		XP_747364.1
XP_752734.1 AFUA_1G13640 AFUB_013130	112	Uncharacterized protein		XP_748779.1
XP_752735.1 AFUA_1G13650 AFUB_013140	103	Uncharacterized protein		XP_755370.1
XP_753194.1 AFUA_5G14630 AFUB_062300	119	Uncharacterized protein		XP_748652.1, XP_750266.1
XP_756073.1 AFUA_2G17380 AFUB_033050	108	Uncharacterized protein		XP_746776.2
XP_756117.1 AFUA_2G17815 AFUB_033490	117	Uncharacterized protein		XP_746600.1, XP_746297.1, XP_750087.1, XP_749995.1
XP_756132.1 AFUA_2G17950 AFUB_033640	116	Uncharacterized protein		XP_754154.1, XP_747181.1

Gene_ID in **bold** are genes of interest. Fold change values have $p < 0.05$ and FDR < 0.05

References

1. Ebbole, D.J. The Conidium. *Cellular and Molecular Biology of Filamentous Fungi* 577-590 (2010).
2. Taha, M.P., Pollard, S.J., Sarkar, U. & Longhurst, P. Estimating fugitive bioaerosol releases from static compost windrows: feasibility of a portable wind tunnel approach. *Waste Manag* **25**, 445-50 (2005).
3. Siqueira, V.M.*, et al.* Filamentous fungi in drinking water, particularly in relation to biofilm formation. *Int J Environ Res Public Health* **8**, 456-69 (2011).
4. Warris, A.*, et al.* Molecular epidemiology of Aspergillus fumigatus isolates recovered from water, air, and patients shows two clusters of genetically distinct strains. *J Clin Microbiol* **41**, 4101-6 (2003).
5. Brakhage, A.A. & Liebmann, B. Aspergillus fumigatus conidial pigment and cAMP signal transduction: significance for virulence. *Medical Mycology* **43**, S75-S82 (2005).
6. Latge, J.P. Aspergillus fumigatus and aspergillosis. *Clin Microbiol Rev* **12**, 310-50 (1999).
7. Nierman, W.C.*, et al.* What the Aspergillus genomes have told us. *Medical Mycology* **43**, S3-S5 (2005).
8. Kwon-Chung, K.J. & Sugui, J.A. Aspergillus fumigatus-What Makes the Species a Ubiquitous Human Fungal Pathogen? *Plos Pathogens* **9**, (2013).
9. Burns, C.*, et al.* Identification, cloning, and functional expression of three glutathione transferase genes from Aspergillus fumigatus. *Fungal Genetics and Biology* **42**, 319-327 (2005).
10. Hillmann, F.*, et al.* Virulence determinants of the human pathogenic fungus Aspergillus fumigatus protect against soil amoeba predation. *Environ Microbiol* **17**, 2858-69 (2015).
11. Novohradska, S., Ferling, I. & Hillmann, F. Exploring Virulence Determinants of Filamentous Fungal Pathogens through Interactions with Soil Amoebae. *Front Cell Infect Microbiol* **7**, 497 (2017).
12. Lamarre, C.*, et al.* Transcriptomic analysis of the exit from dormancy of Aspergillus fumigatus conidia. *BMC Genomics* **9**, 417 (2008).
13. Novodvorska, M.*, et al.* Trancriptional landscape of Aspergillus niger at breaking of conidial dormancy revealed by RNA-sequencing. *BMC Genomics* **14**, 246 (2013).
14. Hagiwara, D.*, et al.* Comparative transcriptome analysis revealing dormant conidia and germination associated genes in Aspergillus species: an essential role for AtfA in conidial dormancy. *BMC Genomics* **17**, 358 (2016).

15. Baltussen, T.J.H., *et al.* Gene co-expression analysis identifies gene clusters associated with isotropic and polarized growth in Aspergillus fumigatus conidia. *Fungal Genet Biol* **116**, 62-72 (2018).

16. Teutschbein, J., *et al.* Proteome profiling and functional classification of intracellular proteins from conidia of the human-pathogenic mold Aspergillus fumigatus. *J Proteome Res* **9**, 3427-42 (2010).

17. Suh, M.J., *et al.* Development stage-specific proteomic profiling uncovers small, lineage specific proteins most abundant in the Aspergillus Fumigatus conidial proteome. *Proteome Sci* **10**, 30 (2012).

18. Anjo, S.I., *et al.* A proteomic and ultrastructural characterization of Aspergillus fumigatus' conidia adaptation at different culture ages. *J Proteomics* **161**, 47-56 (2017).

19. Voltersen, V. Proteome Analysis Reveals the Conidial Surface Protein CcpA Essential for Virulence of the Pathogenic Fungus Aspergillus fumigatus. (2018).

20. Momany, M., Westfall, P.J. & Abramowsky, G. Aspergillus nidulans swo mutants show defects in polarity establishment, polarity maintenance and hyphal morphogenesis. *Genetics* **151**, 557-567 (1999).

21. Upadhyay, S., Torres, G. & Lin, X. Laccases involved in 1,8-dihydroxynaphthalene melanin biosynthesis in Aspergillus fumigatus are regulated by developmental factors and copper homeostasis. *Eukaryot Cell* **12**, 1641-52 (2013).

22. Pertea, M., *et al.* Transcript-level expression analysis of RNA-seq experiments with HISAT, StringTie and Ballgown. *Nat Protoc* **11**, 1650-67 (2016).

23. Stajich, J.E., *et al.* FungiDB: an integrated functional genomics database for fungi. *Nucleic Acids Res* **40**, D675-81 (2012).

24. Frazee, A.C., *et al.* Ballgown bridges the gap between transcriptome assembly and expression analysis. *Nat Biotechnol* **33**, 243-6 (2015).

25. Straub, D. & Wenkel, S. Cross-Species Genome-Wide Identification of Evolutionary Conserved MicroProteins. *Genome Biol Evol* **9**, 777-789 (2017).

26. Leroch, M., *et al.* Transcriptome profiling of Botrytis cinerea conidial germination reveals upregulation of infection-related genes during the prepenetration stage. *Eukaryot Cell* **12**, 614-26 (2013).

27. Sharma, M., *et al.* Genome wide transcriptome profiling of Fusarium oxysporum f sp. ciceris conidial germination reveals new insights into infection-related genes. *Sci Rep* **6**, 37353 (2016).

28. Zhang, Z., Qian, W. & Zhang, J. Positive selection for elevated gene expression noise in yeast. *Mol Syst Biol* **5**, 299 (2009).

29. Monahan, B.J., Fraser, J.A., Hynes, M.J. & Davis, M.A. Isolation and characterization of two ammonium permease genes, meaA and mepA, from Aspergillus nidulans. *Eukaryot Cell* **1**, 85-94 (2002).

30. Calvete, C.L., *et al.* Amino acid permeases in Cryptococcus neoformans are required for high temperature growth and virulence; and are regulated by Ras signaling. *PLoS One* **14**, e0211393 (2019).

31. Martho, K.F., *et al.* Amino Acid Permeases and Virulence in Cryptococcus neoformans. *PLoS One* **11**, e0163919 (2016).

32. Donaton, M.C., *et al.* The Gap1 general amino acid permease acts as an amino acid sensor for activation of protein kinase A targets in the yeast Saccharomyces cerevisiae. *Mol Microbiol* **50**, 911-29 (2003).

33. Crapeau, M., Merhi, A. & Andre, B. Stress conditions promote yeast Gap1 permease ubiquitylation and down-regulation via the arrestin-like Bul and Aly proteins. *J Biol Chem* **289**, 22103-16 (2014).

34. Beaupere, C., *et al.* CAN1 Arginine Permease Deficiency Extends Yeast Replicative Lifespan via Translational Activation of Stress Response Genes. *Cell Rep* **18**, 1884-1892 (2017).

35. Sagaram, U.S., Shaw, B.D. & Shim, W.B. Fusarium verticillioides GAP1, a gene encoding a putative glycolipid-anchored surface protein, participates in conidiation and cell wall structure but not virulence. *Microbiology* **153**, 2850-61 (2007).

36. Palmieri, L., *et al.* Identification of the yeast ACR1 gene product as a succinate-fumarate transporter essential for growth on ethanol or acetate. *FEBS Lett* **417**, 114-8 (1997).

37. Hubert, P., *et al.* Single-spanning transmembrane domains in cell growth and cell-cell interactions: More than meets the eye? *Cell Adh Migr* **4**, 313-24 (2010).

38. Cabrera, I.E., *et al.* Global Analysis of Predicted G Protein-Coupled Receptor Genes in the Filamentous Fungus, Neurospora crassa. *G3 (Bethesda)* **5**, 2729-43 (2015).

39. Robinson, K., Deng, Z., Hou, Y. & Zhang, G. Regulation of the Intestinal Barrier Function by Host Defense Peptides. *Front Vet Sci* **2**, 57 (2015).

40. Long, N., *et al.* Erg4A and Erg4B Are Required for Conidiation and Azole Resistance via Regulation of Ergosterol Biosynthesis in Aspergillus fumigatus. *Appl Environ Microbiol* **83**, (2017).

41. Cui, N., *et al.* Tebuconazole induces triazole-resistance in Aspergillus fumigatus in liquid medium and soil. *Science of the Total Environment* **648**, 1237-1243 (2019).

42. Slaven, J.W., *et al.* Increased expression of a novel Aspergillus fumigatus ABC transporter gene, atrF, in the presence of itraconazole in an itraconazole resistant clinical isolate. *Fungal Genet Biol* **36**, 199-206 (2002).

43. Ukai, Y., *et al.* Contributions of yap1 Mutation and Subsequent atrF Upregulation to Voriconazole Resistance in Aspergillus flavus. *Antimicrob Agents Chemother* **62**, (2018).

44. Moreno, M.A., *et al.* The regulation of zinc homeostasis by the ZafA transcriptional activator is essential for Aspergillus fumigatus virulence. *Mol Microbiol* **64**, 1182-97 (2007).

45. Vicentefranqueira, R., Moreno, M.A., Leal, F. & Calera, J.A. The zrfA and zrfB genes of Aspergillus fumigatus encode the zinc transporter proteins of a zinc uptake system induced in an acid, zinc-depleted environment. *Eukaryot Cell* **4**, 837-48 (2005).

46. Dinamarco, T.M., *et al.* Functional characterization of an Aspergillus fumigatus calcium transporter (PmcA) that is essential for fungal infection. *PLoS One* **7**, e37591 (2012).

47. Wang, J., Zhu, X.G., Ying, S.H. & Feng, M.G. Differential Roles for Six P-Type Calcium ATPases in Sustaining Intracellular Ca(2+) Homeostasis, Asexual Cycle and Environmental Fitness of Beauveria bassiana. *Sci Rep* **7**, 1420 (2017).

48. Portillo, F. Regulation of plasma membrane H(+)-ATPase in fungi and plants. *Biochim Biophys Acta* **1469**, 31-42 (2000).

49. Goossens, A., *et al.* Regulation of yeast H(+)-ATPase by protein kinases belonging to a family dedicated to activation of plasma membrane transporters. *Mol Cell Biol* **20**, 7654-61 (2000).

50. Liu, Y., Li, P., Fan, L. & Wu, M. The nuclear transportation routes of membrane-bound transcription factors. *Cell Commun Signal* **16**, 12 (2018).

51. Kikuma, T., Arioka, M. & Kitamoto, K. Autophagy during conidiation and conidial germination in filamentous fungi. *Autophagy* **3**, 128-9 (2007).

52. Weirauch, M.T., *et al.* Determination and inference of eukaryotic transcription factor sequence specificity. *Cell* **158**, 1431-1443 (2014).

53. Novodvorska, M., *et al.* Metabolic activity in dormant conidia of Aspergillus niger and developmental changes during conidial outgrowth. *Fungal Genet Biol* **94**, 23-31 (2016).

54. Hynes, M.J., Draht, O.W. & Davis, M.A. Regulation of the acuF gene, encoding phosphoenolpyruvate carboxykinase in the filamentous fungus Aspergillus nidulans. *J Bacteriol* **184**, 183-90 (2002).

55. Pongpom, M., *et al.* Divergent targets of Aspergillus fumigatus AcuK and AcuM transcription factors during growth in vitro versus invasive disease. *Infect Immun* **83**, 923-33 (2015).

56. Hynes, M.J., *et al.* Regulatory genes controlling fatty acid catabolism and peroxisomal functions in the filamentous fungus Aspergillus nidulans. *Eukaryot Cell* **5**, 794-805 (2006).

57. Lapp, K., *et al.* Characterization of the Aspergillus fumigatus detoxification systems for reactive nitrogen intermediates and their impact on virulence. *Front Microbiol* **5**, 469 (2014).

58. Han, K.H., *et al.* The conserved and divergent roles of carbonic anhydrases in the filamentous fungi Aspergillus fumigatus and Aspergillus nidulans. *Mol Microbiol* **75**, 1372-88 (2010).

59. Chung, D., *et al.* ChIP-seq and in vivo transcriptome analyses of the Aspergillus fumigatus SREBP SrbA reveals a new regulator of the fungal hypoxia response and virulence. *PLoS Pathog* **10**, e1004487 (2014).

60. Gsaller, F., *et al.* Sterol Biosynthesis and Azole Tolerance Is Governed by the Opposing Actions of SrbA and the CCAAT Binding Complex. *PLoS Pathog* **12**, e1005775 (2016).

61. Blatzer, M., *et al.* SREBP coordinates iron and ergosterol homeostasis to mediate triazole drug and hypoxia responses in the human fungal pathogen Aspergillus fumigatus. *PLoS Genet* **7**, e1002374 (2011).

62. Szklarczyk, D., *et al.* STRING v11: protein-protein association networks with increased coverage, supporting functional discovery in genome-wide experimental datasets. *Nucleic Acids Res* **47**, D607-D613 (2019).

63. Hu, Y., *et al.* The PHD Transcription Factor Rum1 Regulates Morphogenesis and Aflatoxin Biosynthesis in Aspergillus flavus. *Toxins (Basel)* **10**, (2018).

64. Kadamb, R., *et al.* Sin3: insight into its transcription regulatory functions. *Eur J Cell Biol* **92**, 237-46 (2013).

65. Apel, K. & Hirt, H. Reactive oxygen species: metabolism, oxidative stress, and signal transduction. *Annu Rev Plant Biol* **55**, 373-99 (2004).

66. Forrester, S.J., *et al.* Reactive Oxygen Species in Metabolic and Inflammatory Signaling. *Circ Res* **122**, 877-902 (2018).

67. Hong, S.Y., Roze, L.V., Wee, J. & Linz, J.E. Evidence that a transcription factor regulatory network coordinates oxidative stress response and secondary metabolism in aspergilli. *Microbiologyopen* **2**, 144-60 (2013).

68. Venkatesan, K., *et al.* Functional conservation between members of an ancient duplicated transcription factor family, LSF/Grainyhead. *Nucleic Acids Res* **31**, 4304-16 (2003).

69. Narasimha, M., *et al.* Grainy head promotes expression of septate junction proteins and influences epithelial morphogenesis. *J Cell Sci* **121**, 747-52 (2008).

70. Pare, A., *et al.* The functions of grainy head-like proteins in animals and fungi and the evolution of apical extracellular barriers. *PLoS One* **7**, e36254 (2012).

71. Millet, N., *et al.* Aspergillus fumigatus exobeta(1-3)glucanases family GH55 are essential for conidial cell wall morphogenesis. *Cell Microbiol* e13102 (2019).

72. Sanchez, C. Reactive oxygen species and antioxidant properties from mushrooms. *Synth Syst Biotechnol* **2**, 13-22 (2017).

73. Gessler, N.N., Aver'yanov, A.A. & Belozerskaya, T.A. Reactive oxygen species in regulation of fungal development. *Biochemistry (Mosc)* **72**, 1091-109 (2007).

74. Aguirre, J., Hansberg, W. & Navarro, R. Fungal responses to reactive oxygen species. *Med Mycol* **44**, S101-S107 (2006).

75. Aguirre, J., Rios-Momberg, M., Hewitt, D. & Hansberg, W. Reactive oxygen species and development in microbial eukaryotes. *Trends Microbiol* **13**, 111-8 (2005).

76. Joazeiro, C.A. & Weissman, A.M. RING finger proteins: mediators of ubiquitin ligase activity. *Cell* **102**, 549-52 (2000).

77. Teertstra, W.R., *et al.* Maturation of conidia on conidiophores of Aspergillus niger. *Fungal Genet Biol* **98**, 61-70 (2017).

78. Voltersen, V., *et al.* Proteome Analysis Reveals the Conidial Surface Protein CcpA Essential for Virulence of the Pathogenic Fungus Aspergillus fumigatus. *Mbio* **9**, (2018).

79. Hillmann, F., Shekhova, E. & Kniemeyer, O. Insights into the cellular responses to hypoxia in filamentous fungi. *Curr Genet* **61**, 441-55 (2015).

CHAPTER 5

CONCLUSION

Aspergillus fumigatus is a survivor. It is able to tolerate growth in a wide range of environments, sporulates under stress and the asexual propagules, conidia, are whisked away to distant places where they are able to restart. Often this germination environment can be very different than the environment where sporogenesis occurred, yet the conidial developmental stage prepares them to adapt and grow. Even in the presence of synthetic fungicides *A. fumigatus* is able to repurpose genes necessary for basic biological function to rapidly adapt and develop resistance. In this dissertation I set out to understand what allows this organism to be so adaptable and to identify the regulators of survival mechanisms.

In Chapter 2, we were funded by the Centers for Disease Control and Prevention to perform a simple survey of the Southeast for the presence of azole resistant *Aspergillus fumigatus* in agricultural settings. This allowed me go out into the environment and observe *A. fumigatus* in its natural habitat. While *A. fumigatus* is considered a ubiquitous saprophytic fungus it could not be isolated from all decaying plant debris. It was most frequently isolated from within piles of plant debris where it is dark, moist and shielded from the environment. There it grew in competition with other *Aspergillus* spp. and microbes. Even in compost heaps where it was reported to be the most prevalent fungus, *A. fumigatus* was not seen sporulating on the surface of heaps, but rather a few centimeters below the surface in pockets of air. It seized opportunities to sporulate in whatever niche it could.

Whole genome sequencing of the environmental isolates revealed that *Aspergillus fumigatus* is a rather complex species complex. Sequencing a large number of environmental genotypes without clinical bias has finally allowed us to get a better understanding of the population structure. All cyp51A mutant azole resistant isolates clustered into a single clade. The distance between the azole resistant clade and the other clades combined with lack of evidence of genetic recombination between the different clades (Figure 2.2) suggests that the isolates developing rapid resistance are part of a sub species within the

Fumigati complex. There is something genetically inherent about the resistant clade of *A. fumigatus* which allows for adaptation and resistance to agricultural fungicides and requires careful examination.

The complexity of the *A. fumigatus* genome can be further supported by a failed experiment to create a reference core pan-genome using *de novo* assembled genomes of the environmental isolates[1]. The experiment was performed prior to realizing the presence of multiple clades and resulted in a core genome twice the size of the expected genome. Identifying which isolates were contributing to the assembly of the different core genomes posed a challenge prior to having the tree. The experiment should be repeated in the near future with isolates from within clades, then compare the clade specific pan-genomes with each other.

The biggest value of this project wasn't identifying TR_{46}/Y121F/T289A resistant isolates in the United States for the first time. It was the number of high-quality sequences generated of susceptible environmental "WT" isolates. The phylogenetic analysis resulted in identification of pairs of clinical azole resistant isolates of unknown mechanisms with near isogenic susceptible isolates. Previous attempts to sort through SNP data of clinical azole resistant isolates of unknown mechanisms to identify meaningful mutations conferring novel resistance has been challenging due to the vast difference between the reference isolate Af293 and clinical isolates being analyzed (personal communications with Jeffery M. Rybak)[2]. Minimizing the difference between resistant and susceptible isolate pairs should enable us to identify meaningful mutations.

Preliminary analysis of SNPs of clinical azole resistant isolates of unknown mechanisms using Ensembl Variant Effect Predictor[3] showed that the majority of the SNPs are not located in the coding sequences of the genome. Comparison of SNPs found in the 5'UTR region with transcriptomic data from reference isolate A1163 showed that there are SNPs occurring where splicing should occur. Whether or not this changes alternative splicing in the 5'UTR region of resistant isolates should be explored. Interestingly, a gene in the ergosterol pathway contained no SNPs in the coding sequence. However, in all resistant isolates of unknown mechanism the Kozak sequence had been modified, which could change the translation efficiency[4]. There were also examples where no SNPs were present in the coding

sequence but there were several shared SNPs was in the 3'UTR region. In light of advances in RNA structure biology, these SNPs should be modeled to see how they affect the structure of the RNA which could in turn affect the stability of the transcript.

In Chapter 3, we set out to test if the sporulation environment would provide a germination advantage when *Aspergillus fumigatus* re-encountered the same environment where it sporulated and to identify sporulation environments that would result in different germination phenotypes. Indeed, we did identify sporulation environments that resulted in fast and slow germination phenotypes and learned that previous exposure to an environment during sporulation does not always provide a germination advantage. Further experiments will need to be conducted *in vivo* to test if sporulation environment changes the rate of infection.

The biggest impact of this work was being able to detect heterogeneity in a germinating population. In an age where single cell analysis is becoming possible, we were able to establish a procedure to study and measure variation in what had previously been considered to be a homogenous population. In the next chapter I used RNAseq to identify genes that may play a role in regulating germination. I propose using rCas9::mCh[5] and our single cell analysis method to quantify gene expression via fluorescence of the germination regulator genes we identified to observe how the transcript levels effect germination rates in individual conidia.

In Chapter 4, we performed an in-depth transcriptome analysis of conidia. We took a novel approach of comparing conidia exhibiting different germination phenotypes to identify genes that could be important in regulating germination or proper conidial maturation. Then we compared the conidial transcriptome to the hyphal transcriptome which also included conidiophore development. In addition, we used bioinformatics to identify novel regulators in the different developmental stages. By comparing the different developmental stages we were able to identify genes that are expressed during the earliest stages of sporogenesis and identify gene that may be essential for proper conidial development. The next step to understanding conidia includes functional characterization of the genes identified as being important regulators and examination of the conidial transcriptome when the conidia are fully matured[6].

Further experiments are also required to functionally characterize novel transcripts we identified during the first round of analysis[7]. The conidial transcriptome included in Chapter 4 is based on the current annotation (Ensembl v43). Novel transcriptome analysis followed by gene prediction software[8] using transcriptome data showed that there may be approximately 172 unannotated transcripts in the genome. 43 are enriched in the conidia and 54 are enriched in conidophore. Annotation of novel genes using SWISS-MODEL[9], Phobius[10], and WoLF PSORT[11] predicted that in conidia there are many secreted toxins, proteins that could be easily washed away prior to mass spectrometry analysis for proteomics based annotations. In the conidiophore transcriptome there were several novel lectins and a novel transcription factor with protein homology with SPO16, sporulation-specific protein 16. Further characterization and protein expression of these transcripts should be performed.

In addition to unannotated genes, there were over 2000 novel isoforms that appear to be developmentally- or stress-regulated. Many of these splice variants occurred in the UTR regions of the transcripts and therefore may be important for translation of the gene. There were also splice variants in the coding sequence which included novel isoforms and co-transcription with neighboring "proteins of unknown function" for a large number of transmembrane proteins and metabolic genes. Under stress these transcripts could be translated into novel proteins offering new function. While this occurrence has been described for small ORFs, it has not been fully explored for larger ORFs[12]. These isoforms warrant further investigation[13].

Finally, SNP analysis of mRNA revealed that there are a handful of transcripts with development specific post transcriptional modifications. It is important to note that rarely did I observe 100% of the transcript being modified in a cell type. There were always a small number of transcripts in each cell type that would or would not be modified, but the ratio of these modifications changed between cell types. Due to the coverage depth of the datasets we can be confident that these observations are not due to sequencing errors. In the rare occasions that I did observe 100% of the transcripts being modified I could not be confident whether the modification was due to a SNP in the lab strain compared to the reference genome. Therefore, it is important to sequence the gene with predicted post-transcriptional modification

prior to making any conclusive statements. Post-transcriptional modifications of mRNA have been shown to play important roles in development[14].

References

1 Jandrasits, C., Dabrowski, P. W., Fuchs, S. & Renard, B. Y. seq-seq-pan: building a computational pan-genome data structure on whole genome alignment. *BMC Genomics* **19**, 47, doi:10.1186/s12864-017-4401-3 (2018).

2 Rybak, J. M. *et al.* Mutations in hmg1, Challenging the Paradigm of Clinical Triazole Resistance in Aspergillus fumigatus. *MBio* **10**, doi:10.1128/mBio.00437-19 (2019).

3 McLaren, W. *et al.* The Ensembl Variant Effect Predictor. *Genome Biol* **17**, 122, doi:10.1186/s13059-016-0974-4 (2016).

4 Nakagawa, S., Niimura, Y., Gojobori, T., Tanaka, H. & Miura, K. Diversity of preferred nucleotide sequences around the translation initiation codon in eukaryote genomes. *Nucleic Acids Res* **36**, 861-871, doi:10.1093/nar/gkm1102 (2008).

5 Nelles, D. A. *et al.* Programmable RNA Tracking in Live Cells with CRISPR/Cas9. *Cell* **165**, 488-496, doi:10.1016/j.cell.2016.02.054 (2016).

6 Anjo, S. I., Figueiredo, F., Fernandes, R., Manadas, B. & Oliveira, M. A proteomic and ultrastructural characterization of Aspergillus fumigatus' conidia adaptation at different culture ages. *J Proteomics* **161**, 47-56, doi:10.1016/j.jprot.2017.03.021 (2017).

7 Pertea, M., Kim, D., Pertea, G. M., Leek, J. T. & Salzberg, S. L. Transcript-level expression analysis of RNA-seq experiments with HISAT, StringTie and Ballgown. *Nat Protoc* **11**, 1650-1667, doi:10.1038/nprot.2016.095 (2016).

8 Ter-Hovhannisyan, V., Lomsadze, A., Chernoff, Y. O. & Borodovsky, M. Gene prediction in novel fungal genomes using an ab initio algorithm with unsupervised training. *Genome Res* **18**, 1979-1990, doi:10.1101/gr.081612.108 (2008).

9 Waterhouse, A. *et al.* SWISS-MODEL: homology modelling of protein structures and complexes. *Nucleic Acids Res* **46**, W296-W303, doi:10.1093/nar/gky427 (2018).

10 Kall, L. Prediction of transmembrane topology and signal peptide given a protein's amino acid sequence. *Methods Mol Biol* **673**, 53-62, doi:10.1007/978-1-60761-842-3_4 (2010).

11 Horton, P. *et al.* WoLF PSORT: protein localization predictor. *Nucleic Acids Res* **35**, W585-587, doi:10.1093/nar/gkm259 (2007).

12 Kastenmayer, J. P. *et al.* Functional genomics of genes with small open reading frames (sORFs) in S. cerevisiae. *Genome Res* **16**, 365-373, doi:10.1101/gr.4355406 (2006).

13 Roach, N. P. *et al.* The full-length transcriptome of C. elegans using direct RNA sequencing. *bioRxiv*, 598763, doi:10.1101/598763 (2019).

14 Frye, M. & Blanco, S. Post-transcriptional modifications in development and stem cells. *Development* **143**, 3871-3881, doi:10.1242/dev.136556 (2016).